POLYMER BLEND BASED MIXED MATRIX GAS SEPARATION MEMBRANES

A THESIS SUBMITTED TO
THE GRADUATE SCHOOL OF NATURAL AND APPLIED SCIENCES
OF
MIDDLE EAST TECHNICAL UNIVERSITY

BY

MELİS KARĞILI

IN PARTIAL FULFILLMENT OF THE REQUIREMENTS
FOR
THE DEGREE OF MASTER OF SCIENCE
IN
POLYMER SCIENCE AND TECHNOLOGY

SEPTEMBER 2015

Approval of the thesis:

POLYMER BLEND BASED MIXED MATRIX GAS SEPARATION MEMBRANES

submitted by **MELİS KARĞILI** in partial fulfillment of the requirements for the degree of **Master of Science in Polymer Science and Technology Department, Middle East Technical University** by,

Prof. Dr. Gülbin Dural Ünver
Dean, Graduate School of **Natural and Applied Sciences** _____

Prof. Dr. Necati Özkan
Head of Department, **Polymer Science and Technology** _____

Prof. Dr. Levent Yılmaz
Supervisor, **Chemical Engineering Dept., METU** _____

Prof. Dr. Halil Kalıpçılar
Co-supervisor, **Chemical Engineering Dept., METU** _____

Examining Committee Members:

Prof. Dr. Nihal Aydoğan
Chemical Engineering Dept., Hacettepe University _____

Prof. Dr. Levent Yılmaz
Chemical Engineering Dept., METU _____

Prof. Dr. Halil Kalıpçılar
Chemical Engineering Dept., METU _____

Assist. Prof. Dr. Pınar Zeynep Çulfaz Emecen
Chemical Engineering Dept., METU _____

Assist. Prof. Dr. Erhan Bat
Chemical Engineering Dept., METU _____

Date: 02.09.2015

I hereby declare that all information in this document has been obtained and presented in accordance with academic rules and ethical conduct. I also declare that, as required by these rules and conduct, I have fully cited and referenced all material and results that are not original to this work.

Name, Last name : Melis KARĞILI

Signature :

ABSTRACT

POLYMER BLEND BASED MIXED MATRIX GAS SEPARATION MEMBRANES

Kargılı, Melis

M.S., Polymer Science and Technology

Supervisor : Prof. Dr. Levent Yılmaz

Co-Supervisor: Prof. Dr. Halil Kalıpçılar

September 2015, 97 pages

Polymer blending and mixed matrix membranes are two methods suggested to improve performance of gas separation membranes. Dense and asymmetric membranes of PES/PI blends with different compositions were prepared and the effect of blend composition on gas separation performances was investigated. In addition, PES/PI/ZIF-8 blend based mixed matrix membranes were prepared in order to investigate the effect of nano-porous filler addition to polymer blends.

ZIF-8 particles with size of 83 nm were synthesized. Particles were characterized through scanning electron microscopy (SEM), X-Ray diffractometer (XRD), and thermogravimetric analysis (TGA).

Dense PES/PI blend membranes were prepared in DMF with PI composition in range of 5 to 95%. Membranes were characterized through SEM, TGA, and differential scanning calorimetry (DSC). Glass transition temperatures of the blend membranes

were in between the values of pristine membranes. Gas permeation test were conducted for H_2, CO_2, and CH_4 at 3 bar feed pressure. It was determined that no phase separation occurred based on SEM or DSC characterization. The permeability of all gases increased as the amount of the PI in the blend increased. H_2/CO_2, CO_2/CH_4, and H_2/CH_4 selectivity values increased with increasing PI composition. PES/PI 20/80 membranes performed best for all gas pairs among the blend membranes.

Polymer blend based dense, mixed matrix membranes were prepared by addition of 10 wt% ZIF-8 particles into the PES/PI 20/80 matrix. Membranes were characterized through TGA, SEM, and DSC. The decomposition temperature of PES/PI/ZIF-8 membrane was found below PES/PI 20/80 membranes. ZIF-8 particles were dispersed in the polymer matrix homogeneously and formed sieve-in-cage structure. ZIF-8 addition improved the permeability of the membranes due to high porosity of the particles, while selectivity values remained almost same for all gas pairs, compared to PES/PI 20/80 blend membranes. Furthermore, CO_2/CH_4 separation performance of PES/PI/ZIF-8 membrane was found better than PI/ZIF-8 membranes.

PES/PI 20/80 asymmetric blend membranes were prepared by immersing polymer blend/DMF solution casted on a glass plate into DMF/IPA mixture. Thermal characters of the asymmetric membranes were improved very little in terms of the decomposition temperature and weight losses. According to the SEM micrographs, membranes have thin, nanoporous skin layer on sponge-like microporous support layer. The permeances of the asymmetric membranes were significantly higher than the dense membranes, due to the high porous structure. Besides, H_2/CO_2 and H_2/CH_4 selectivity values were improved by preparation of asymmetric membranes, relative to dense membranes.

Keywords: Gas separation, Polymer Blends, Polyethersulfone, Polyimide, Zeolitic Imıdazolate Framework-8 (ZIF-8), Mixed Matrix Membranes

ÖZ

POLİMER HARMANINA DAYALI KARIŞIK MATRİSLİ GAZ AYIRMA MEMBRANLARI

Kargılı, Melis

Yüksek Lisans, Polimer Bilimi ve Teknolojisi Bölümü

Tez Yöneticisi : Prof. Dr. Levent Yılmaz

Ortak Tez Yöneticisi: Prof. Dr. Halil Kalıpçılar

Eylül 2015, 97 sayfa

Polimer harmanlama ve karışık matrisli membranlar gaz ayırma membranlarının performanslarını arttırmak için önerilmiş iki yöntemdir. İnce film ve asimetrik PES/PI membranlar iki polimerin farklı oranlarda harmanlanmasıyla üretilmiş ve harman komposizyonunun gaz ayırım performansına etkileri incelenmiştir. Ayrıca, PES/PI/ZIF-8 harman temelli karışık matrisli membranlar üretilerek nano-gözenekli dolgu malzemesinin harman membranların gaz ayırım performansına etkileri incelenmiştir.

Sentezlenen ZIF-8 dolgu malzemesinin ortalama parçacık boyutu 83nm'dir. Partiküller taramalı elektron mikroskobu (SEM) , X-Ray kırınımı (XRD) ve termogravimetrik (TGA) yöntemlerle analiz edilmiştir.

PI oranı %5 ile %95 arasında değişen PES/PI harman membranlar, polimerlerin DMF içerisinde çözünmesiyle çözücü uçurma yöntemine göre hazırlanmıştır. Membranlar SEM, TGA ve diferansiyel taramalı kalorimetri yöntemiyle analiz edilmiştir. Harman membranların camsı geçiş sıcaklıkları saf polimerlerin camsı geçiş sıcaklıkları arasındadır. H_2, CO_2 ve CH_4 gaz geçirgenlik testleri 3 bar besleme

basıncında yapılmıştır. SEM ve DSC analizlerinde iki polimer arasında bir faz ayırımı gözlenmemiştir. Membranların gaz geçirgenlikleri ve seçicilikleri harman içerisindeki PI oranı arttıkça artmaktadır. PES/PI 20/80 oranına sahip membran, harman membranlar içerisindeki en iyi gaz ayırım performansını göstermiştir.

Polimer harmanına dayalı karışık matrisli membranlar PES/PI 20/80 membrana kütlece %10 ZIf-8 eklenmesiyle hazırlanmıştır. PES/PI/ZIF-8 membranların termal ve yapısal karakteri TGA, SEM ve DSC ile incelenmiştir. ZIF-8 ekli membranların dekomposizyon sıcaklığı ince film PES/PI 20/80 membranlardan daha aşağıda tespit edilmiştir. ZIF-8 partikülleri PES/PI matrisi içerisinde homojen olarak dağılmış ve kafes içinde elek adı verilen yapıyı oluşturmuşlardır. PES/PI/ZIF-8 membranların gaz geçirgenlikleri, ince film PES/PI 20/80 membranlara kıyasla ZIF-8 parçacıklarının yüksek gözenekli yapısı sayesinde artarken, seçiciliklerinde önemli denilebilecek bir değişme görülmemiştir. Dahası, PES/PI/ZIF-8 membranların CO_2/CH_4 seçicilikleri PI/ZIF-8 membranların seçiciliklerinden bile daha yüksek bulunmuştur.

Asimetrik PES/PI 20/80 membranlar cam üzerine yayılan Polimer/DMF çözeltisinin IPA/DMF çökeltme banyosuna batırılmasıyla elde edilmiştir. Dekomposizyon sıcaklığı ve kayıp kütle miktarları incelendiğinde, asimetrik membranların termal karakterinin ince film PES/PI 20/80 membranlar göre daha iyi olduğu görülmüştür. SEM analizleri incelendiğinde, membranların mikro-gözenekli süngerimsi bir destek tabaka üzerindeki nano-gözenekli ince kabuk tabakadan oluştuğu gözlenmiştir. Asimetrik membranların akıları, membranların gözenekli yapılarından dolayı, ince film membranlara kıyasla oldukça yüksektir. Ayrıca, asimetrik membranların H_2/CO_2 ve H_2/CH_4 seçiciliklerinde de ince film membranlar oranla artış gözlenmiştir.

Anahtar Kelimeler: Gaz ayırım, Polimer Harman, Polietersülfon, Poliimid, Zeolitik İmidazolat Çatı-8 (ZIF-8), Karışık Matrisli Membranlar

To My Dearest Family,

ACKNOWLEDGMENTS

First, I am deeply grateful to my supervisor Prof. Dr. Levent Yılmaz for his significant contributions, patience, and guidance throughout this study. I would like to show my appreciation to my co-supervisor Prof. Dr. Halil Kalıpçılar for his precious suggestions and support. It was a pleasing honor for me to work with them.

Moreover, I would like to thank to TÜBİTAK (The Scientific and Technological Research Council of Turkey) for financial supports through grant number 213M546. I am also grateful to Middle East Technical University Chemical Engineering Department technicians for their helps and advices.

I would like to present my sincere thanks to my dear lab colleagues Elif İrem Şenyurt, Fırat Ozanırk, Gülçin Kaltalı, İlhan Ayas, Burcu Tüzün, Fatma Şahin Çakanyıldırım and Yiğit Gencal for their kind friendship, help and useful cooperation.

I would also like to thank to my dear friends Burçin Kavcı and Alyaan Khan for their endless friendships and supports. Also, I sincerely thank to all my comrades of higher education Umut Çaçan, Emir Demirtaş, Türkan Güler, Burcu Sarı, Başak Kanya, Elif Topçuoğlu, Özge Çimen, Berrak Erkmen, Merve Özkutlu, Dilara Gülçin Çağlayan, who were beside me during my graduate study.

Finally yet importantly, my very special thanks go to my family for their great support, encouragement, and unlimited patience and love.

TABLE OF CONTENTS

LIST OF TABLES

TABLES

LIST OF FIGURES

FIGURES

CHAPTER 1

INTRODUCTION

Fossil fuels can be counted as the world's most preferred energy sources. However, increase in the need of energy around the world and the harmful effects of the fossil fuels on the nature direct the research on renewable and more efficient energy sources. Natural gas is counted as a replacement of fossil fuel and coal. Purification of the natural gas from the impurity gases, mostly CO_2, is enhances the quality of the natural gas and decrease the corrosion of the pipelines during transportation [1].

There are several methods to separate carbon dioxide from methane; such as cryogenic distillation, absorption, amine adsorption, and membrane separation. Even though amine adsorption is the most developed commercial method, this method has several disadvantages, such as high energy consumption during regeneration of the solvent, corrosion of the equipment and flow problems [1]. Separation of gas mixtures by membranes has numerous advantages over the other methods, for example low operation and capital cost, ease of operation and low energy consumption [1,2].

Hydrogen is one of the most vastly used chemicals in various industries, such ammonia production, oil refining, or food. Also, it has been gained importance as one of the clean energy sources alternative to fossil fuels [3]. Therefore, production, storage, and separation of hydrogen have been gaining importance. Water-gas shift reaction is the major hydrogen production method and products of this reaction are CO_2 and H_2. The presence of carbon dioxide decreases the yield of the process and quality of the product [4]. The conventional H_2/CO_2 separation methods can be listed

as pressure swing adsorption, temperature swing adsorption, and cryogenic distillation. However, these methods are not energy or cost effective, compared with membrane separation methods [5]. Moreover, H_2 is used extensively in steam refining process, therefore it is required to be separated from CH_4 and regained [6].

Gas separation membranes can be classified to four groups, based on materials they are produced, facilitated-transport membranes, inorganic membranes, polymeric membranes, and mixed matrix membranes. The theory of facilitated-transport membranes is to establish strong bonds between interested gas molecules and membrane to facilitate the diffusion of interested gas [7]. They possess some disadvantages such as mechanical instability, low diffusivity, and defect formation. Inorganic membranes may have good separation performance, chemical and thermal stability [2]. However, since they are quite expensive, hard to handle and process, they are not preferred to be used in industrial applications. Polymeric membranes are cost effective, easy to produce and operate. However, since they are chemically and thermally vulnerable, their usage is limited by low-temperature and non-reactive gases. Mixed matrix membranes are developed by combining inorganic and polymeric membranes to overcome these problems. They have mechanical and thermal stability, cost-effectiveness, and easy operation condition as well as excellent gas separation properties [2]. Polymer blending is another method to obtain an enhanced polymeric membrane by combining different polymers with different properties. It is time and cost effective method to derive a polymeric membrane with certain performance rather than synthesizing a new polymer [8]. Polymeric membranes may suffer from CO2 plasticization at relatively higher temperatures and pressures, which may be required for natural gas purification. Blending of two or more polymers are suggested to overcome or increase the resistance against plasticization [9] and also to increase the mechanical and thermal properties [8].

Polymer based membranes can also be classified depending on their morphology as symmetric, asymmetric and composite. Symmetric membranes can be porous or non-porous (dense).The permeability of a symmetric membrane depends on its thickness,

which means thinner the membrane higher the permeation rate. Asymmetric membranes have thin skin layer on porous sublayer. The thickness of an asymmetric membranes can be decreased to 0.1 to 0.5 microns which decreases the resistance of the membrane against permeate and increases the permeability of the membrane, yet not much changes the selectivity [10].

Separation mechanism of non-porous, also called dense, polymeric membranes is sorption of the gas molecules at one side of the membrane, diffusion, and passing through the membrane, and desorption at the other side under the driving force of pressure gradient. Solubility of the gas molecules in the polymer matrix are playing an important role while separating similar sized gases [9].

The permeability, and the ideal selectivity are the key features while determining the gas separation performance of a dense membrane, which are calculated by following formulas [6].

$$P(Barrer) = (J \times l)/\Delta p \qquad \text{Equation 1.1}$$

$$\alpha = P_A/P_B \qquad \text{Equation 1.2}$$

where P is the permeability of the membrane for certain gases, Barrer,

α is the selectivity of A gas to B gas,

J is the flux of gas through membrane, cm^3/cm^2 s,

l is the membrane thickness, cm,

Δp is the difference of the partial pressures of feed and permeate, atm.

$$Barrer = 1 \times 10^{-10}\ \ (cm^3(STP).cm)/(cm^2.s.cmHg) \qquad \text{Equation 1.3}$$

During calculating gas separation performance of an asymmetric membrane, permeance is calculated instead of permeation. Permeance can be simply defined as

thickness independent permeation and can be calculated by using following formula: [11]

$$P'(GPU) = \frac{P}{l} = \frac{Q}{A \times \Delta p} = \frac{J}{\Delta p} \qquad \text{Equation 1.4}$$

where P' is the permeance, GPU (gas permeation unit),

Q is the volumetric flow rate, cm^3/s,

A is the cross-sectional area, cm^2.

$$GPU = 1 \times 10^{-6}\,(cm^3(STP))/(cm^2.s.cmHg) \qquad \text{Equation 1.5}$$

A gas separation membrane has to have both high selectivity and high permeability in order to be used as an industrial gas separation method. However, Robeson mentioned that there is a tradeoff between selectivity and permeability [12,13]. For example, rubbery polymers show very high permeability, but low selectivity because of the high chain mobility. On the other hand, glassy polymers exhibit high selectivity and low permeability. The addition of inorganic fillers such as zeolites, silicates, CNTs to the glassy polymers is suggested to enhance the performance of the polymeric membranes. These type of membranes are called mixed matrix membranes [2].

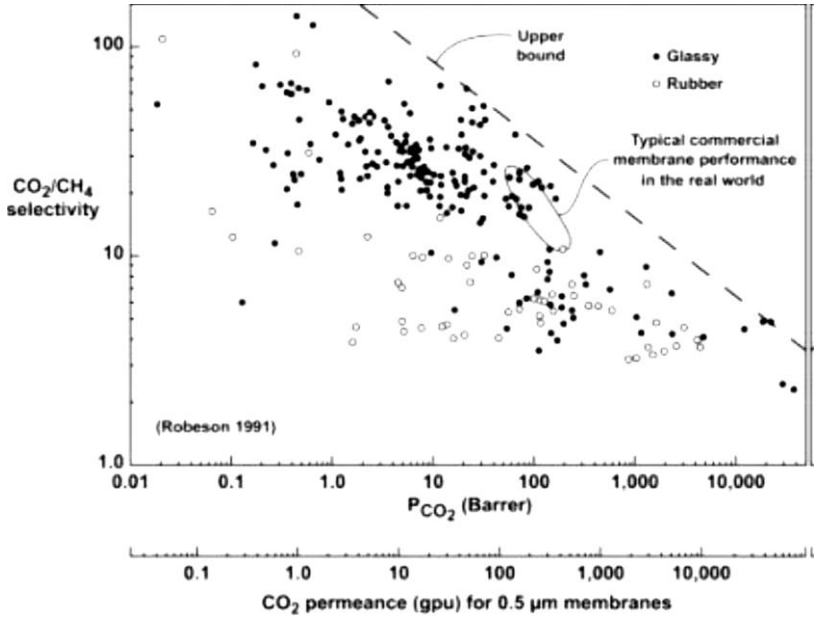

Figure 1.1 Robeson upper bound trade off [9]

At this study, glassy polymers with different properties are blended in order to see the effect of blending on gas separation performance. At the beginning of this study, Polycarbonate/Polyethersulfone (PES), Poly (vinyl alcohol)/Polyethersulfone, and Poly (vinyl acetate)/Polyethersulfone blends were prepared However, because of the incompatibility of these polymers with PES, we were unable to prepare homogeneous and usable membranes. Therefore, we continued with literature survey and came up with Matrimid ® 5218 (a type of polyimide, abbreviated as PI), a superior polymeric material for gas separation membranes.

Since only PES/PI pair produces homogeneous, workable membranes, rest of the study focused on membranes based on PES/PI blends. Based on this polymer pair, the effect of blending composition, structure of the blend membrane (dense vs. asymmetric), and ZIF-8 addition to a dense polymer blend on the gas separation performance of PES/PI and PES/PI/ZIF-8 membranes were investigated.

CHAPTER 2

LITERATURE RESEARCH

2.1. Polymeric gas separation membranes

First gas separation membranes were used by Monsanto for H_2 recovery system in 1977. First CO_2 separation membrane was cellulose acetate based. However, plasticization of cellulose acetate membranes under harsh flue gas conditions urged the researchers to investigate new membranes with better permeability, selectivity, and mechanical and thermal durability. There has been using numerous polymeric membranes with reasonable gas separation performances, such as polyamides, polycarbonate, polysulfones, and polyimides. [7]

One of the major problems of polymeric membranes is the trade-off between permeability and selectivity. It was reported by Robeson that rubbery polymers have very high permeability values because of the loose chain packing; therefore, they are suffering from lack of selectivity. On the other hand, glassy polymers have considerably high selectivity values and low permeability values, but in order to be feasible for industrial applications, membrane area should be very large [9]. However, superior gas separation performance is not the only important aspect for polymeric membrane to be industrially attractive. Mechanical and thermal stabilities are also important aspect in industrial gas separation [7]. According to the patent application study conducted by Ekiner revealed that percent elongation of ternary

blend of PES, aromatic polyimide and alkyl substituted aromatic polyimide is higher than pristine polymers' [14].

Another major problem of polymeric membranes is the CO_2 plasticization at high temperature pressure processes. CO_2 molecules cause to increase the free volume within the polymer matrix and make the membrane looser as they diffuse through the membrane. This bring about increase in permeation and decrease in selectivity, especially in CO_2/CH_4 separation processes [1,15,16]. In order to overcome or at least enhance the resistance against plasticization three possible solutions has been suggested, which are polymer blending, crosslinking and thermal treatment [8,16,17].

2.2. Advancements in polymeric membranes

Polymeric membrane technology for gas separation processes has been being studied extensively because of the advantages as easy processability, low cost of preparation and operation, aside from the disadvantages as low chemical and thermal stability, unsatisfying gas separation performance for industrial applications, and plasticization at certain operation conditions [1,2]. In order to improve the gas separation performance and overcome the problems several methods have been proposed such as polymer blending, copolymerization and grafting of backbone, sulfonation, hollow-fiber spinning, crosslinking and thermal treatment, and combination with inorganic fillers, i.e. mixed matrix membranes [1].

2.2.1. Mixed matrix membranes

Mixed matrix membranes were designed by dispersing filler materials in the polymer matrix in order to overcome the problems of both inorganic and polymeric

membranes and to create the synergistic effect of increasing of both permeability and selectivity [2]. Zeolites, carbon molecular sieves, and metal organic frameworks are the most used fillers in the mixed matrix membranes [18,19]. However, due to the limitations as poor polymer-filler bonding, filler segregation, or pore blocking, zeolites, carbon molecular sieves or silicas were not much preferred to use in the industrial membranes as MMM fillers. Zeolites are one of the most preferred filler material among them, even though severe interfacial non-selective void formation and aggregation. Several methods have been suggested to overcome these problems of zeolite based MMMs, such as priming, silanation, chemical treatment, low molecular weight additives, thermal treatment, copolymerization and crosslinking [16,20,21]. Recently discovered metal organic frameworks are the most attention gathering fillers thanks to their high surface and pore volume, tunable pore size and structure, and compatibility with organic materials [22,23]. MOFs are crystalline materials where metal ions are connected to each other with organic linkers. The gas permeation mechanism of the MOFs is based on the adsorption of the gas molecules on the MOF surface requiring physical or chemical interaction, and sieving according to the molecular size. It is possible to tailor the MOF materials by changing the organic linker types to reach the desired cage opening or affinity to certain gases. Zeolitic imidazolate frameworks are one of the subclasses of MOFs. They have sodalite like structures with certain affinity to small sized gases. ZIF-8 has a pore size of 3.4 Å, which makes ZIF-8 a very good sieving material for H_2/CH_4 and CO_2/CH_4 separation [24]. ZIF-8 is synthesized in methanol medium where $Zn(NO_3)_2$ used as a metal donor and HMIM as organic linker [25].

2.2.2. Polymer blends gas separation membranes

Robeson described several upper bounds for different gas pairs by considering permeability and selectivity performances of numerous polymeric membranes used in gas separation industry. For example, it can be clearly seen from the Figure 1.1 that

the CO_2/CH_4 separation performances of the most of the polymeric membranes are below the upper bound [12]. Therefore, most of the recent research is aimed to develop composite materials that reach or go further than the upper bound.

According to the upper bound described by Robeson, while membranes of glassy polymers show better selectivity performances, membranes of rubbery polymers show better permeation performances [2]. In the light of these results, research are focused on producing a highly perm-selective membranes by combining glassy and rubbery polymers [26]. The reason of blending is to come up with membranes that have the high permeability characteristic of rubbery polymers and high selectivity of glassy polymers. However, not all polymers are compatible with each other [27]. Polymer blends are categorized by miscible, i.e. completely dissolved in each other in molecular level, and phase-separated, i.e. partially or not dissolved, blends by Robeson [8]. There are several methods have been used to blend the polymers, e.g. melt mixing [28] and solution mixing [8,29].

2.2.2.1. Dense Polymer Blend Membranes

Kapantaidakis and his research group have been studying the gas permeation of dense PSF/PI membranes. Dense PSF/PI membranes were prepared by solvent evaporation method using methylene chloride as a solvent in three different proportions as 1:4, 1:1, and 4:1. Single gas permeation experiments were done in variable volume setup with upstream pressure of 1-45 atm and downstream pressure of atmospheric conditions. Gas separation experiments were carried out for He, H_2, O_2, CO_2 and N_2. Membranes performed monotonous increase in permeability of gases except H_2 and CO_2 as the ratio of the PI in the blend decreased. The pure PI membranes had the highest H_2 permeability values. The permeability of CO_2 of all blend membranes were below that of the pure polymers and showing an inflection point, because of the CO_2 plasticization under that experimental conditions. The CO_2

permeation experiments were conducted at different pressures to determine the plasticization pressure of each membrane at 40°C. The results showed that PSF membranes have the highest resistance and PI membranes have the lowest resistance to CO_2 plasticization. The plasticization pressures of the blend membranes were in between the pure polymers and adding PSF into the PI matrix significantly increased the resistance. The CO_2/N_2 selectivity of the blend membranes fell below the predicted values because of the decrease in the CO_2 permeability. The selectivity of O_2 over N_2 did not affected by the blending and H_2/CO_2 selectivity increased compared to the pure polymers. In case of O_2/N_2 selectivity, the effect of blending was insignificant. There was the inflection points observed at 50/50 wt% blend ratios for selectivity for the all gas pairs investigated [30].

Hosseini, Teoh and Chung blended Matrimid ® 5218 and PBI with compositions of (w/w) 25/75, 50/50 and 75/25. In order to prove the miscibility of these polymer blends, DSC analysis were conducted. Single glass transition temperatures in the results confirmed these two polymer are miscible with each other. Gas permeation test were conducted at 35°C, and 3.5 atm for H_2 and 10 atm for other gases based on variable pressure-constant volume method. According to the gas permeation test, the permeabilities of all gases were decreasing with increasing PBI concentration. As expected, the selectivities were increasing with increase in PBI concentration. Surprisingly, H_2/N_2 and H_2/CO_2 selectivities of Matrimid/PBI 25/75 membranes were higher than the pure polymer membranes [31].

Another study on PES/PI blend membranes was done by Ekiner for a patent application [14]. He investigated the mechanical properties and O_2/N_2 separation performances of both binary and ternary blend membranes. First, PES: aromatic polyimide binary blend dense membranes were prepared. In the resulting scans of DSC of these membranes, only one phase transition temperature in between the pristine polymers T_g's occurred on the first scan proving that these polymers are compatible. However, on the second scan two different temperatures observed showing a phase separation between polymers when membranes are annealed above

T_g. The gas separation tests were conducted with a mixture of O_2 and N_2 (21/79) at 30°C. O_2 permeability was found as 1.12 Barrers and O2/N2 selectivity as 6.4. Researcher further investigated the ternary blends of PES: aromatic polyimide: alkyl substituted aromatic polyimide membranes. According to the results, pure alkyl substituted aromatic polyimide has the highest O_2 permeability, while aromatic polyimide has the highest selectivity. Pure PES membranes have the lowest permeability, while ternary blend with 80:10:10 composition has the lowest selectivity values. The permeability and selectivity values of the blend membranes were increased as the amount of PES in the blend decreased [14].

2.2.2.2. Asymmetric Polymer Blend Membranes

The theory of the asymmetric membrane preparation is based on exchange of the solvent with non-solvent. During exchange process, as the solvent diffused out of the polymer matrix, non-solvent penetrated into the matrix, causing polymer to precipitate with formation of an asymmetric structure with porous substructure. Skin layer formation depends on the interactions between polymer-solvent and polymer-non-solvent. The reason of addition solvent into the coagulation bath is to delay the demixing and obtain an asymmetric membranes with thicker skin layer [32].

Han et.al. were studied the compatibility and thermal stability of PES and Matrimid® 5218 and their blends [33]. Membranes are produced by dry/wet phase inversion with w/w blending ratios of PES/MI 90/10, 80/20, 70/30, 60/40, 50/50, 40/60, 30/70 20/80 and 10/90 as weight percent. NMP and DMF has been used as solvents, and ultra-purified water has been used as a non-solvent. According to the SEM micrographs of the cross-sections, the blend membranes with 90/10, 80/20, 70/30 and 10/90 PES/MI ratios have finger-like macro pores, while other blend membranes have sponge-like pore structures. Formation of sponge-like pore implies that the interpenetration of the non-solvent into the polymer matrix is slow, because

of strong polymer-polymer interactions. The skin layers of the finger-like polymer membranes are changing between 5 to 10 microns, while sponge-like membranes have approximately 0.7 micron skin layer thickness. There is no evidence of incompatibility between these two polymers has been observed in the SEM micrographs. Since the finger-like macro pores cause to increase in the gas permeability and decrease in the selectivity, the gas permeation tests of the membranes with finger-like pores are not conducted. Gas permeation experiments of H_2, N_2 and O_2 gases were conducted at different feed pressures. The results showed that as the feed pressure increased permeances of all gases were increased, while the selectivities of O_2/N_2 and H_2/N_2 decreased [33].

Another interesting study on polymer blend gas separation membranes were done with Matrimid® and Polybenzimidazole (PBI). The membranes was dual-layer hollow fibers where the inner support was made of PSf. Research group was studied the effects of air gap, dope liquid composition, rate of elongational drawing, and chemical modification on gas separation performances of the membranes. The drawing the fibers in elongational direction after coagulation bath affected the gas separation performance positively. The permeability of the drawn membranes for H_2 and CO_2 gases increased, while he CH_4 permeability decreased. Owing to this method, it is possible to produce membranes with considerably high CO_2/CH_4 selectivities. According to the SEM micrographs, PSf support layer had finger-like large pores, while the outer M/PBI blend layer had sponge-like porous structure. There was no evidence of debonding or incompatibility in between inner and outer layers [34].

In another study on polymer blend gas separation membranes were done by using Matrimid® 9725 (M) and polysulfone (PSf) [15]. The membranes were prepared by dry/wet phase inversion method with the w/w ratios of M/PSf 1/3, 1/1, and 3/1. Binary gas mixture separation performance of the membranes was measured at 35°C and 10 bar for different CO_2/CH_4 compositions. The pure Matrimid membranes showed the highest and pure PSf membranes showed the lowest selectivity and

permeance performances among the membranes studied within this work. As the CO_2 concentration increased in the feed mixture, the selectivities off all membranes decreased. The gas separation performance of the pure Matrimid membranes were affected the most by the increase of CO_2 concentration in the feed mixture, so that values decreased to the half. On the other hand, blend membranes were affected least by the concentration change of CO_2 in feed stream indicating that blending Matrimid with PSf increases the membrane stability at the high CO_2 concentration processes. Basu et al., also investigated the effect of feed temperature on the binary gas separation process for two different feed compositions, which are 10/90 vol% and 75/25 vol% at 10 bar. Permeation characteristics of pure Matrimid membrane was affected the most from the temperature change among the studied membranes. The results, where the feed contained 75/25 vol% CO_2, showed that selectivity of the membranes decreased with the increase in temperature from 35°C to 95°C due to the increase in the permeation of the membranes, as expected. The CO_2 permeance increased up to 65°C due to the increasing kinetic energy of the gas molecules and chain mobility. However, when temperature were increased even more, the CO_2 permeance decreased sharply which may be due to the chain relaxation causing to decrease of free volume. The results of the experiments that the feed composition was set to 10/90 vol% CO_2 showed that as the temperature increased, the permeance of CO_2 and CH_4 increased, especially in case of pure Matrimid membranes. On the other hand, blend membranes showed steady and smaller change as a function of increasing temperature. The effect of feed pressure on the membranes were also studied at 4, 8, 10, 12, 13, and 14 bar with feed composition of 75/25 vol% CO_2/CH_4. The selectivity of CO_2 over CH_4 increased with increasing feed pressure. However, in case of pure Matrimid, the selectivity suddenly decreased after 12 bar, because of the CO_2 plasticization of Matrimid membranes. Having the stable gas permeance and selectivity values at high pressures, blending of Matrimid can be offered to overcome the CO_2 plasticization [15].

Another research conducted by Kapantaidakis and his group was on the gas separation performance of PES/PI blend hollow fiber membranes with three different

w/w blending ratios (20/80, 50/50 and 80/20). The hollow fiber membranes were prepared by dry/wet phase inversion method with NMP as solvent and water as non-solvent. In addition, the effect of PDMS coating on gas separation performance was investigated. Single gas permeations of N_2 and CO_2 were measured in a lab-scale system by employing constant volume variable pressure method. Glass transition temperatures of the blend membranes were in between the pure polymers and matching with the Taylor-Gordon equation when the k is 1 [29]. CO_2 and N_2 gas permeance of the uncoated PES/PI 80/20 membranes increased as the air gap distance increased from 1 to 10 cm, since the increasing air gap distance may cause prolonging of the coagulation time and production of a membrane structure with higher free volume. The CO_2 and N_2 permeance of uncoated PES/PI 20/80 were much higher than other membranes, especially in case of N_2, revealing that high PI containing blends have more porous skin layer and looser structure. The CO_2/N_2 selectivity of the uncoated membranes decreased from 2.2 to 1.3 as the air gap distance increased from 6 to 31 cm. On the other hand, the CO_2/N_2 selectivity of the coated membranes remained similar to PES/PI 80/20 and 50/50 membranes. The hollow fiber membrane with high PI concentration in the blend showed higher gas permeance as expected, because PI is more permeable polymer than PES. As a result, the gas separation performances of the PES/PI blend membranes were better than the commercial CO_2 separation membranes and a good candidate to study and improve further [35].

A study carried out by Rafiq et al. (2011) on blending of PSf and Matrimid 5218 [36]. PSf and PI were blended in five w/w compositions (100/0, 95/5, 90/10, 85/5 and 80/20) in different NMP/DMF mixtures. They prepared PSf/PI membranes by dry wet phase inversion method using ethanol as non-solvent. They analyzed the thermal character of the membranes and reported that both glass transition and decomposition temperatures were increased as the PI content in the blend increases. The group were investigated the effect of feed pressure and solvent mixture on gas separation performance of PSf/PI blend membranes. As the feed pressure increased, not only CO_2, but also CH_4 permeance was decreased. Permeance values of the

membranes increased as amount of PI in the blend increased, which is expected because of higher free volume of the PI. The ideal selectivity of CO_2 over CH_4 was also increased as the PI content increased. However, as the feed pressure increased, the ideal selectivities were decreased and membranes prepared in NMP/DMF 80/20 mixture appeared as the least affected from the feed pressure [36].

Ekiner also investigated the gas separation performance of asymmetric hollow fiber PES: aromatic polyimide and PES: aromatic polyimide: alkyl substituted aromatic polyimide blend membranes. The gas permeation tests were conducted under 100psig bore feed pressure and 21°C for 21/79 O_2/N_2 mixture. According to the results, highest O_2 permeance values were obtained from 50:50 wt% and 50:25:25 wt% membranes. On the other hand, highest O_2/N_2 selective membrane was 10:10:80 wt. % membrane, which is expected [14].

2.2.3. Polymer blend based mixed matrix membranes

The addition of nanoparticles into the polymer blend matrix is one of the newest research areas of membrane technology. Nonselective void formation because of poor adhesion of the nanoparticles in the polymer matrix is one of the major problems of mixed matrix membranes. Usage of polymer blends instead of single polymer is suggested to improve adhesion [37].

2.2.3.1. Dense Polymer Blend Based Mixed Matrix Membranes

The polymer blend mixed matrix membranes based on polysulfone and polyimide as base polymers and ZSM-5 as filler was studied [37]. Membranes were prepared by solution casting method with DCM (dichloromethane) as solvent. Polymer blend compositions of 0/100, 30/70, 50/50, 70/30, and 100/0 membranes were prepared

without and with ZSM-5 to be able the see the effect of ZSM-5 addition on the gas separation performance. The gas permeation of the membranes were tested in a constant volume system with feed pressure changing between 2 to 5 bar and 35°C for O_2, N_2, CO_2, and CH_4. According to the results of the gas permeation tests, the gas permeability of the membranes decreased and the selectivities increased as the concentration of the PI in the blend increased. PES/PI 50/50 membranes had the highest O_2/N_2 and CO_2/CH_4 selectivities among the blend membranes. The addition of the ZSM-5 particles to the polymer matrix caused to increase the gas permeabilities significantly, and thus decreased the selectivities. The reason of this increment is the nonselective void formed between the particles and polymers [37].

Another study on polymer blend based mixed matrix membranes was conducted by Ismail et.al [38]. They added Zeolite 4A into the blend of 50/50 PES and Matrimid ® 5218 and investigated the gas separation performances. Membranes were produced according to the solvent evaporation method where the solvent was NMP. Gas separation performances of the membranes were investigated in terms of O_2 and N_2 separation. O_2 and N_2 gas permeations were increased as the zeolite loading increased. However, O_2/N_2 selectivity of membranes were very low [38].

2.2.3.2. Asymmetric Polymer Blend Based Mixed Matrix Membranes

Basu et al. also studied the effect of PSf addition with the ratio of PI/PSF 3/1 to PI/[$Cu(BTC)_2$] asymmetric, mixed matrix membranes. [$Cu(BTC)_2$] is a metal organic framework with high gas absorptivity. Membranes were containing 20 wt.% polymer and 10, 20, and 30 wt% MOF. There was no evidence of phase separation between PI and PSf occurred in the SEM micrographs. The selectivity of CO_2/CH_4 and CO_2/N_2 of the PI/PSF 3/1 membranes were lower than the pure PI and PI/MOF membranes and decreased as the CO_2 content in the feed increased. The addition of

filler didn't affect much on the selectivities of the PI/PSf blend membranes also [39].

Another study on this topic was conducted with addition of silica nanoparticles to PSF/PI matrix [40]. PI content in PSF matrix was fixed to 20wt% and silica content was set as 5.2, 10.1, 15.2, and 20.1wt%. According to the SEM images, a sponge-like layer was supporting a relatively denser skin layer. Silica particles were homogeneously distributed through the membrane, except 20.1 wt%. At that much of loading, particles had been started to agglomerate and cause interfacial voids. Glass transition and decomposition temperatures of the membranes increased as the silica content increased. Both CO_2 and CH_4 permeances increased gradually as the amount of silica in the membrane increased. The permeances of the membranes tend to decrease upon increase of feed pressure, due to plasticization of the membranes. Therefore, membranes were heat treated at 120°C for 1h. After heat treatment, the permeances of the membranes decreased because of reduction of interfacial voids between silica particle and polymer matrix. In addition, heat treatment enhanced the selectivity of the membranes [40].

As a brief summary of the literature so far, most of the studies were focused on O_2/N_2 separation. The major outcome from these studies was indicating that the addition of zeolites to polymer blends might increase the O_2 permeability of the membranes, but decrease the O_2/N_2 selectivity. Another possible inference is that asymmetric membranes allow more gas to permeate through because of their porous structure, as expected.

Table 2.1 Gas Separation Performance of Blend and Blend Based Mixed Matrix Membranes

Ref.	Polymers (+ Additive)	Prep. Method and Test Cond.	Nanopart. wt%	O_2 (Barrer)	N_2 (Barrer)	O_2/N_2 Select.
Ismail et al. [38]	PES/PI 50/50 Zeolite 4A	Dense memb., 1 bar, T_{room}	10	9.4	13.06	0.72
			30	12.8	15.06	0.85
Ekiner [14]	PES/PI 50/50	Dense memb., 30°C	0	1.12	0.18	6.40
Dorosti et al. [37]	PI/PSf 50/50 ZSM-5	Dense memb., 2 bar, 35°C	0	0.86	0.27	3.16
			10	0.87	0.29	3.02
			20	1.16	0.50	2.30
Kapantaidakis et al. [30]	PSf/PI 50/50	Dense memb., 10 atm, 40°C	0	0.88	0.18	5.00

CHAPTER 3

EXPERIMENTAL METHODOLOGY

3.1. Preparation of PES/PI and PES/PI/ZIF-8 Membranes

3.1.1. Materials of PES/PI and PES/PI/ZIF-8 Membranes

Radel A-100 grade Polyethersulfone was provided by Solvay. The glass transition temperature, density, and molecular weight are 220°C, 1.37 g/m3 and 53,000 g/mol, respectively. Matrimid ® 5218 polyimide resin, of which T_g, density and molecular weight are 300°C, 1.2 g/cm3, and 80,000 g/mol, was purchased from Alfa Aesar. Polymers were dried in the oven at 80°C at least for 1 night prior to use for removal of any absorbed vapor. N,N-Dimethylformamide (DMF), purchased from Sigma-Aldrich, was chosen as the solvent and used as received. IPA is purchased from Sigma-Aldrich and used as received as non-solvent.

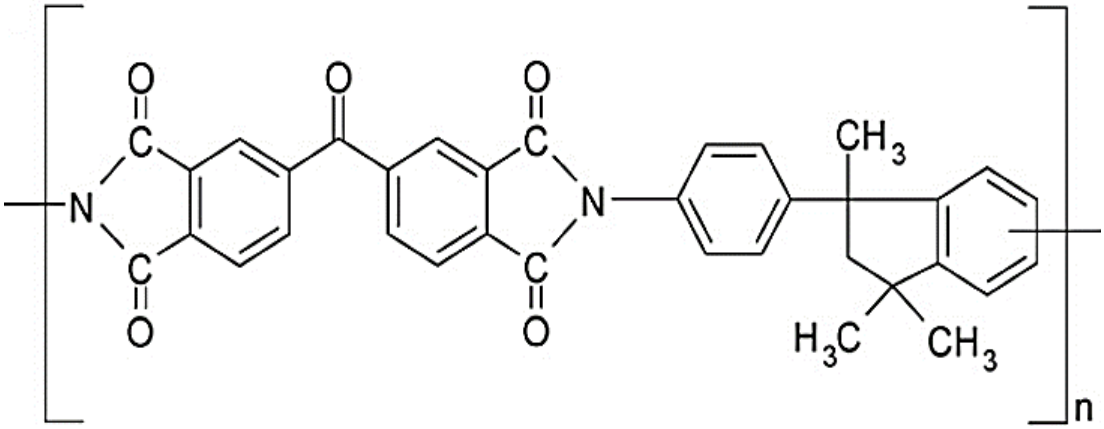

Figure 3.1. Open Formula of Polyimide [33]

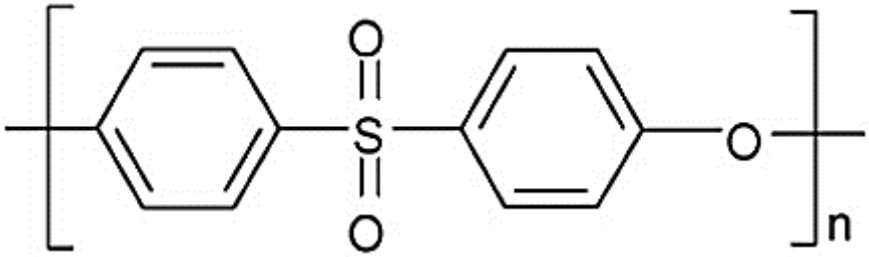

Figure 3.2 Open Formula of PES [33]

3.1.2. Materials and Preparation Method of ZIF-8

Zinc nitrate hexahydrate (Zn $(NO_3)_2.6H_2O$) is purchased from Across, 2-methyl imidazole and methanol were bought from Sigma-Aldrich to synthesize ZIF-8.

ZIF-8 crystals were synthesized as explained in Keser Demir et. al. [25]. In one beaker, 4.8 g zinc nitrate hexahydrate were dissolved in 180.8 g methanol. In another beaker, 10.6 g 2-methyl imidazole were dissolved in 180.8 g methanol. After a short while of stirring, both solutions became clear and zinc nitrate hexahydrate-methanol solution was poured in the 2-methyl imidazole solution. The mixture of these solutions started to whiten immediately indicating that reaction between zinc nitrate hexahydrate and 2-methyl imidazole had started. The reaction mixture was stirred for 1 hr at 300 rpm in order to complete the ZIF-8 crystal formation. After one hour,

ZIF-8 crystals were precipitated in centrifuge. The crystals were washed with methanol twice to remove any remaining zinc nitrate hexahydrate or 2-methyl imidazole may clogged the pores of the ZIF-8 particles. ZIF-8 particles were activated at 180°C in an oven overnight before adding to the membrane preparation solution.

3.1.3. Membrane Preparation Methodology

3.1.2.1. Dense Membrane Preparation

All compositions of the PES/PI and PES/PI/ZIF-8 membranes were prepared according to the previously described thin film dense membrane preparation method [6,41]. Polymer blend membranes were prepared by dissolution of the polymers one by one in the DMF by priming. For example, during the preparation of the PES/PI 60/40 membranes, first, 1.2 g PES was dissolved in 10 mL DMF by priming, and stirred overnight. Next day, 0.8 g PI was added into the PES-DMF solution, again by priming, and stirred overnight. Polymer solution was ultrasonicated between each polymer addition in order to enhance the interaction between polymer-solvent and polymer-polymer, therefore the homogeneity. Membrane solution was casted into a thin film on the third day and placed into an oven at 80°C, 0.2 bar N_2 atmosphere for 8 hours in order to remove the solvent. After removal of the solvent, film was removed from the glass, placed on metal holders and put in the oven at 180°C with 0.8 bar N_2 atmosphere for 1 week in order to remove any remaining solvent and anneal the membrane. Membrane thicknesses were measured with micrometer.

Preparation of polymer blend based mixed matrix membranes is similar, but ZIF-8 crystals were added to DMF a day before addition of polymers and stirred at room temperature overnight. ZIF-8 addition was done by priming with 30 min ultrasonication between each addition in order to prevent from agglomeration of the

crystals. Polymer addition to the ZIF-8-DMF mixture was done as explained above. The thickness of the polymer blend based mixed matrix membranes were measured with micrometer.

The recipe of the blend membranes and polymer blend based mixed matrix membranes was given in the Table 3.1 and Table 3.2, respectively.

Table 3.1 The recipe of the polymer blend membranes

PES wt%	PES (g)	PI wt%	PI (g)	Total Amount of Solid (g)	Amount of DMF (mL)	Membrane Code
0	0.00	100	2.00	2.00	10	Pure PI
5	0.10	95	1.90	2.00	10	PES/PI 5/95
10	0.20	90	1.80	2.00	10	PES/PI 10/90
20	0.40	80	1.60	2.00	10	PES/PI 20/80
25	0.50	75	1.50	2.00	10	PES/PI 25/75
40	0.80	60	1.20	2.00	10	PES/PI 40/60
50	1.00	50	1.00	2.00	10	PES/PI 50/50
60	1.20	40	0.80	2.00	10	PES/PI 60/40
75	1.50	25	0.50	2.00	10	PES/PI 75/25
90	1.80	10	0.20	2.00	10	PES/PI 90/10
95	1.90	5	0.10	2.00	10	PES/PI 95/5
100	2.00	0	0.00	2.00	10	Pure PES

Table 3.2 The recipe of the polymer blend based mixed matrix membranes

PES wt%	PES (g)	PI wt%	PI (g)	ZIF-8 wt%	ZIF-8 (g)	Total Amount of Solid (g)	Amount of DMF (mL)	Membrane Code
20	0.40	80	1.60	10	0.20	2.20	10	PES/PI/ZIF-8 20/80/10

3.1.2.2. Asymmetric Membrane Preparation

Asymmetric membranes were prepared only for PES/PI 20/80 blend composition. The preparation steps of the asymmetric membranes were same with dense membrane preparation method up to solvent removal part. During preparation of asymmetric membranes, glass plate with polymer casted on it, was placed into the coagulation bath, which is composed of 375 mL (75 vol %) IPA and 125mL (25 vol %) DMF. The coagulation of the polymer film on the glass plate completed in approximately 15 min. A completely precipitated film was removed from the coagulation bath and soaked into a distilled water bath for overnight in order to remove of the IPA and DMF from the pores of the membrane. After water bath, membrane was removed and gently wiped with paper towel before be placed into the vacuum oven for drying. Asymmetric membrane was placed on the metal holders and remaining water entrapped in the porous layer of the membrane was removed at 120°C, under vacuum for 24 hr. Next day, the temperature of the oven was increased to 180°C and membrane was heat treated for 48 hr.

3.2. Characterization of Blend and Mixed Matrix Membranes and ZIF-8 Crystals

3.2.1. TGA

Thermal character and the amount of solvent entrapped in the membranes were determined by Shimadzu DTG-60H TGA analysis device. A piece of membrane was heated from room temperature to 650°C with heating rate of 10°C/min. under N_2 atmosphere.

3.2.2. DSC

Differential scanning calorimeter analysis were conducted with Shimadzu DSC-60 to determine the glass transition temperature of the blend and mixed matrix membranes. Approximately 4 mg of membrane piece was placed in the chamber and heated up to 350°C with the heating rate of 20°C/min under N_2 atmosphere and analyses were conducted as double run.

3.2.3. SEM

The morphology of both polymer blend and mixed matrix membranes were visualized by scanning electron microscopy in METU Central Laboratory with QUANTA 400F Field Emission series scanning device. A small piece of membrane were dipped in liquid nitrogen and fractured by using tweezers. The aim of dipping membranes in liquid nitrogen is to immobilize the atoms and keep the structure still.

3.2.4. XRD

The patterns of the X-ray diffractometer analysis of the ZIF-8 particles were compared with the pattern given in the literature. The area under the characteristic peaks of the ZIF-8, of which belongs the planes of (011), (002), (112), (022), (013), (222), (114), and (134), is used to determine the percent crystallinity of the particles [42]. XRD analyses were conducted at the Philips PW 1729 X-Ray Diffractometer, with Cu-Kα tube at 30 kV voltage and 24 mA current, and 0.05 % scan rate for Bragg angles between 5-40°.

3.3. Gas permeation Measurements of Membranes

Gas permeation experiments were carried on a system designed based on constant volume-variable pressure method and used previously [6]. The diagram of the test set-up is given in the Figure 3.3., made-up of a gas tank, a pressure gauge, a membrane cell, a pressure transducer, a computer, a heating tape and temperature controller, and vacuum pump. Feed gas tank was made up of seamless stainless steel to be enduring for high pressures. The pressure of the feed gas tank was measured with an electronic pressure gauge. All the piping and fittings were ¼" stainless steel, bought from Swagelok and Hoke. The stainless steel membrane cell was purchased from Millipore (part no. XX45047 00) with effective membrane area of 9.6 cm^2. Two Viton O-Rings were placed on the cell to prevent any gas leakage during experiments. One of the O-rings were worn out, therefore it replaced with an original spare. The pressure change on the permeate side were measured with MKS Baratron pressure transducer (0-1000 Torr, ± 0.1 Torr) and recorded on the computer. The two-stage Edwards vacuum pump was used to evacuate the set-up. The temperature of the set-up was regulated with a heating tape and controlled with J-type thermocouple and PID controller.

Gas permeation tests were carried under 3 bar absolute pressure and 35°C. Primarily, a piece of membrane with 9.6 cm^2 area was cut and placed into the membrane cell and the set-up was evacuated for 1.5 hr in order to remove the atmospheric gas or remaining gas from the previous test. Then, feed tank was filled with penetrant gas up to absolute 3 bar and immediately allowed to fill the feed and permeate sides of the membrane cell. This pressure difference acts as driving force of this process. The increment on the permeate site was measured through pressure transducer and recorded to the computer. A sample calculation of the membrane's permeability was given in APPENDIX A. In order to show the reproducibility of the membranes, each formulation was casted at least three times and two pieces from each cast were tested

twice. Gas permeation experiments were conducted for H_2 (Linde, 99.99%), CO_2 (Linde, 99.9%) and CH_4 (Linde, 99.95%).

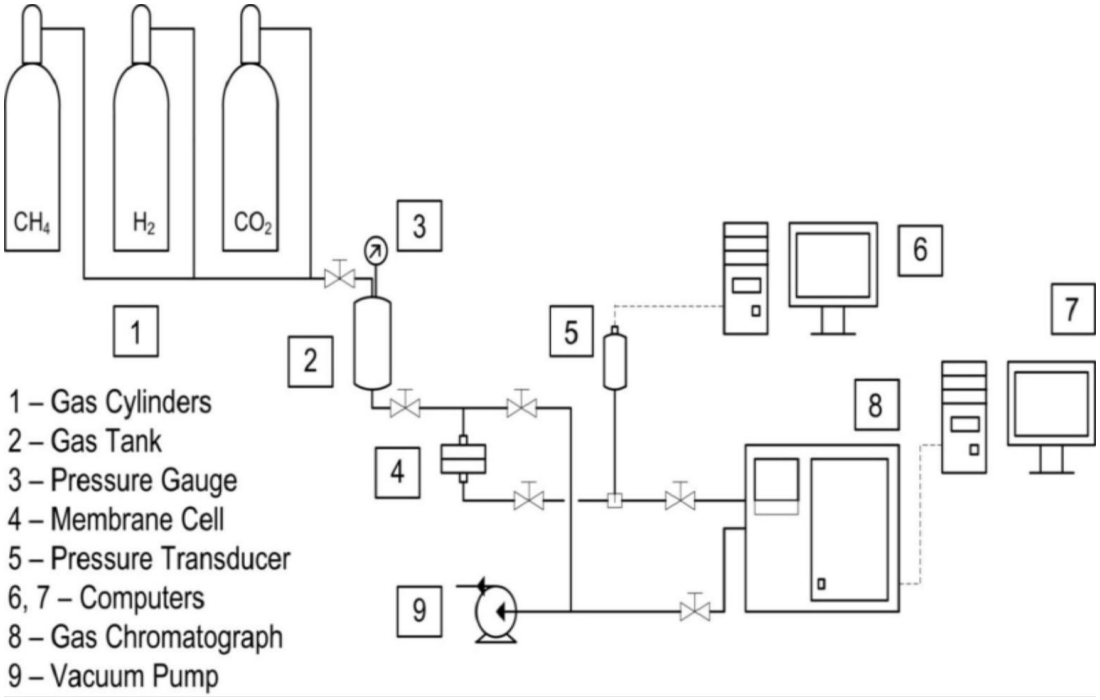

Figure 3.3 The Diagram of the Gas Permeation Test Set-Up [6]

CHAPTER 4

RESULTS AND DISCUSSION

4.1. Characterization of ZIF-8 Crystals

4.1.1. XRD

Synthesized ZIF-8 crystals were analyzed through X-Ray Diffractometer. After synthesis, crystals were dried in oven at 80°C overnight in order to remove the methanol. After drying crystals were crushed in the mortar and activated in the oven at 180°C overnight. In Figure 4.1, the peaks of two different synthesis of ZIF-8 are matching one by one with the reference peaks [25], showing that ZIF-8 crystals are successfully produced.

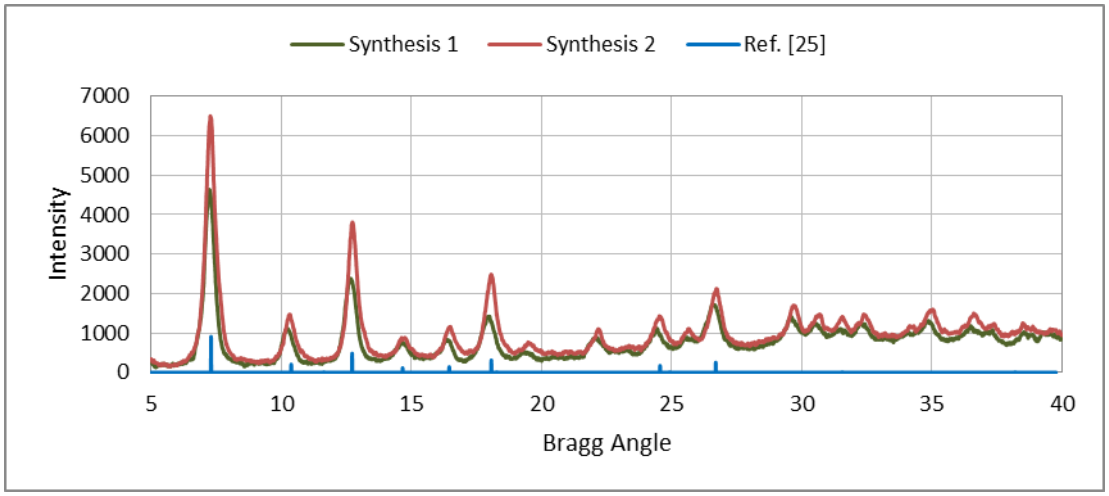

Figure 4.1 X-Ray Pattern of Synthesized ZIF-8 crystals

The calculation of percent crystallization is done through the areas under the characteristic peaks of ZIF-8. The reference area is assumed as 100% crystalline and relative percent crystallizations were calculated according to Equation 4.1.

$$\%Cryst. = \frac{Total\ Area\ of\ Synthesis \times 100}{Total\ Area\ of\ Reference\ Synthesis} \qquad \text{Equation 4.1}$$

The percent crystallizations of ZIF-8 particles of Synthesis 1 and 2 are calculated as 71% and 78%, respectively.

Table 4.1 Peak Areas and % Crystallizations

	Peak Areas		
Planes of Peaks	Reference [25]	Synthesis 1	Synthesis 2
(011)	2090	1410	1727
(002)	346	296	236
(112)	1120	860	1019
(022)	162	64	74
(013)	216	127	169
(222)	700	518	438
(114)	250	202	146
(134)	497	359	400
Total Peak Area	5381	3836	4209
%Crystallinity	100	71	78

4.1.2. SEM

In order to visually characterize and determine the particle size of the ZIF-8 particles SEM analysis is conducted. The SEM micrographs were given in Figure 4.2. The synthesized particles were fine, well dispersed, hexagonal in shape, and coherent with the literature [6]. The average size of the particles was calculated as 83 ±16 nm, which can be considered close to the expected size, 60 nm. The size of the particles is not only fine enough to be considered as nanoparticle, but also large enough to prevent agglomeration [41]. Observations and measurements were presented in APPENDIX B.

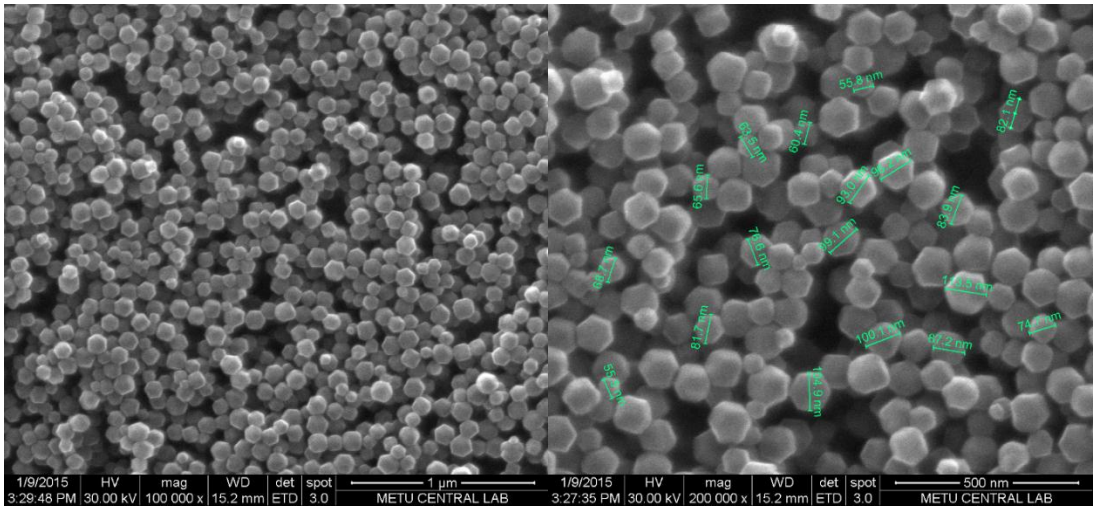

Figure 4.2 SEM micrographs of ZIF-8 particles

4.2. Characterization of PES/PI and PES/PI/ZIF-8 Membranes

4.2.1. TGA

Thermal gravimetric analyses were done to calculate the amount of remaining solvent entrapped in the membranes and decomposition temperature of the membranes in order to have an idea about thermal stability of the membranes. Thermogravimetric analysis is based on the rate of change in weight of the polymer at a constant rate of heating [43]. The detailed TGA results of Pure PES, Pure PI, PES/ZIF-8, PES/PI 20/80, and PES/PI/ZIF-8 20/80/10 membranes were presented in Table 4.2. All thermograms of conducted analyses were given in APPENDIX C.

Table 4.2 TGA Results of PES, PI, PES/PI 20/80, PES/ZIF-8, and PES/PI/ZIF-8 20/80/10 Membranes

Weight %		Membrane Type	Wt % ZIF-8	T_d (°C)	Weight Loss (%)
PES	PI				
0	100	Dense	0	514	40.89
20	80	Dense	0	513	40.1
			10	493	43.6
100	0	Dense	0	577	58.27
		Dense	10	511 [6]	60.86 [6]

TGA thermograms results of Pure PI, Pure PES, and PES/PI 20/80 dense membranes were given in Figure 4.3 and Figure 4.4. According to the Figure 4.3, major weight loss was after 450°C, which is coherent with the literature [33,44]. The decomposition temperatures of dense Pure PES membrane and Pure PI were found as 577°C and 514°C, respectively. These values are consistent with the literature [6,45] and indicating that PES is more thermally stable than PI. On the other hand, it can be

stated that PI is more thermally durable than PES based on the amounts of the weight losses given in Table 4.2 and Figure 4.3, because the weight loss of Pure PI membrane is significantly lower than Pure PES membrane.

The average decomposition temperatures of dense PES/PI 20/80 blend membranes were found as 513°C ass shown in Figure 4.4, which is close to the T_d of PI. The amount of lost weight of PES/PI 20/80 dense membranes is also very similar to Pure PI membrane, which is an indication of blend of PES and PI is as durable as Pure PI.

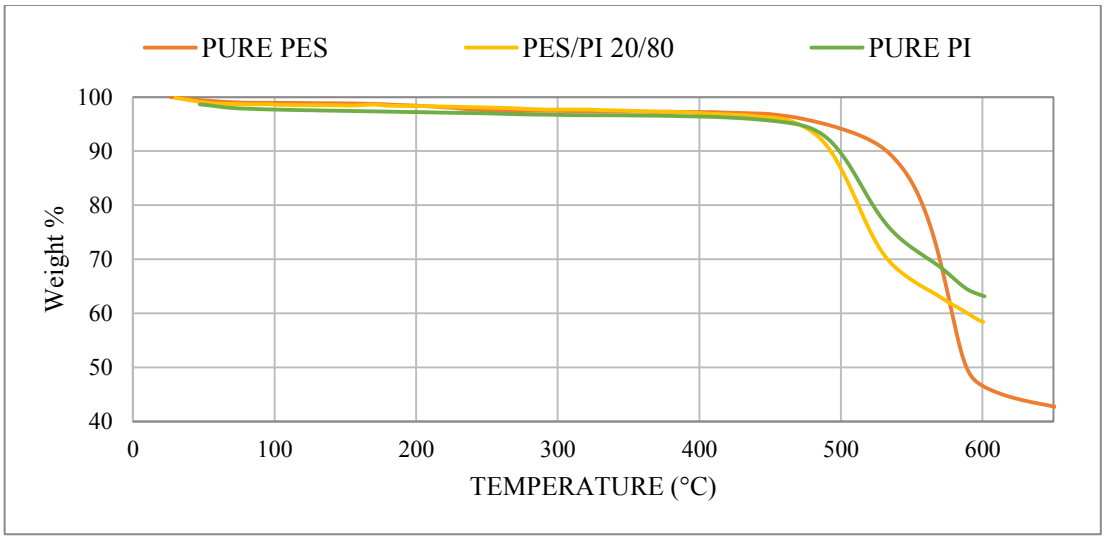

Figure 4.3 TGA Results of Pure PI, Pure PES, and PES/PI 20/80 Membranes

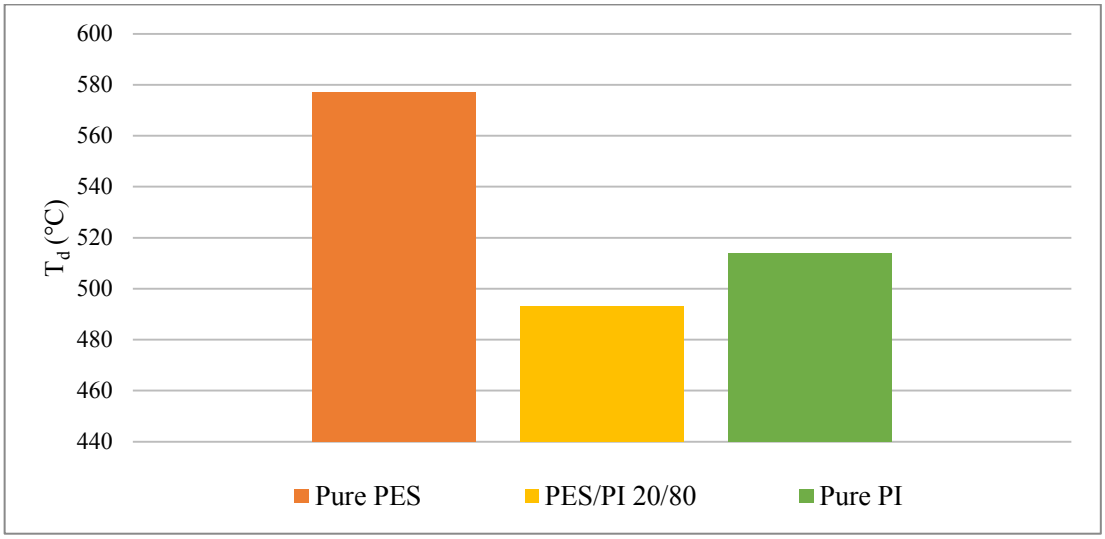

Figure 4.4 T_d of Pure PES, PES/PI 20/80 Dense and Pure PI Membranes

In Figure 4.5 and Figure 4.6, the TGA thermograms and decomposition temperatures of PES/PI 20/80 and PES/PI/ZIF-8 20/80/10 membranes were given. The addition of ZIF-8 to PES/PI matrix caused a significant decrease on T_d of the membranes. This fact is observed before also for PES/ZIF-8 membranes [6]. Lower decomposition temperature indicates less stable material upon high temperature processes. Moreover, the amount of weight lost to the polymer matrix increased with ZIF-8 addition, causing to decrease the durability of the membranes at high temperatures.

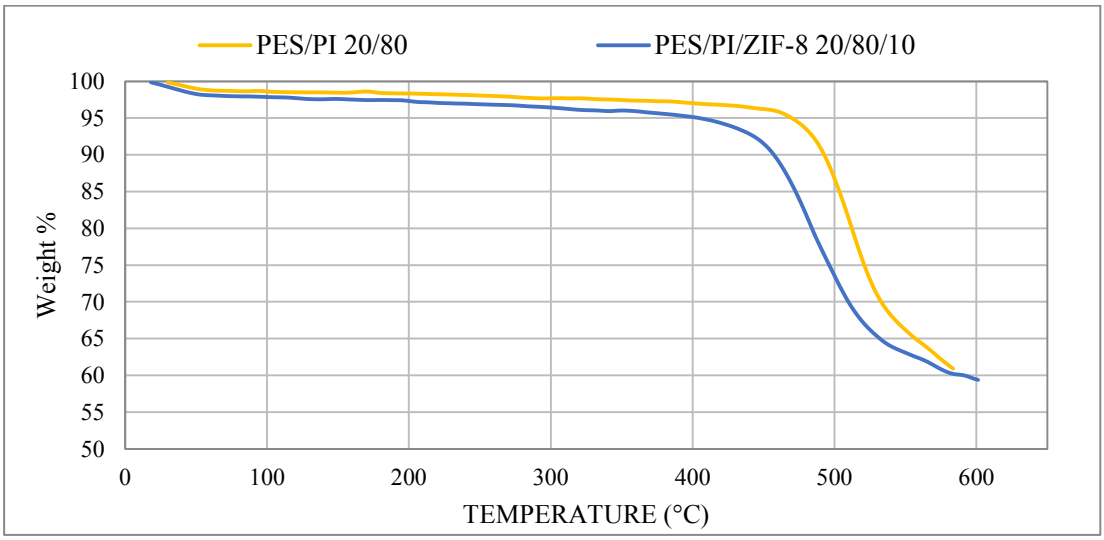

Figure 4.5 TGA Results of PES/PI 20/80 and PES/PI/ZIF-8 20/80/10 Membranes

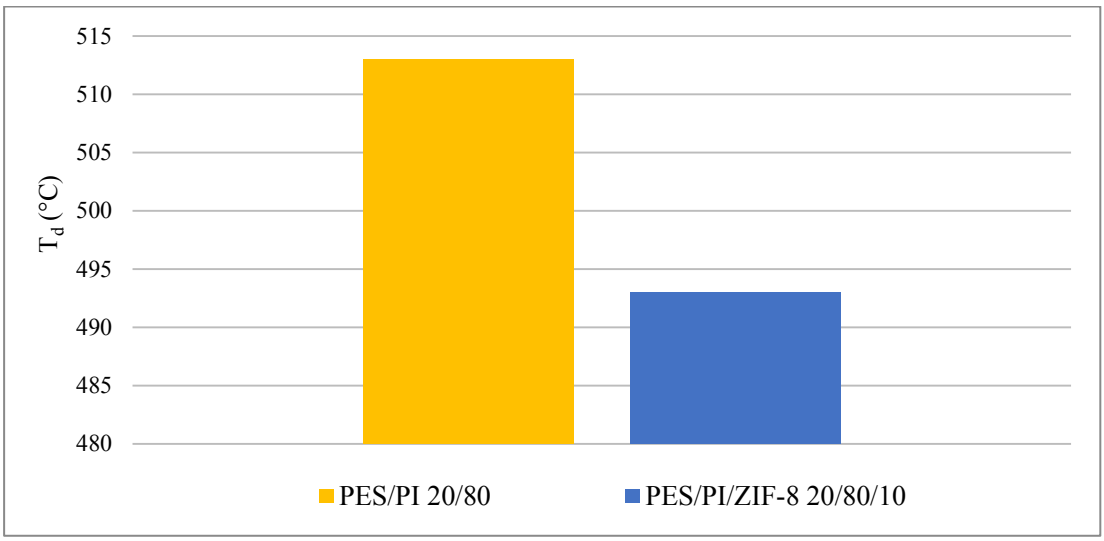

Figure 4.6 T_d of PES/PI 20/80 and PES/PI/ZIF-8 20/80/10 Membranes

Membrane preparation method does not cause a significant difference on decomposition temperatures, as presented in Figure 4.7 and Figure 4.8. The decomposition temperatures of the dense and asymmetric PES/PI 20/80 membranes were found similar, for dense 512.5 ±0.5°C and for asymmetric 517.4°C. Asymmetric membrane lost 37.3 g and dense blend membranes lost 40.1 ±1.3 g. The fact that, asymmetric blend membrane lost lesser amount of their weights compared to dense blend membranes means that asymmetric blend membranes are more durable than dense blend membranes.

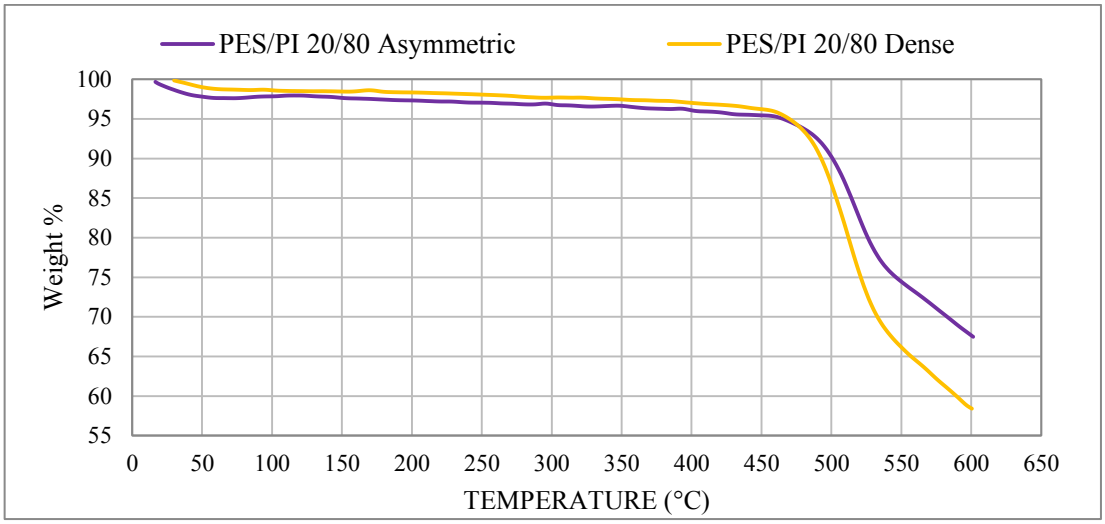

Figure 4.7 TGA Results of PES/PI 20/80 Dense and Asymmetric Membranes

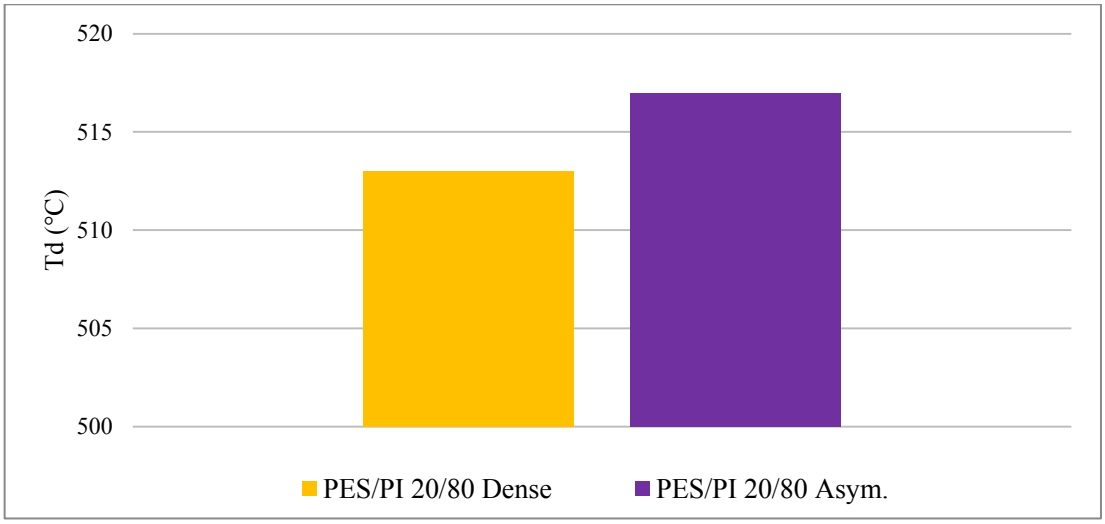

Figure 4.8 T_d of Dense and Asymmetric PES/PI 20/80 Membranes

4.2.2. DSC

Differential scanning calorimeter (DSC) is a well-known method to determine the miscibility of polymers. Observation of one phase transition indicates the miscibility and compatibility of two polymers, while more than one phase transitions indicate formation of different phases within the inner structure and immiscibility of the polymers.

Firstly, PES/PC wt/wt 1:1 and 1:2 blends were prepared according to method explained in 3.1.2.1. Phase separation between PES and PC was observed visually on both casting solutions and casted membranes. Resulting films were heterogeneous, which cannot be used as membranes. DSC scan analyses of these membranes were given in Figure 4.9 and Figure 4.10. DSC analysis results showed that these two polymers are not compatible. In Figure 4.9 and Figure 4.10, two different glass transition temperatures were observed at 148°C which belongs to T_g of pure PC, and 217°C which belongs to T_g of pure PES [27], proving these two polymers are incompatible.

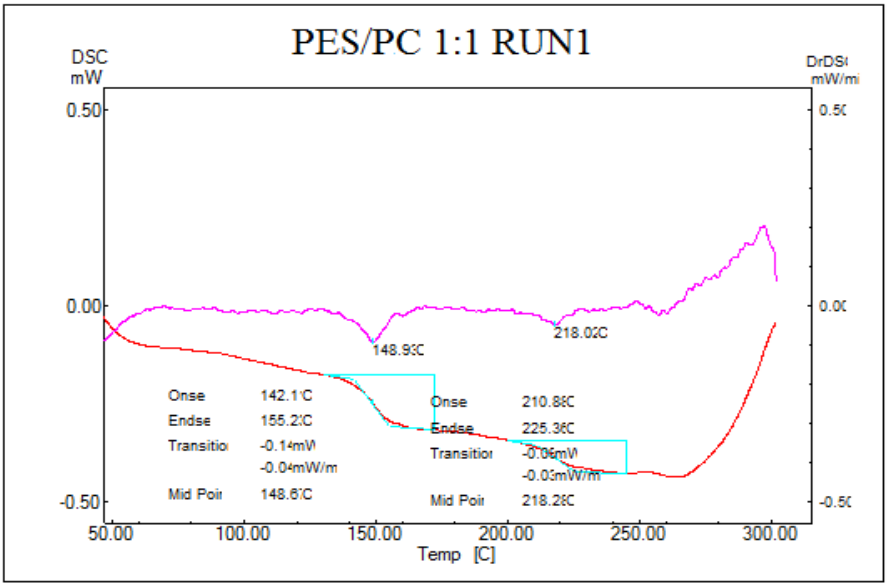

Figure 4.9 DSC result of PES/PC 1:1 Membrane

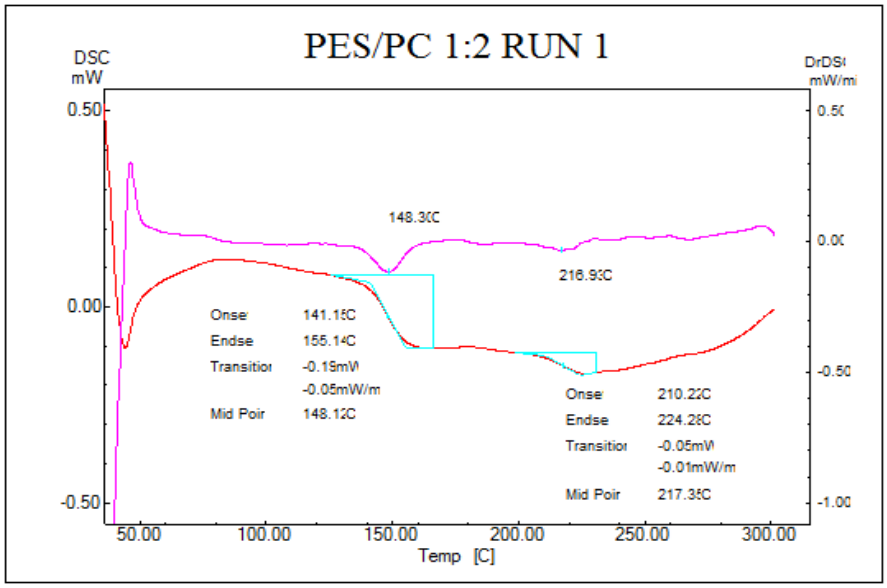

Figure 4.10 DSC result of PES/PC 1:2 Membrane

After shoving that PES and PC are not compatible and resulting films are not usable as a membrane, a PES compatible polymer was searched through literature. One of the PES-compatible polymers mentioned in the literature was PI [29]. Therefore, further studies were conducted on blending of PES and PI.

In order to prove the miscibility and compatibility of PES and PI, we also conducted DSC analysis. In order to remove the thermal history of the membranes, DSC scans were conducted twice [6]. However, two different glass transitions were observed in the second runs of the analyses at the temperatures of each polymers in DSC scans of some PES/PI blends, and in other analyses single value is observed very close to T_g of the pure polymers, as presented in Table 4.3. This fact is mentioned in the literature by Liang et al. as an indication of a phase separation [29, 43]. They stated that when the PES/PI polymer blend is heated up to 350°C for 30 min, which is above the glass transition temperature of PI, caused to phase separation of the polymers. Resulting films became cloudy, as a visual proof of phase separation. Further rheological measurements conducted by them, suggesting that the reason of phase separation may because of the change in viscoelastic properties at higher

temperatures [29]. In addition, the reason of increase in opacity of the polymer blend films may be an indication of increase in crystallinity. Heating the polymer films above T_g increases the chain mobility [47]. Therefore, polymer chains rearrange themselves and chains of each polymer may contract individually, thereby may cause phase separation. Therefore, further DSC analyses of ZIF-8 containing and asymmetric blend membranes were conducted as single run through this study. A sample scan of PES/PI 25/75 dense blend membranes was given in the Figure 4.11. All DSC thermograms of blend membranes were given in APPENDIX D.

Table 4.3 DSC Results of Dense Blend Membranes

Weight % PI	T_g 1st Run	T_g 2nd Run	
		PI dominated phase	PES dominated phase
100	317	N/A	
95	310	313	
90	303		
80	290	313	
75	252	307	227
50	260		227
25	240		226
10	232		224
0	220 [48]	N/A	

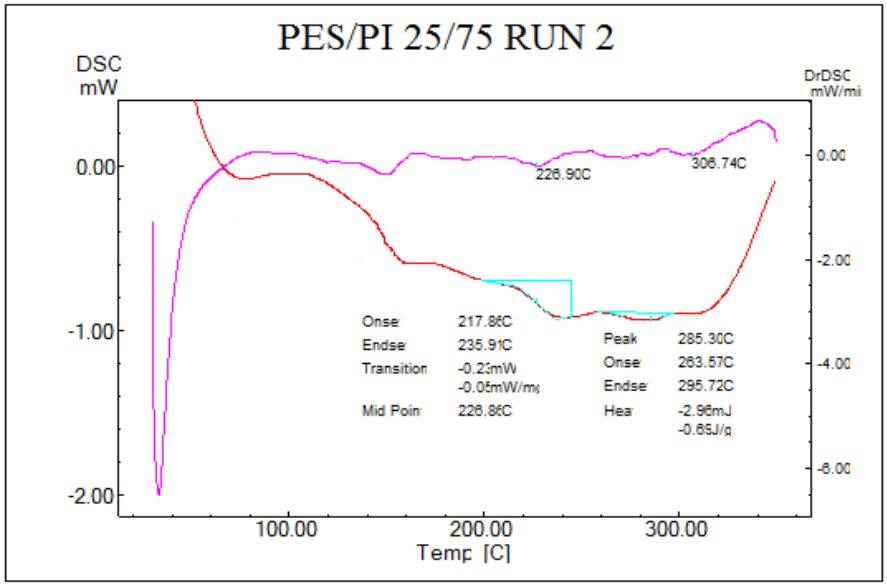

Figure 4.11 DSC scan of PES/PI 25/75 Run 2

The experimental results were compared with a theoretical model. Taylor-Gordon equation (Eq. 4.2) is one of the most used equations to predict the T_g of the miscible polymer blends. In this equation, w_1 and w_2 are the mass fractions; and T_{g1} and T_{g2} are the glass transition temperatures of the pristine polymer. The k is a constant indicating the strength of the interaction between the polymers. When k closer to 1 the weak interactions are expected between the polymers [29].

$$T_g = \frac{w_1 T_{g1} + k w_2 T_{g2}}{w_1 + k w_2} \text{ [29]} \qquad \text{Equation 4.2}$$

Table 4.4 Measured Glass Transition Temperatures of PES/PI Blends

Weight %		T_g (°C)
PI	PES	
0	100	220 [48]
10	90	230
25	75	240
40	60	256
50	50	258
80	20	290
90	10	303
95	5	310
100	0	317

Graphical interpretation of Table 4.4 and comparison with Taylor-Gordon model is given in Figure 4.12. The deviation between the theoretical and experimental values became smallest when k constant is 0.74. This k constant is slightly higher than the k constant given in the literature found by same analysis method. However, the solvent used during film preparation and heating rate of DSC analysis affect the glass transition temperatures, and thereby k values [29]. Therefore, the k value we found is different from the literature. To sum up, the k value once more indicates that these two polymers are miscible and the interaction between the polymer chains is considerably high.

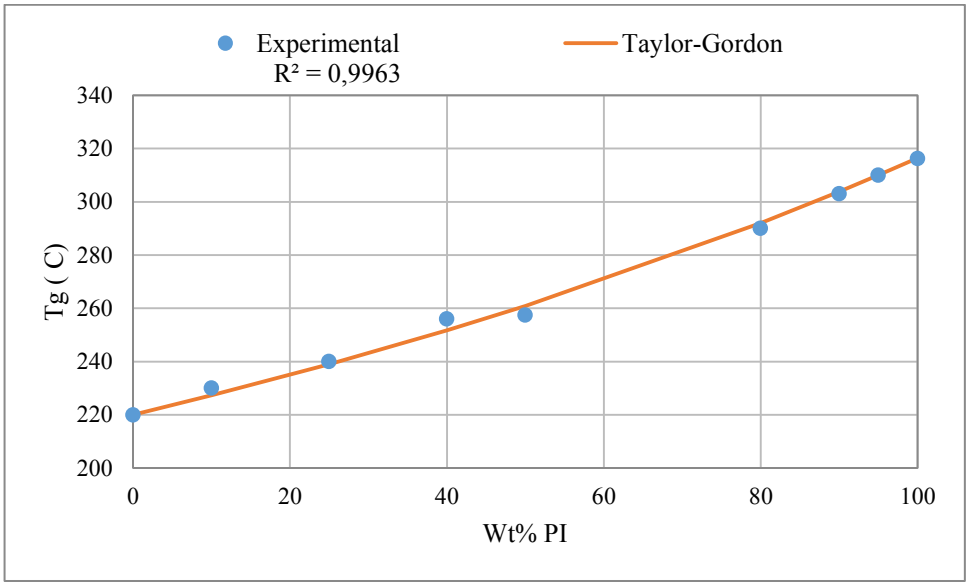

Figure 4.12 Experimental vs. Taylor-Gordon Eqn. T_g Results

4.2.3. SEM

PES/PI (dense and asymmetric) and PES/PI/ZIF-8 membranes are characterized through SEM analysis in order to determine the morphology of the membranes. SEM micrographs of some of the dense polymeric membranes are given in the Figure 4.13 and Figure 4.14.

In Figure 4.13, membrane is appeared as homogeneous and the thickness is measured as 51.5 µm, which is close to the micrometer measurements, 55 µm. The droplet-like, rough structure is observed at the cross sectional view of the membrane. This feature is also observed in the literature before [49–51].

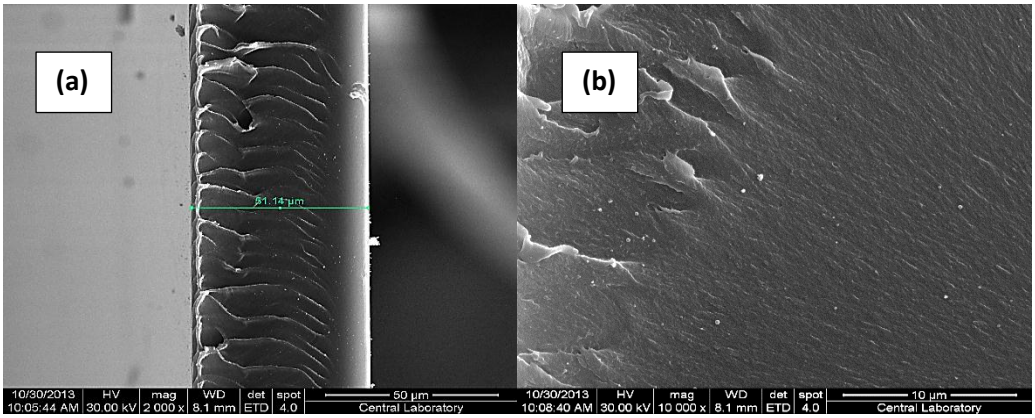

Figure 4.13 SEM Micrograph of Pure PI Dense Membrane (a) low magnification; (b) high magnification

In Figure 4.14, the cross-sectional morphology of Pure PI, PES/PI 10/90, PES/PI 20/80, PES/PI 75/25, PES/PI 50/50, PES/PI 75/25, and PES/PI 90/10 membranes are given for comparison. The cross-sectional roughness is observed in all PES/PI blend membranes and also indicated in the literature [37,44]. There are no phase separations or defects observed in the SEM micrographs, indicating that PES/PI couple is miscible and compatible.

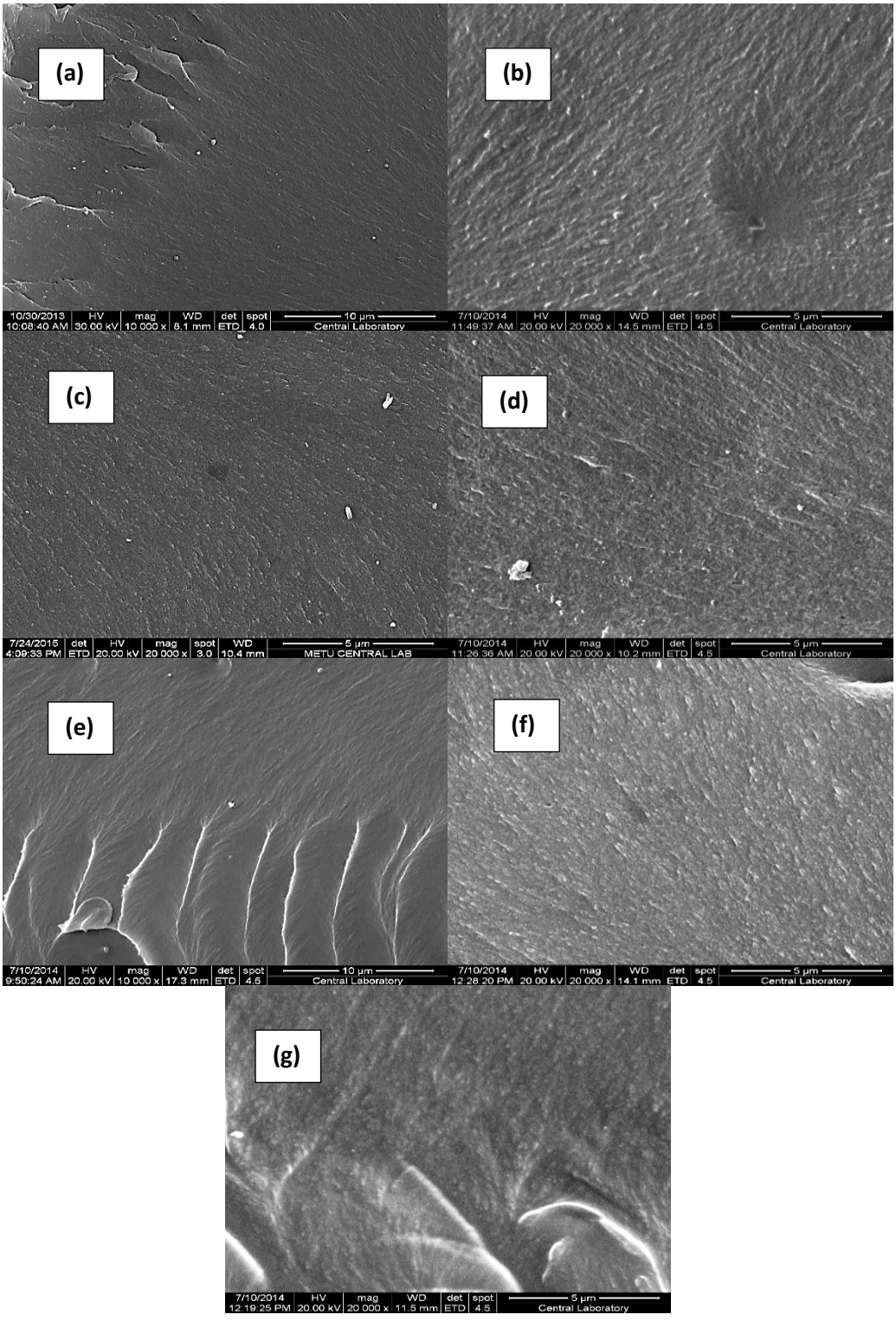

Figure 4.14 SEM micrographs of cross-sections of (a) Pure PI; (b) PES/PI 10/90; (c) PES/PI 20/80; (d) PES/PI 75/25; (e) PES/PI 50/50; (f) PES/PI 75/25; (g) PES/PI 90/10 membranes at high magnification

The SEM micrographs of PES/PI/ZIF-8 20/80/10 membrane are given in the Figure 4.15 and Figure 4.16. The ZIF-8 particles are homogeneously dispersed through the membrane and the average particle size of the ZIF-8 particles in the membrane is calculated as 79 ±20 nm. Similar membrane structure observed in the literature is stated as the result of good interaction between filler and polymer matrix [37,51–53]. On the other hand, this structure is also described as sieve in cage as an indication of partial incompatibility of polymer matrix and filler material.

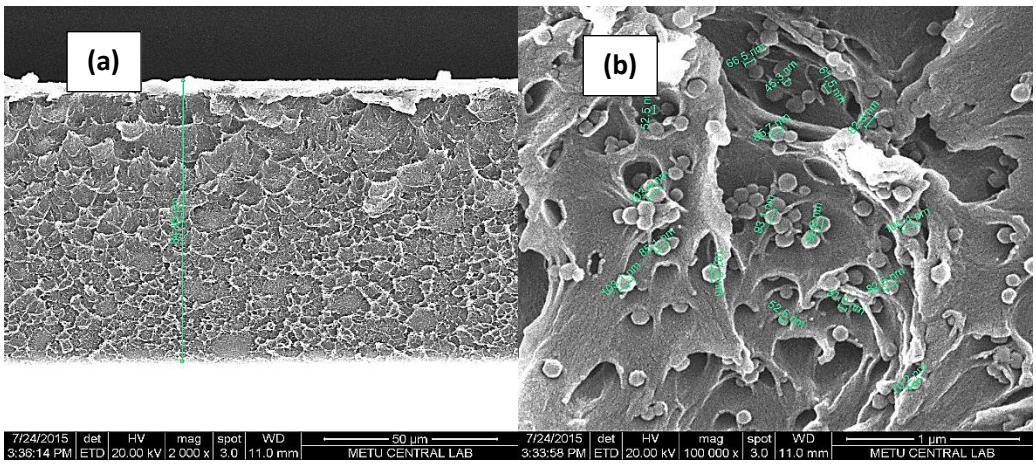

Figure 4.15 SEM micrographs of cross-sections of PES/PI/ZIF-8 20/80/10 membranes at (a) low; (b) high magnification

In Figure 4.16, cross sectional morphologies from different points of PES/PI/ZIF-8 20/80/10 membrane are given at high magnification. It can be commented as approximately 5 to 10 particles of ZIF-8 are tend to agglomerate, which is considerably low when compared with the literature [37,54,55]. Stretchings and sieve in cage structure are observed between polymer matrix and ZIF-8 particles, showed in Figure 4.16. The reason of these stretchings may because of the concentrated bond stress at the interface, mentioned in the literature for similar polymer-MOF couples [51–54]. There are also few particles embedded into the polymer matrix indicating the good interaction between ZIF-8 particles and polymers [51]. Stretchings and embeddings were marked with red circles in Figure 4.16. Interfacial void formations

are also clearly observed at all SEM micrographs, as an indication that PES/PI polymer matrix is not completely compatible with ZIF-8 particles [37,56]. Another possible reason of occurring of interfacial voids is stated in the literature as freeze fracturing in liquid nitrogen [15,39,51–53].

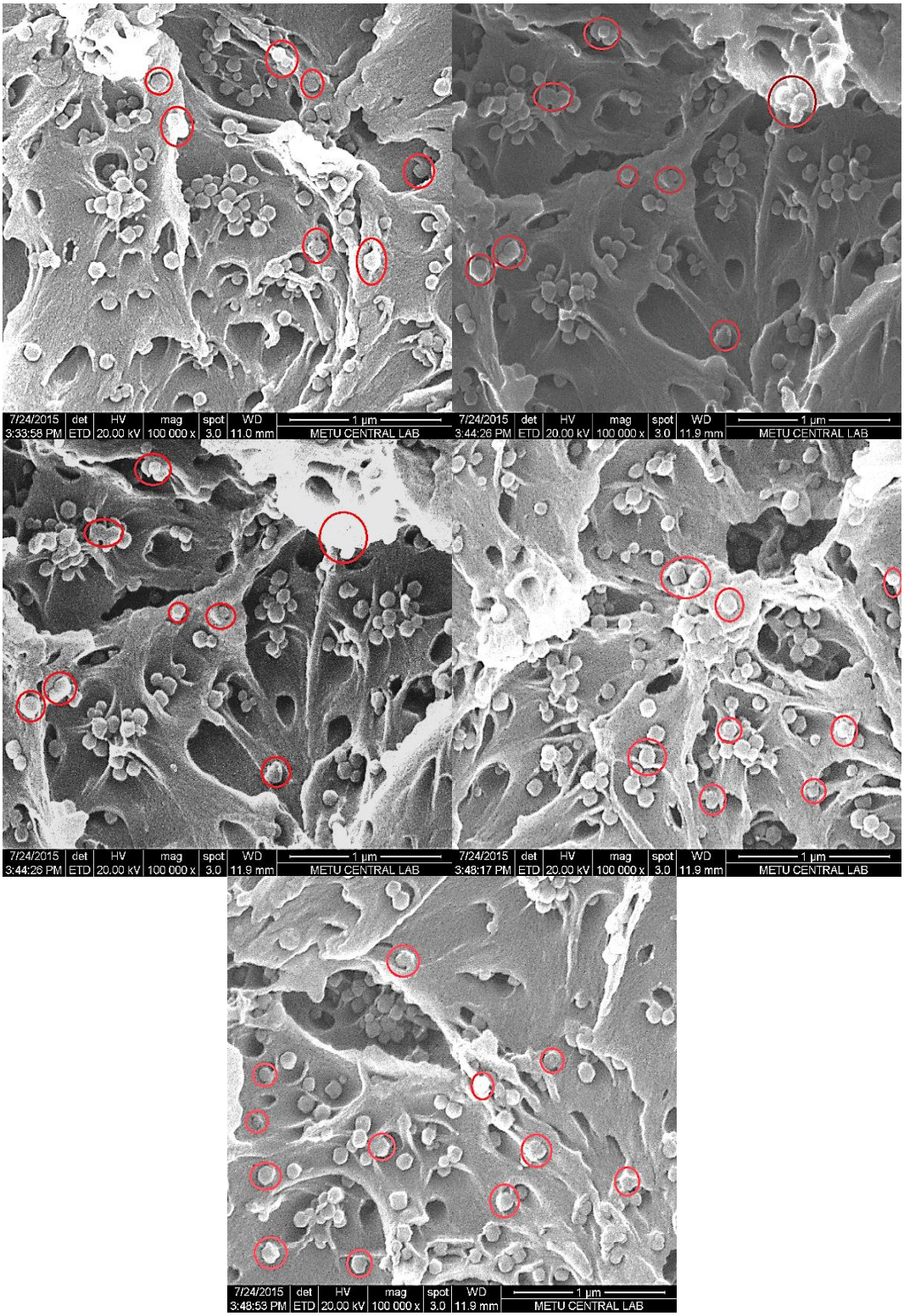

Figure 4.16 High magnification SEM micrographs of PES/PI/ZIF-8 20/80/10 membranes where Polymer Matrix-ZIF-8 attachments marked

In Figure 4.17, the SEM micrographs of asymmetric PES/PI 20/80 membranes are given with different magnifications. A sponge-like nano-porous skin layer on top of sponge-like micro-porous support layer is observed. Similar asymmetric structures were mentioned in the literature before for similar polymer couples [11,33,36].

The thicknesses of skin layer and overall membrane are measured as 14 and 174 μm, respectively. In addition, pore size of the support layer is approximately 1 micron and pores size of the skin layer is below micron size.

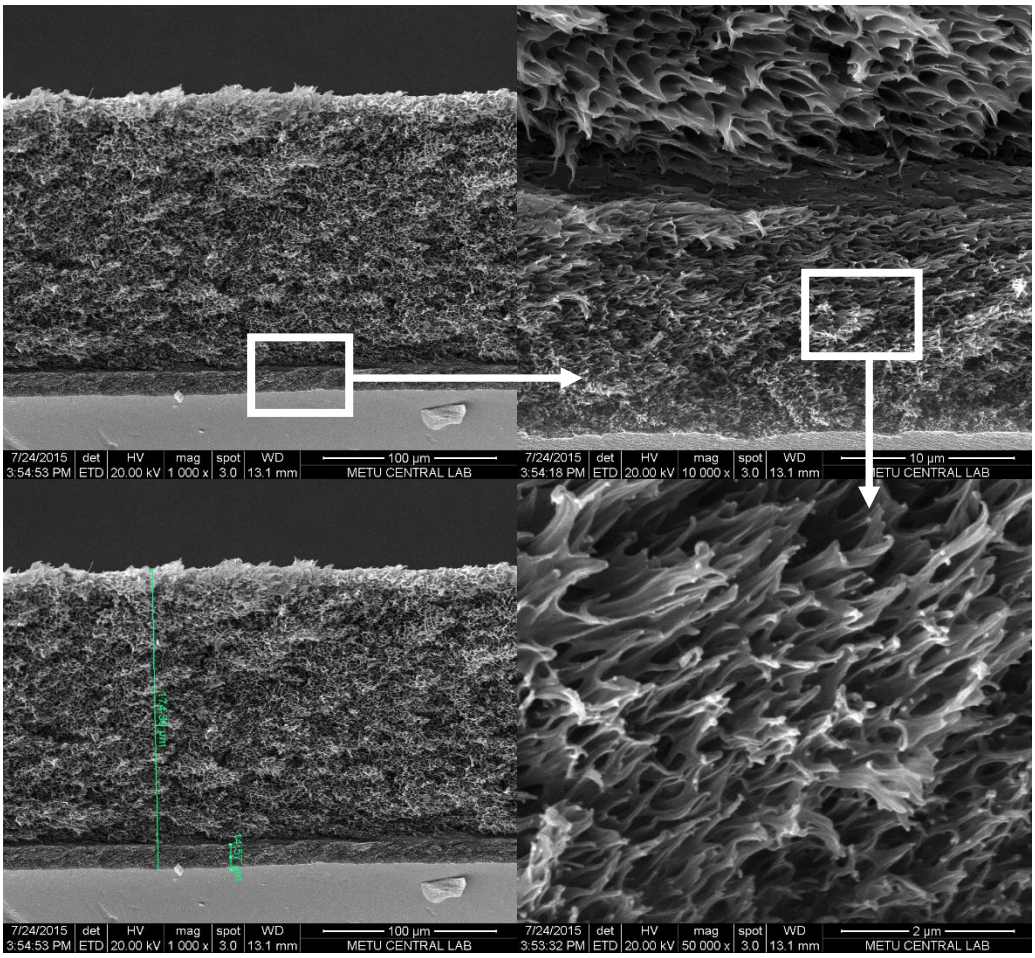

Figure 4.17 SEM micrographs of Asymmetric PES/PI 20/80 Membrane

4.3. Gas Permeation Results of Dense and Asymmetric Membranes

4.3.1. Gas Permeation Results of Dense Membranes

Firstly, in order to investigate the effect of miscible blending of PES and PI, H_2, CO_2, and CH_4 permeability of PES/PI dense blend membranes with composition range of 25 to 90 wt/wt% PI were measured. Permeability and selectivity of the dense blend membranes are given in Table 4.5 and Figure 4.18 to Figure 4.32. According to these results, as the amount of PI in the blend increases, both permeability and selectivity values increase, as expected [30,31]. Moreover, H_2 is affected most by the change in blend concentration because of having the smallest kinetic diameter among the tested gases. Reproducibility results of dense membranes were given in APPENDIX E.

Table 4.5 Permeability and Selectivity Values of the PES/PI Dense Blend Membranes

	Permeability (Barrer)			**Selectivity**		
	H_2	**CO_2**	**CH_4**	**H_2/CO_2**	**CO_2/CH_4**	**H_2/CH_4**
Pure PI	32.6±1.1	9.6±0.3	0.27±0.01	3.4±0.1	36.2±1.4	122.0±2.7
PES/PI 10/90	24.1±0.1	7.5±0.1	0.21±0.01	3.2±0.1	36.6±1.6	117.3±7.4
PES/PI 20/80	24.6±0.5	7.8±0.3	0.22±0.01	3.2±0.1	35.6±1.5	112.1±4.0
PES/PI 25/75	21.5±1.0	7.1±0.2	0.23±0.02	3.0±0.1	31.1±2.3	93.3±9.1
PES/PI 30/70	22.4±0.3	8.0±0.0	0.20±0.00	2.8±0.0	40.2±0.3	111.9±1.7
PES/PI 60/40	17.5±0.4	6.8±0.3	0.19±0.01	2.6±0.1	36.9±1.2	95.0±1.8
PES/PI 75/25	16.2±0.3	6.3±0.2	0.26±0.02	2.6±0.1	31.3±3.8	78.2±7.9
Pure PES	10.8±0.6	4.8±0.2	0.14±0.02	2.3±0.1	33.9±3.4	77.4±4.6

The experimental values were compared with the following formula derived from a theoretical model suggested by Hopfenberg and Paul [57] for copolymers and polymer blends:

$$\ln P_b = w_1 \ln P_1 + w_2 \ln P_2 \qquad \text{Equation 4.3}$$

This formula is derived by assuming the polymers dissolved in DMF and in each other ideally. There were some deviations observed from the actual model, may because of some specific molecular interactions between polymer chains [58].

Table 4.6 Theoretical Permeability Results According to Eq. 4.3

	Permeability (Barrer)			**Selectivity**		
wt% PI	**H_2**	**CO_2**	**CH_4**	**H_2/CO2**	**CO_2/CH_4**	**H_2/CH_4**
100	32.6	9.6	0.27	3.4	36.2	122.0
90	29.1	9.0	0.25	3.2	35.9	116.6
80	26.1	8.4	0.23	3.1	35.7	111.4
75	24.7	8.1	0.23	3.1	35.6	108.9
70	23.4	7.8	0.22	3.0	35.5	106.5
40	16.8	6.3	0.18	2.7	34.8	92.9
25	14.2	5.7	0.16	2.5	34.5	86.7
0	10.8	4.8	0.14	2.3	33.9	77.4

The gas permeability of the membranes also compared with theoretical models in terms of mol percent. A sample mol calculation is given in Equation 4.4. Calculated mol percent for each blend composition are tabulated in Table 4.7.

$$n_{PI} = \frac{1\ mol\ PI}{80000\ g\ PI} \times 2\ g\ PI = 2.5 \times 10^{-5} mol\ PI \qquad \text{Equation 4.4}$$

Table 4.7 The Amount of Mol of PI in Blends

Weight % PI	Gram PI	Mol PI	Gram PES	Mol PES	Mol % PI
100	2.0	2.5E-05	0	0	100
90	1.8	2.3E-05	0.2	3.8E-06	85.64
80	1.6	2.0E-05	0.4	7.6E-06	72.60
75	1.5	1.9E-05	0.5	9.4E-06	66.53
70	1.4	1.8E-05	0.6	1.1E-05	60.72
40	0.8	1.0E-05	1.2	2.3E-05	30.64
25	0.5	6.3E-06	1.5	2.8E-05	18.09
0	0	0	2	3.8E-05	0

The amount of PI to the blend in terms of mol fractions is smaller than mass fractions, because molecular weight of PI is higher than molecular weight of PES. However, the contribution of PI to the gas separation performance of the blend membranes was similar for both weight percent and mol percent interpretations.

The results given in Table 4.5 and Table 4.6 were also presented on Figure 4.18, Figure 4.20, and Figure 4.22. The decrease in the permeability with decreasing weight percent of PES can be more clearly observed in the Figure 4.18, Figure 4.20, and Figure 4.22. H_2 and CO_2 permeability values match with both logarithmic and linear models with very small deviations. However, the deviations of CH_4 permeability of the blend membranes from the theoretical models are larger. The minimum leak rate of the test set-up was calculated as 0.002 Barrer. This value is considerably low to affect H_2 and CO_2 permeabilities; however, it may somewhat affect CH_4 permeability. The solution and diffusion of CH_4 molecules through the membrane is slower than H_2 and CO_2, because of the larger kinetic size of the CH_4. Because of this larger kinetic size, its permeation may be affected by interaction and molecular conformation of two different polymer chains of the blend.

The effect of PI content in the blend on H_2 permeation was presented on a graphic in Figure 4.18. H_2 permeability increased as PI content in the blend increases. A similar trend is observed in the literature for PSF/PI blend membranes [30]. The reason of higher permeation value of PI was stated as that PI chains arrange themselves in a

less compacted manner than PES chains, due to the bulkier repeating unit of PI [31]. It can be seen in the Figure 4.18 that experimental permeability values are matching with the logarithmic model [30,31] better than linear model. There are some small deviations were observed from the theoretical models. PES/PI 10/90 membranes had the highest deviation from the theoretical models for H_2 permeation.

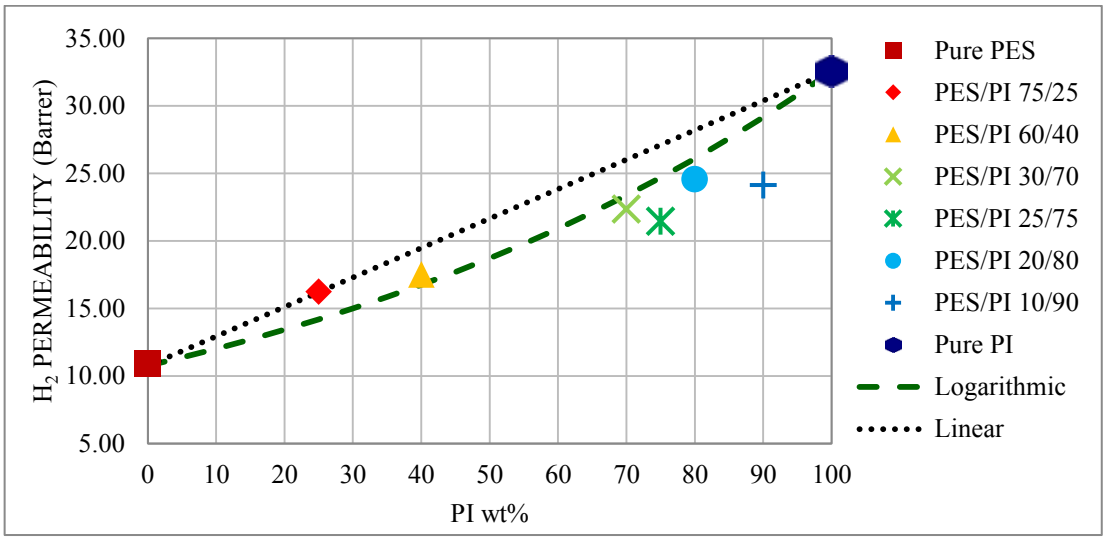

Figure 4.18 PI wt% vs. H_2 Permeability

Hydrogen permeability of blend membranes were also compared with theoretical models based on mol percentages of the polymers in the blend and graphically interpreted in Figure 4.19. Membrane code names are kept same as weight percentages for simplicity. Similar to weight percent case, the permeability of the membranes increased as the PI content increased. In addition, the deviations from the theoretical models were found smaller in case of mol percent interpretation.

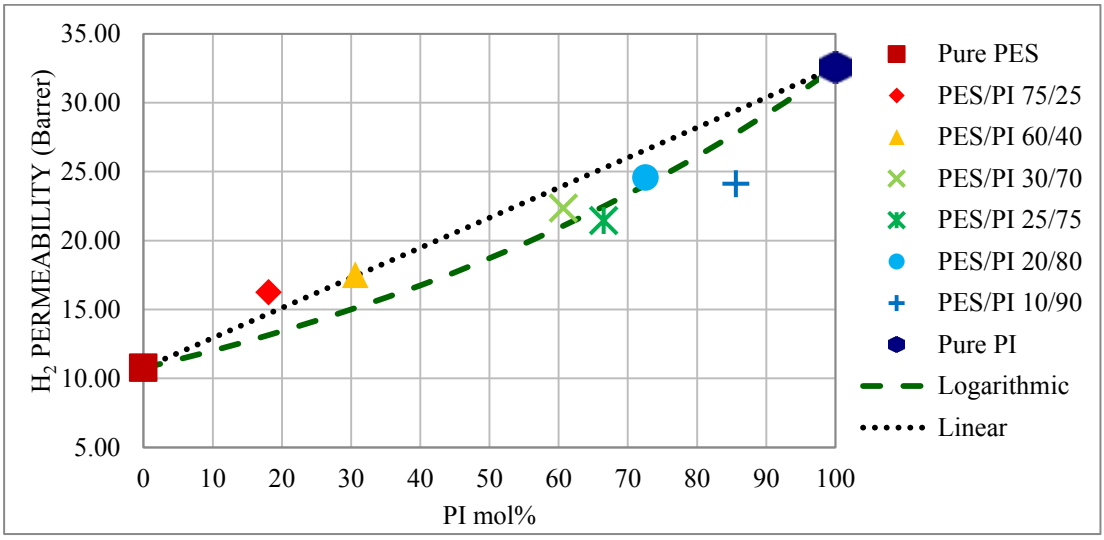

Figure 4.19 PI mol% vs. H_2 Permeability

The permeability results of CO_2 are similar with H_2, seen in Figure 4.20. Permeability values increase as the PI composition increases, coherent with the literature [17,31,37,59]. The CO_2 permeability of PES/PI 10/90 differs from the theoretical values as similar in case of H_2 permeability. The deviation of PES/PI 10/90 from the logarithmic model is calculated as 17%.

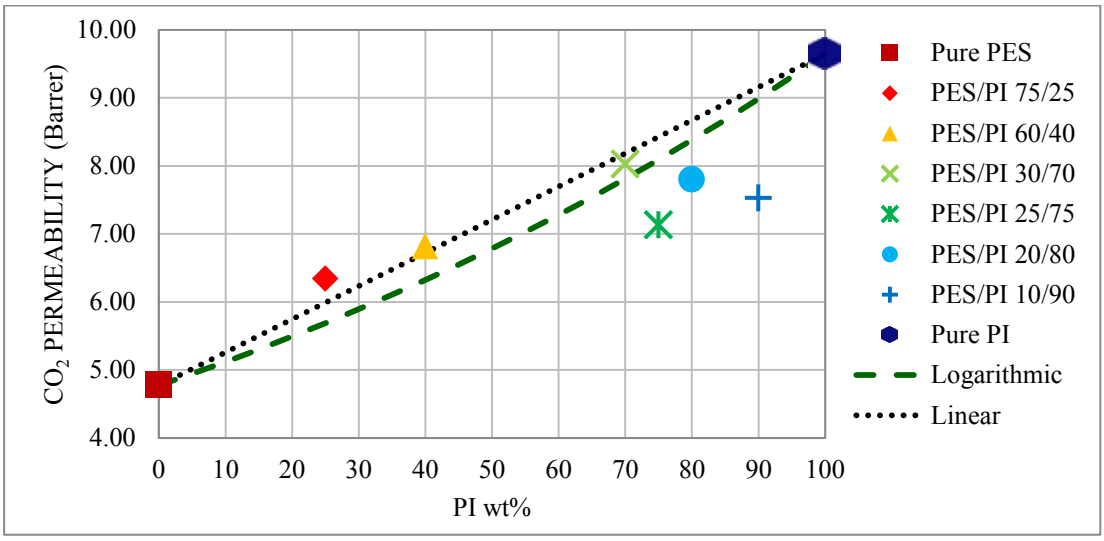

Figure 4.20 PI wt% vs. CO_2 Permeability

CO_2 permeability of blend membranes versus amount of PI in the blend as mol percent is presented in Figure 4.21. The difference between theoretical models and experimental results were smaller than weight percent interpretation of the results. For example, the deviation from the logarithmic model of PES/PI 10/90 was calculated as 14%. Again, the permeability increased as the amount of PI in the blend increased.

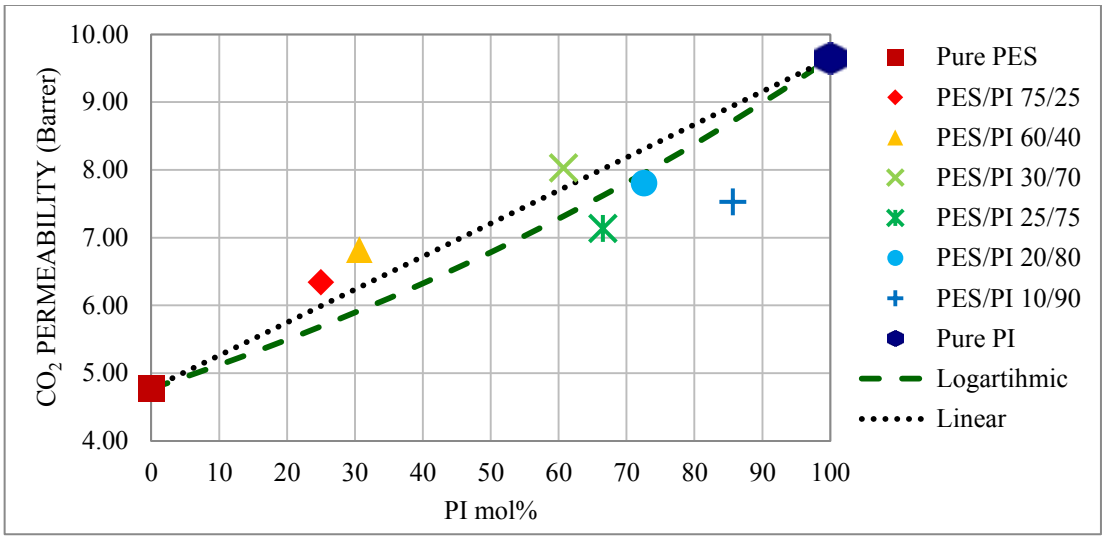

Figure 4.21 PI mol% vs. CO_2 Permeability

In Figure 4.22, PI content in the blend versus the CH_4 permeability values of the dense blend membranes can be seen. It can be stated that CH_4 permeability values of the blend membranes increased as the amount of PI in the blend increased, agreeing with the literature [31,37], except PES/PI 75/25 membrane. The CH_4 permeability of PES/PI 75/25 membrane deviates from the theoretical models clearly, e.g. 39% deviation from the logarithmic model. Nevertheless, all CH_4 permeability values of the blend membranes were in between the CH_4 permeability values of Pure PI and Pure PES.

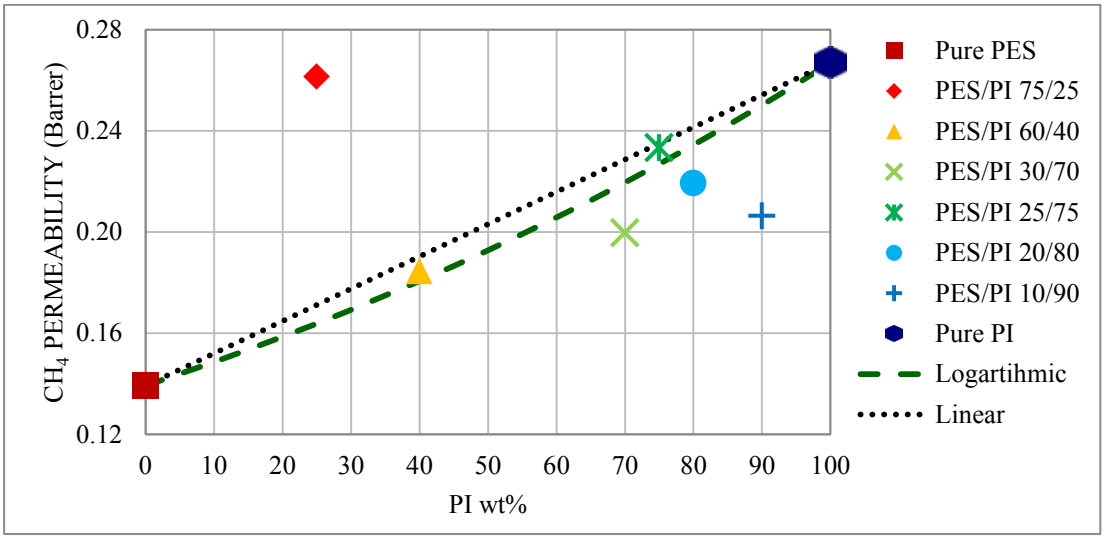

Figure 4.22 PI wt% vs. CH_4 Permeability

The effect of increase in PI amount in terms of mol percent on CH_4 permeability of the blend membranes can be observed in Figure 4.23. There is no significant difference is observed between weight or mol percent interpretations.

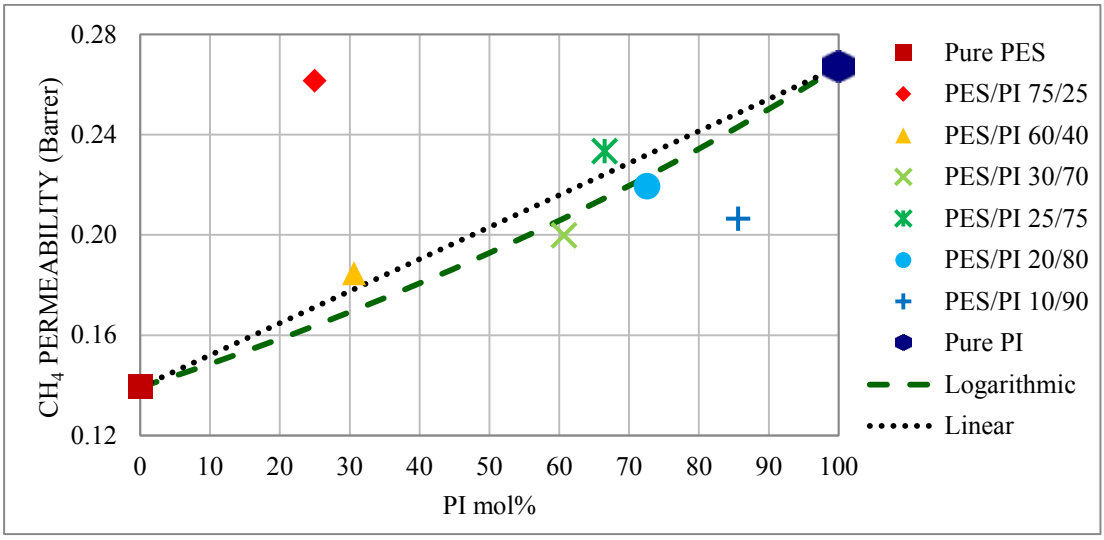

Figure 4.23 PI mol% vs. CH_4 Permeability

The effect of change in PI composition on H_2/CO_2 selectivity was presented in Figure 4.24. According to graphic, H_2/CO_2 selectivity values are increasing as the amount of PI in the blend increased. In a similar study, blend of PBI and Matrimid performed a synergetic effect of H_2/CO_2 selectivity. The H_2/CO_2 selectivity of Matrimid/PBI 25/75 membrane is higher than the Pure PBI and Pure Matrimid membranes [31]. The possible reason of this difference between our experiments and literature values could be different interactions between polymers and difference in interactions between CO_2 and polymeric components of blend membrane. All H_2/CO_2 selectivity values of the blend membranes matched with the both logarithmic and linear models.

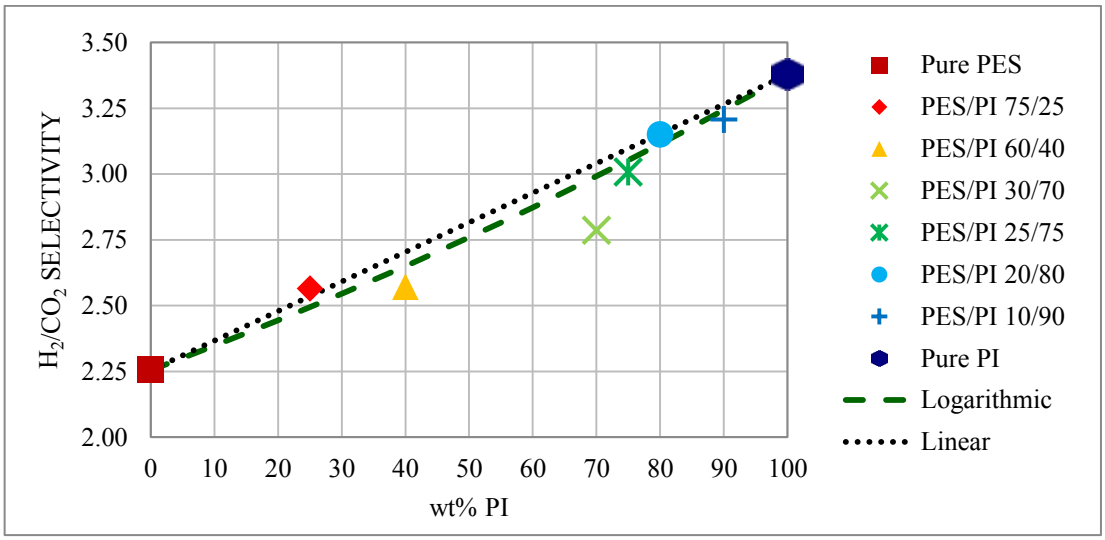

Figure 4.24 PI wt% vs. H_2/CO_2 Selectivity

The selectivity of H_2/CO_2 depending on the mol percent of PI is given in Figure 4.25. The experimental selectivity values and theoretical values were similar to each other. The deviations from the theoretical models in case of mol percent PI were found similar to weight percent PI interpretation.

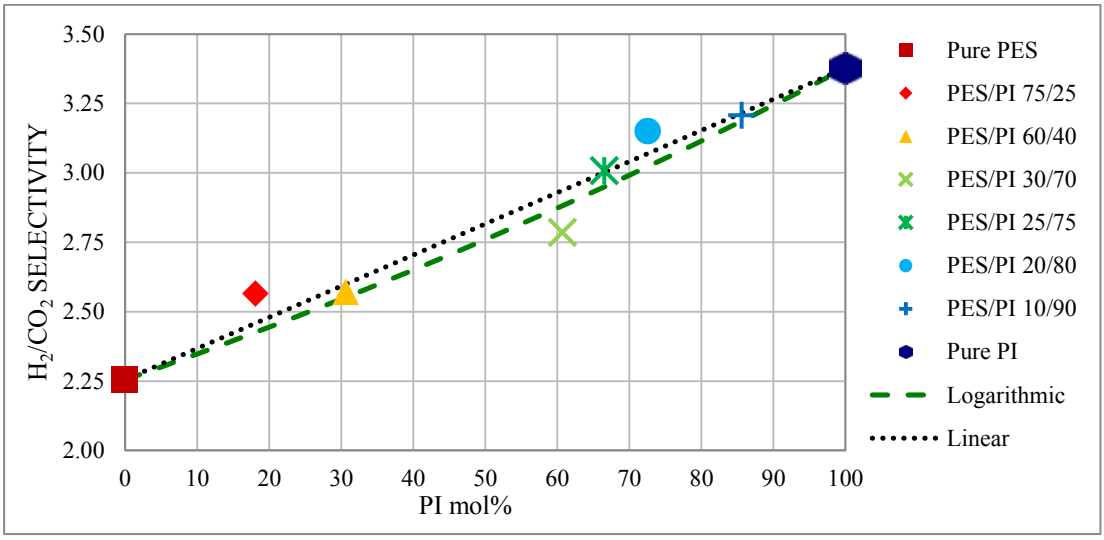

Figure 4.25 PI mol% vs. H_2/CO_2 Selectivity

In Figure 4.26, H_2 permeability versus H_2/CO_2 selectivity values of PES/PI blend membranes were given with respect to theoretical upper bound [12]. It can be obviously seen that H_2/CO_2 separation performance of PI is closer to the theoretical upper bound drawn by Robeson and both H_2 permeability and H_2/CO_2 selectivity values of blend membranes are increasing as the PI content increased, because PI chains are less compacted than PES chains thanks to bulkier repeating unit [36].

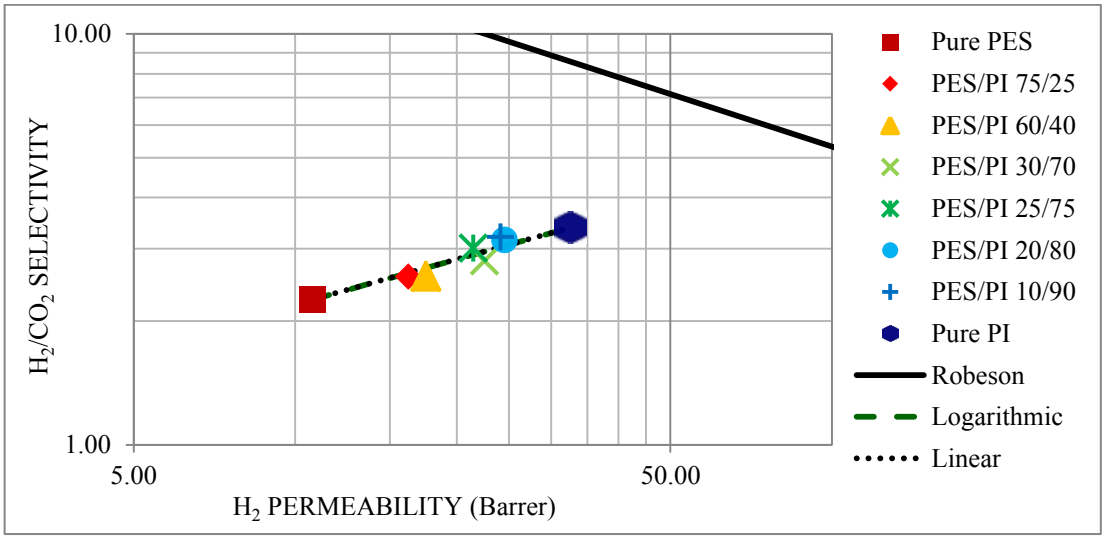

Figure 4.26 Single gas permeabilities of blend membranes with reference line for H_2/CO_2 pair

CO_2/CH_4 selectivity as a function of blend composition (PI wt%) is given in Figure 4.27. It can be clearly seen that linear and theoretical models are exactly coinciding. Some of the experimental values are deviating from the theoretical models. PES/PI 20/80 membrane's CO_2/CH_4 selectivity is overlapping with the theoretical models. The CO_2/CH_4 selectivity of PES/PI 60/40 and PES/PI 30/70 membranes are above; PES/PI 75/25 and PES/PI 25/75 membranes are below the theoretical models. As it is stated above, CH_4 permeation may be affected by the leak rate of the experimental set-up. Since the molecular diameter of the CH_4 is comparatively larger than H_2 and CO_2, CH_4 molecules move slower through the solution and diffusion. Therefore, test set-up is subject to leaks for longer duration. In addition, CO_2 molecules may interact with polymer chains and affect the conformation of the chains. CO_2 diffusion may be affected by differing chain conformations at different blend compositions. Since the diffusion of H_2 through the membrane is considerably fast, because of very small kinetic diameter, the effect of change in conformation may not affect H_2 diffusion.

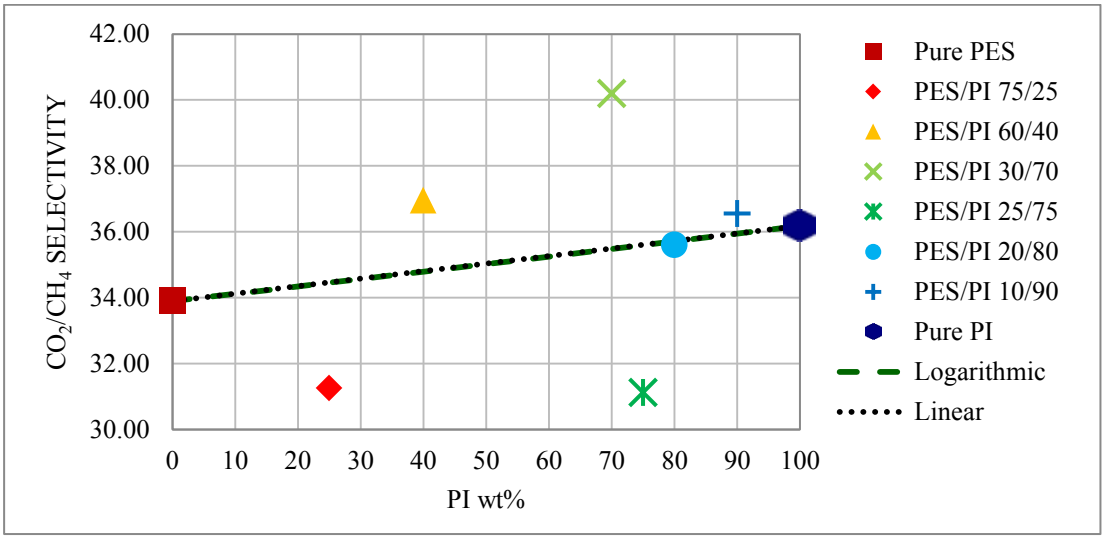

Figure 4.27 PI wt% vs. CO_2/CH_4 Selectivity

The CO_2/CH_4 selectivity of the blend membranes in terms of mol percent of PI is given in Figure 4.28. The contribution of mol of PI to the CO_2/CH_4 selectivity performance of the blend membranes was found almost same with the contribution of weight of PI. Therefore, the interactions of CO2 and CH4 molecules with polymer chains are dominant than the interaction of polymer chains with each other.

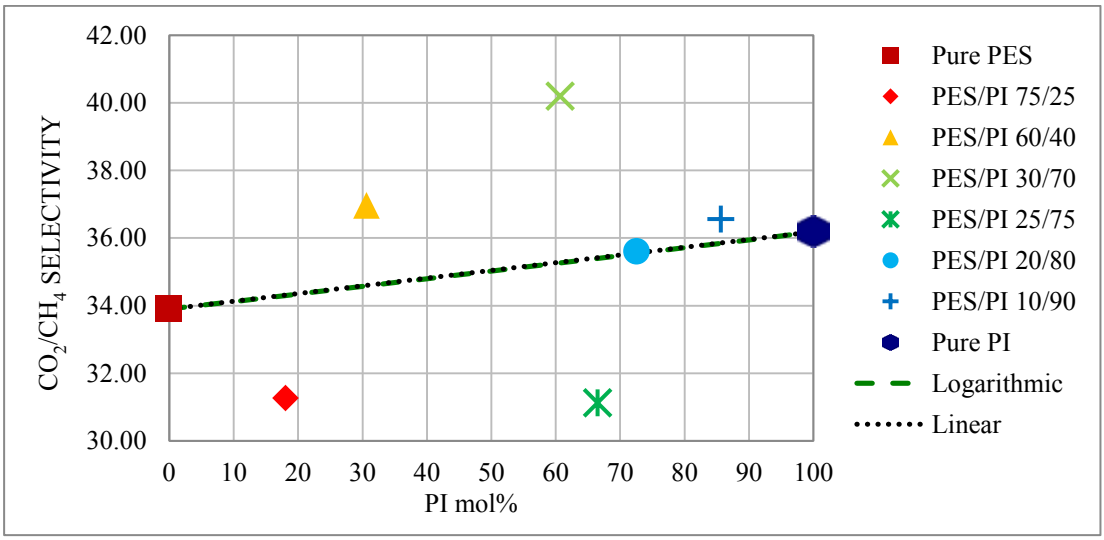

Figure 4.28 PI mol% vs. CO_2/CH_4 Selectivity

In Figure 4.29, CO_2/CH_4 separation performance of dense blend membranes was described. CO_2/CH_4 selectivities of PES/PI 60/40, 30/70 and 10/90 membranes were higher than the theoretical values. Furthermore, both CO_2 permeability and CO_2/CH_4 selectivity of PES/PI 30/70 membrane is higher than PES/PI 20/80 and 10/90 membranes.

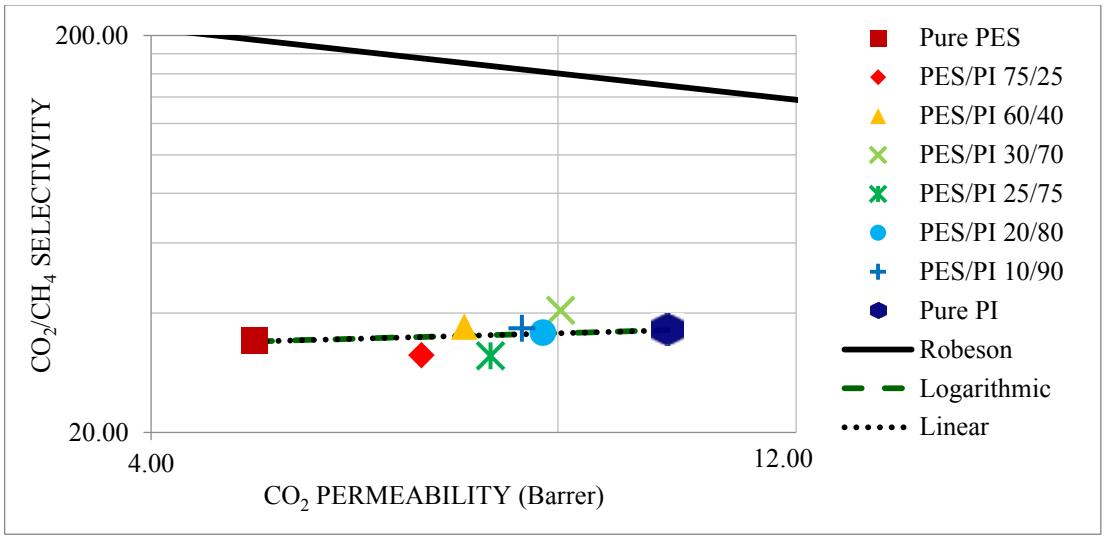

Figure 4.29 Single gas permeabilities of blend membranes with reference line for CO_2/CH_4 pair

The effect of PI content on H_2/CH_4 selectivity is similar to H_2/CO_2 selectivity, as shown in Figure 4.30. All the selectivity values of the blend membranes are lying in between the pristine membrane values given in Figure 4.30. However, PES/PI 75/25 and 25/75 membrane deviates from the theoretical models. There is only one research has been done on H_2/CH_4 separation with miscible polymeric blend membranes [31]. Surprisingly, H_2/CH_4 selectivity of Matrimid/PBI 25/75 membrane, synthesized by this group, is higher than the pristine polymers. They stated that the reason of this synergistic effect might because of the hydrogen bonding between Matrimid and PBI.

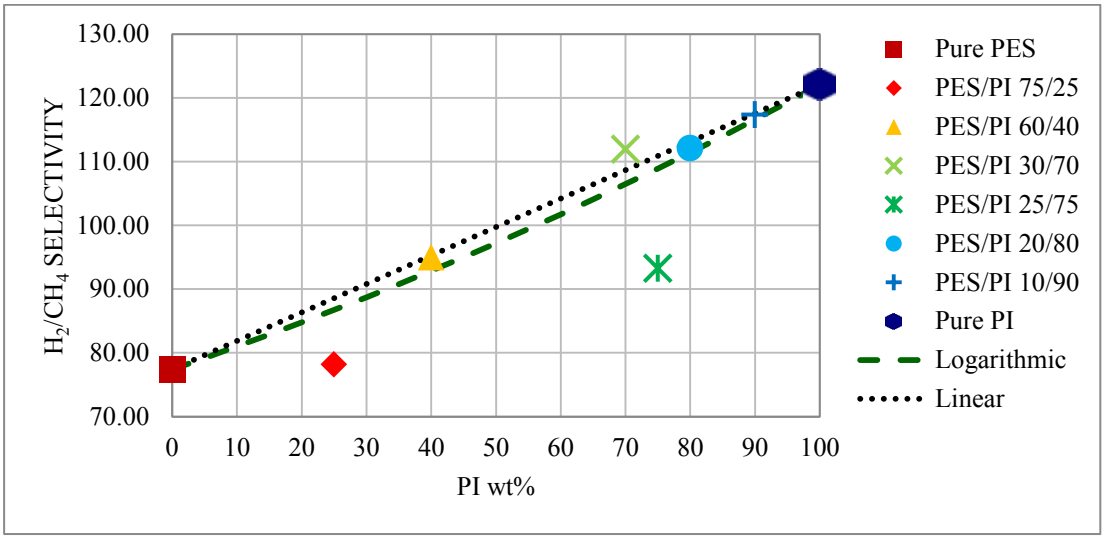

Figure 4.30 PI wt% vs. H_2/CH_4 Selectivity

The selectivity of H_2 over CH_4 with respect to mol percent of PI is given in Figure 4.31. The results presented in Figure 4.31 were found very similar to results presented in Figure 4.30. Therefore, it can be suggested that blending two polymers based on mass or mol fractions is not resulted significantly different from each other.

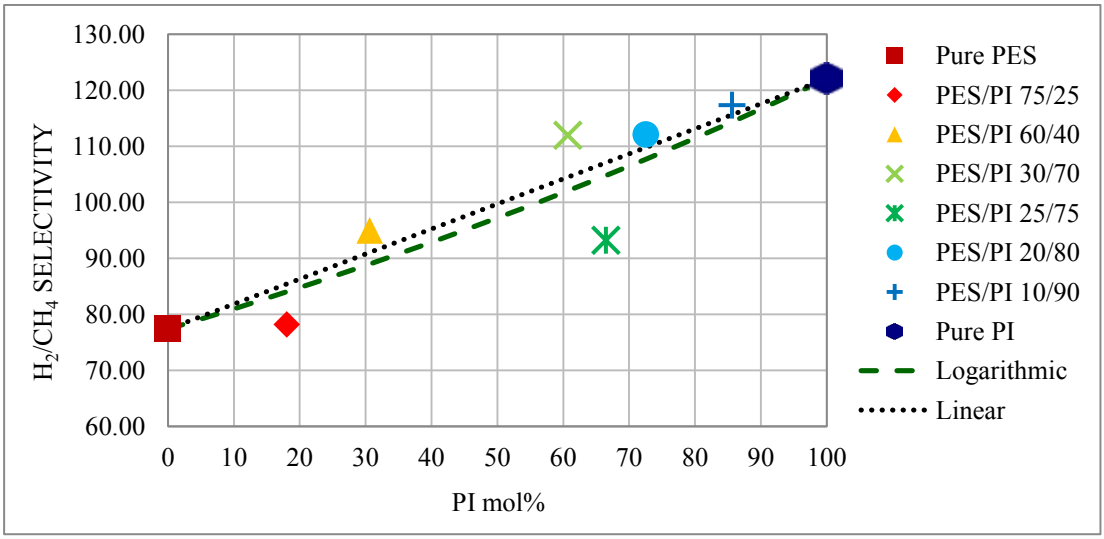

Figure 4.31 PI mol% vs. H_2/CH_4 Selectivity

In Figure 4.32, H_2/CH_4 separation performance of the blend membranes on Robeson plot is given. Both permeability and selectivity values increased as the PI content in the blend increased, because of higher free volume of PI compared to PES [31].

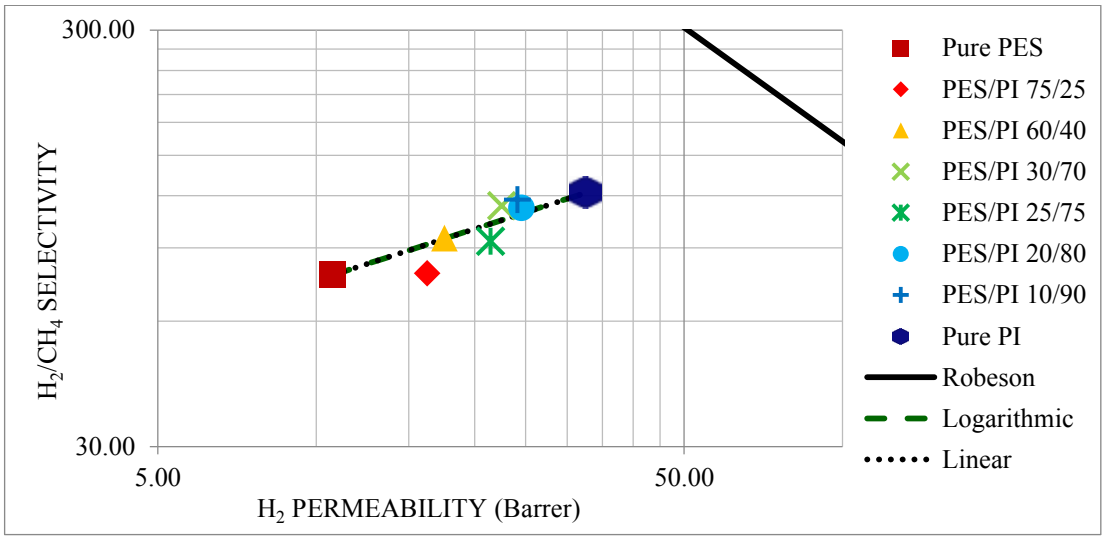

Figure 4.32 Single gas permeabilities of blend membranes with reference line for H_2/CH_4 pair

As a brief summary, PES/PI blend membranes with different compositions were prepared and gas permeations tests were conducted for H_2, CO_2, and CH_4. PES/PI 20/80 membranes performed best among the tested membranes. In addition, separation performance of only PES/PI 20/80 membrane for all gas pairs was coinciding with the theoretical models. Therefore, further mixed matrix membrane and asymmetric membrane studies were conducted through this polymer composition.

4.3.2. Gas Permeation Results of PES/PI/ZIF-8 Membranes

After completing gas permeation tests of PES/PI dense blend membranes, PES/PI/ZIF-8 membranes were synthesized. The gas separation results of PES/PI/ZIF-8 20/80/10 membranes were given in Table 4.8 and Figure 4.33 to Figure 4.35 in comparison with PES/PI 20/80 dense membranes. All H_2, CO_2 and CH_4 permeability values of the PES/PI/ZIF-8 20/80/10 membranes increased significantly, while the decrease in selectivity is not significant, as expected [6]. Even a very small increase in CO_2/CH_4 selectivity is observed with ZIF-8 addition to the polymer matrix. Therefore, PES/PI/ZIF-8 blend based mixed matrix membranes can be considered advantageous in terms of enhancing the CO_2/CH_4 separation.

Table 4.8 Comparison of Permeability and Selectivity Values of the PES/ZIF-8 (10%), PES/PI/ZIF-8 20/80/10 and PI/ZIF-8 (10%) Dense Blend Membranes

	Permeability (Barrer)			**Selectivity**		
	H_2	**CO_2**	**CH_4**	**H_2/CO_2**	**CO_2/CH_4**	**H_2/CH_4**
PES/ZIF-8 (10%) [6]	15.4	7.2	0.24	2.1	34.5	72.9
PES/PI/ZIF-8 20/80/10	39.6 ±1.7	13.5 ±0.5	0.37 ±0.02	2.9 ±0.1	36.8 ±0.7	106.4 ±2.5
PI/ZIF-8 (10%) [56]	52.6	13.7	0.26	3.8	30.6	117.7

In Figure 4.33, H_2 permeability vs. H_2/CO_2 selectivity values of Pure PES, Pure PI, PES/PI 20/80, PES/ZIF-8, PI/ZIF-8, and PES/PI/ZIF-8 20/80/10 are presented on Robeson plot [12]. It can be clearly seen from the figure that, ZIF-8 addition enhances the permeability of the membranes, while it has little or no effect on selectivity [6]. Separation performance of PES/PI/ZIF-8 20/80/10 membrane is found even better than Pure PI membranes. The H_2 and CO_2 permeability values of PES/PI 20/80 membranes were increased upon ZIF-8 addition by 61% and 73%,

respectively. The nano-porous structure of ZIF-8 and sieve-in-cage mixed matrix structure are responsible these increases. However, voids formed between the ZIF-8 particles and polymer matrix cause to decrease the selectivity. Gas molecules prefer to go through these non-resistant voids instead of polymer matrix or filler pores [6]. In spite of the fact these drastic increases in permeability values; the H_2/CO_2 selectivity decreased only 7% upon 10 wt% ZIF-8 addition to PES/PI 20/80 matrix.

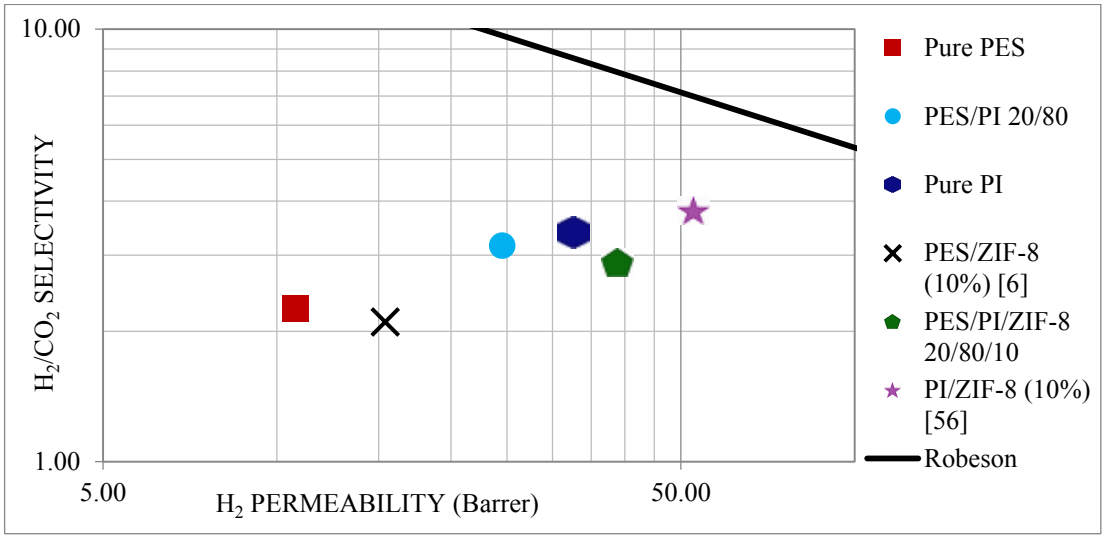

Figure 4.33 H_2/CO_2 vs. H_2 Permeation of PES/ZIF-8, PI/ZIF-8, PES/PI/ZIF-8 20/80/10, Pure PES, Pure PI and PES/PI 20/80 membranes

CO_2 permeability vs. CO_2/CH_4 selectivity values of PES/PI, PES/PI/ZIF-8, PES/ZIF-8, and PI/ZIF-8 on corresponding Robeson plot are given in Figure 4.34. The CO_2 and CH_4 permeability of PES/PI 20/80 membranes were increased by 73% and 68%, respectively. Unlikely H_2/CO_2 and H_2/CH_4 selectivity values, CO_2/CH_4 selectivity increased by 3% with ZIF-8 addition to the matrix. Moreover, CO_2/CH_4 selectivity of PES/PI/ZIF-8 membrane is found 20% higher than the PI/ZIF-8. Therefore, ZIF-8 addition into the PES/PI blend can be a promising method to produce industrial membranes for CO_2/CH_4 separation processes.

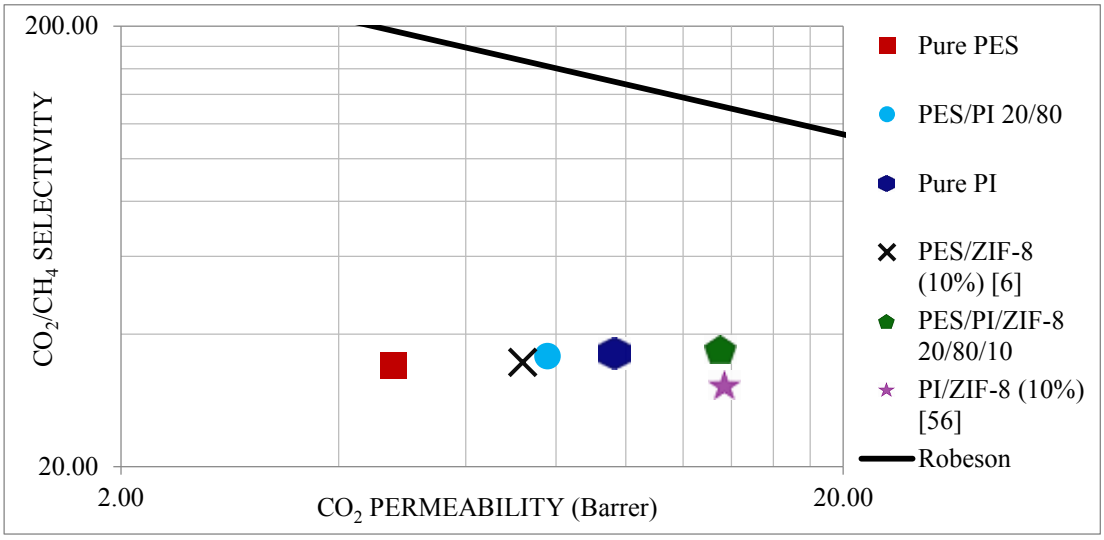

Figure 4.34 CO_2/CH_4 vs. CO_2 Permeation of PES/ZIF-8, PI/ZIF-8, PES/PI/ZIF-8 20/80/10, Pure PES, Pure PI and PES/PI 20/80 membranes

H_2 permeability versus H_2/CH_4 selectivity values of PES/PI blend and PES/PI/ZIF-8 20/80/10 membranes on Robeson plot is given in Figure 4.35. Methane permeability increased by 68% by ZIF-8 addition to PES/PI 20/80 blend due to high porosity of ZIF-8 [6]. On the other hand, H_2/CH_4 selectivity decreased only 5%. The amount of decrease in H_2/CH_4 selectivity is smaller than H_2/CO_2 selectivity. This may indicate that non-selective interfacial voids are smaller than the molecular size of CH_4; therefore, non-selective voids may become insignificant upon large molecule permeations.

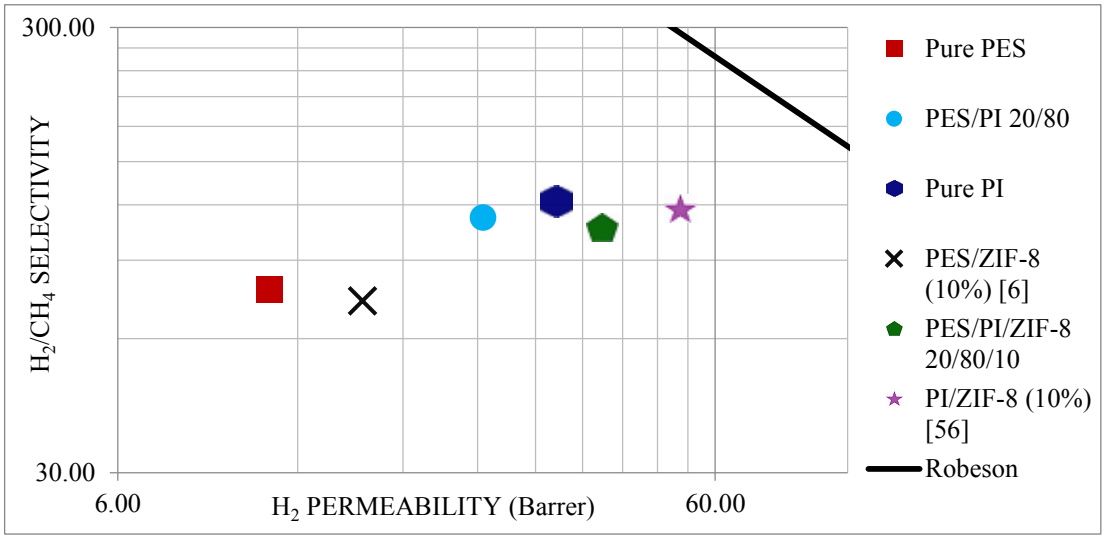

Figure 4.35 H_2/CH_4 vs. H_2 Permeation of PES/ZIF-8, PI/ZIF-8, PES/PI/ZIF-8 20/80/10, Pure PES, Pure PI and PES/PI 20/80 membranes

4.3.3. Gas Permeation Results of PES/PI 20/80 Asymmetric Membranes

The permeance and selectivity values of PES/PI 20/80 asymmetric membranes were given in Table 4.9, Figure 4.36, and Figure 4.37. Five PES/PI 20/80 asymmetric membranes were synthesized at different times to observe the reproducibility of the membranes. According to the results, it is possible to produce reproducible asymmetric membranes with method explained in Section 3.1.2.2.

Table 4.9 Permeance and Selectivity Values of PES/PI 20/80 Asymmetric Membranes

	Permeance (GPU)			Selectivity		
	H_2	CO_2	CH_4	H_2/CO_2	CO_2/CH_4	H_2/CH_4
M1	1.407	0.426	0.01192	3.30	35.74	118.02
M2	1.438	0.403	0.01095	3.57	36.82	131.39
M3	1.508	0.403	0.01341	3.74	30.09	112.48
M4	1.437	0.394	0.01204	3.64	32.77	119.38
M5	1.508	0.403	0.01341	3.79	23.81	90.20
Average	1.496	0.415	0.01341	3.61	31.85	114.29
Std. Dev.	0.102	0.019	0.00277	0.17	4.66	13.53

The permeance values of PES/PI 20/80 dense membranes were calculated by Equation 1.4. H_2 permeances of asymmetric PES/PI 20/80 membranes were ~3.5 fold of the dense membranes, due to the highly porous structure of the membrane. Gas molecules prefer to go through less resistive pores, consequently permeation rates of the gases trough the membrane increase significantly. In addition, very thin skin layer with sub-micron size pores decreases the resistance against the gas molecules. Asymmetric membrane production is advantageous compared to dense membranes, because industrial gas separation membranes should have high permeance values. The permeance values have found during this study are different than literature values, may because of different membrane structures [14,15,33]. The trend of increase in CO_2 and CH_4 permeances were found similar to H_2 permeances.

Table 4.10 Permeance and Selectivity Values of PES/PI 20/80 Asymmetric Membranes

	Permeance (GPU)			**Selectivity**		
	H_2	**CO_2**	**CH_4**	**H_2/CO_2**	**CO_2/CH_4**	**H_2/CH_4**
PES/PI 20/80 Dense	0.422	0.135	0.00379	3.13	35.6	111.35
PES/PI 20/80 Asymmetric	1.496	0.415	0.01341	3.61	31.85	114.29
Dense vs. Asym.	+255%	+207%	+254%	+15%	-3%	+3%

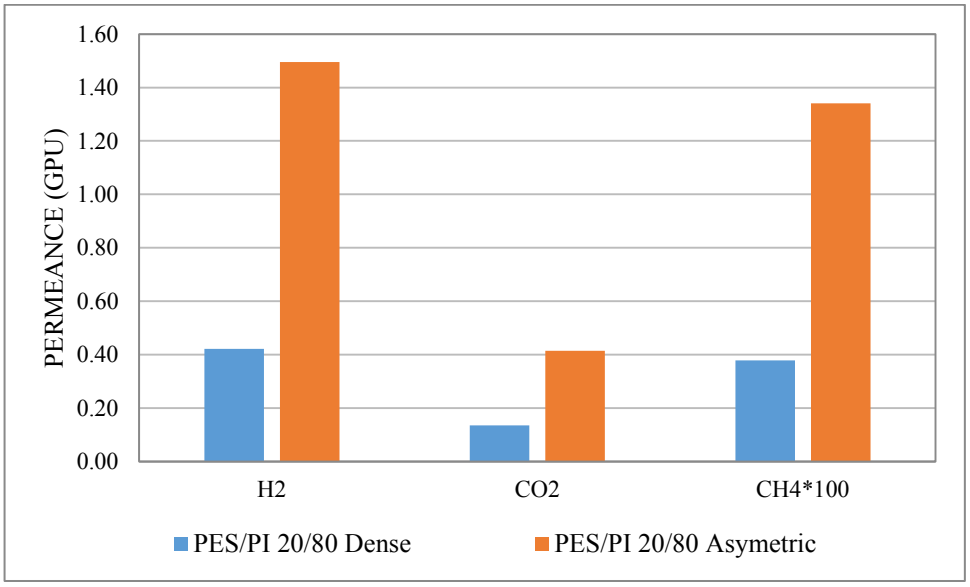

Figure 4.36 H_2, CO_2, and CH_4 Permeances of PES/PI 20/80 Dense and Asymmetric Membranes

Selectivity values of dense and asymmetric membranes were shown in Figure 4.37. Although the great increase in permeances, selectivity values were found close to that of PES/PI 20/80 dense membranes. In fact, H_2/CO_2 and H_2/CH_4 selectivity values increased by 15% and 3%, respectively. CO_2/CH_4 selectivity decreased only by 3%, which is considerably low.

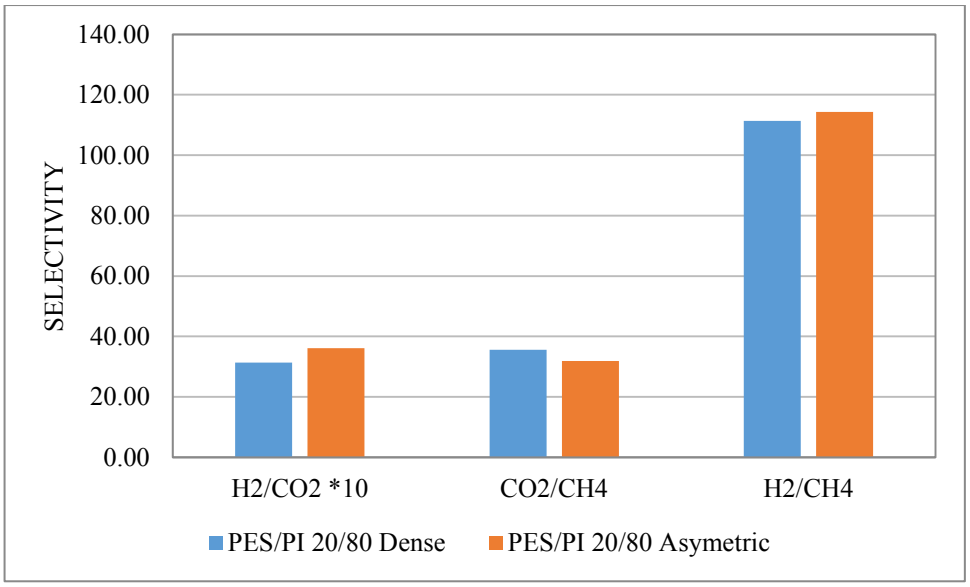

Figure 4.37 H_2/CO_2, CO_2/CH_4, and H_2/CH_4 Selectivities of PES/PI 20/80 Dense and Asymmetric Membranes

As a conclusion, the permeances of the PES/PI 20/80 membranes improved considerably by altering the membrane structure from dense to asymmetric. Moreover, selectivity values were not affected significantly by asymmetric membrane production method. Therefore, it can be suggested that PES/PI blend asymmetric membranes are worthy to investigate further and they can be good candidates as an industrial membranes.

CHAPTER 5

CONCLUSION

In this study, the effects of blend composition on gas separation performances of polymer blend based membranes were studied. At the beginning of the study PES/PC blend membranes were prepared and characterized with DSC. The results revealed that PES and PC are not compatible with each other, and prepared membranes were not suitable for the purpose of this study. Then, dense PES/PI membranes were prepared at different compositions. Further, 83nm ZIF-8 particles were added to PES/PI 20/80 membrane to investigate the effect of ZIF-8 on gas separation performances. Finally, asymmetric PES/PI 20/80 membranes were prepared and gas permeation test were conducted. The conclusions were listed as follows:

1. Dense blend membranes were prepared according to solvent evaporation method. Resulting membranes were clear as an early indication of miscibility and compatibility of PES and PI. Further, DSC analysis were conducted to prove the miscibility and compatibility. At the first runs of scans, only one glass transition temperature in between the temperatures of the pure polymers. The glass transition of the blend membranes increased as the %PI in the blend increased. The glass transition temperatures were applied to Gordon-Taylor model and k constant was calculated as 0.7, which is an indication of good interaction between the polymers.

2. Gas separation performance of PI is better than PES, and gas separation performance of the membranes increased as amount of PI in the blend increased. Results were compared with linear and logarithmic theoretical models. H_2 and

CO_2 permeability and H_2/CO_2 and H_2/CH_4 selectivity values were in accordance with the theoretical models. There were some deviations from these theoretical models in case of CH_4 permeability and CO_2/CH_4 selectivity. Interaction of CO_2 molecules with polymer chains may alter the chain conformation and free volume, consequently affected the CO_2/CH_4 selectivity. Since kinetic diameters of H_2 and CO_2 were comparatively smaller than CH_4, the permeabilities of H_2 and CO_2 were not affected by leak rate and free volume as much as CH_4. The gas separation performance of PES/PI 20/80 membranes were the best among the blend membranes for all gas pairs.

3. The incorporation of ZIF-8 with PES/PI 20/80 increased the H_2, CO_2, and CH_4 permeabilities. H_2/CO_2 and H_2/CH_4 selectivities were decreased 5% and 6%, respectively. On the other hand, CO_2/CH_4 selectivity increased 3% with addition of ZIF-8 to PES/PI 20/80 matrix.

4. Asymmetric PES/PI 20/80 blend membranes were prepared by wet phase inversion method. Coagulation bath was composed of v/v 75%IPA and 25% DMF. Membranes had 14 micron thick nano-porous skin layer on sponge-like porous support layer. This porous structure leaded to increase the permeance of the membranes for all gas pair. On the other hand, H_2/CO_2 and H_2/CH_4 selectivity values increased 15% and 3%, respectively. Unlikely, CO_2/CH_4 selectivity decreased approximately 3%.

REFERENCES

[1] J.K. Adewole, a. L. Ahmad, S. Ismail, C.P. Leo, Current challenges in membrane separation of CO2 from natural gas: A review, Int. J. Greenh. Gas Control. 17 (2013) 46–65. doi:10.1016/j.ijggc.2013.04.012 Review.

[2] R. Nasir, H. Mukhtar, Z. Man, D.F. Mohshim, Material Advancements in Fabrication of Mixed-Matrix Membranes, Chem. Eng. Technol. 36 (2013) 717–727. doi:10.1002/ceat.201200734.

[3] Hydrogen, RSC. (2014). http://www.rsc.org/periodic-table/element/1/hydrogen.

[4] Y. Li, F. Liang, H. Bux, W. Yang, J. Caro, Zeolitic imidazolate framework ZIF-7 based molecular sieve membrane for hydrogen separation, J. Memb. Sci. 354 (2010) 48–54. doi:10.1016/j.memsci.2010.02.074.

[5] L. Shao, B.T. Low, T.S. Chung, A.R. Greenberg, Polymeric membranes for the hydrogen economy: Contemporary approaches and prospects for the future, J. Memb. Sci. 327 (2009) 18–31. doi:DOI 10.1016/j.memsci.2008.11.019.

[6] N. Keser, PRODUCTION AND PERFORMANCE EVALUATION OF ZIF-8 BASED BINARY AND TERNARY MIXED MATRIX GAS SEPARATION MEMBRANES, Middle East Technical University, 2012.

[7] S. Kentish, C. Scholes, G. Stevens, Carbon Dioxide Separation through Polymeric Membrane Systems for Flue Gas Applications, Recent Patents Chem. Eng. 1 (2008) 52–66. doi:10.2174/2211334710801010052.

[8] H.A. Mannan, H. Mukhtar, T. Murugesan, R. Nasir, D.F. Mohshim, A. Mushtaq, Recent Applications of Polymer Blends in Gas Separation Membranes, Chem. Eng. Technol. 36 (2013) 1838–1846. doi:10.1002/ceat.201300342.

[9] A. Mushtaq, H. Mukhtar, A.M. Shariff, H.A. Mannan, A Review : Development of Polymeric Blend Membrane for Removal of CO2 from Natural Gas, Int. J. Eng. Technol. IJET-IJENS. 13 (2013) 53–60.

[10] M. Mulder, Basic Principles of Membrane Technology, Zeitschrift Für Phys. Chemie. 72 (1998) 564.

[11] S.S. Madaeni, A. Farhadian, V. Vatanpour, Effects of Phase Inversion and Composition of Casting Solution on Morphology and Gas Permeance of Polyethersulfone / Polyimide Blend Membranes, Adv. Polym. Technol. 31 (2012) 298–309. doi:10.1002/adv.

[12] L.M. Robeson, The upper bound revisited, J. Memb. Sci. 320 (2008) 390–400. doi:10.1016/j.memsci.2008.04.030.

[13] B.D. Freeman, Basis of Permeability/Selectivity Tradeoff Relations in Polymeric Gas Separation Membranes, Macromolecules. 32 (1999) 375–380. doi:10.1021/ma9814548.

[14] O.M. Ekiner, Blends of polyethersulfones with aromatic polyimides, polyamides or polyamide-imides and gas separation membranes made therefrom., EP 0 648 812 A2, 1994.

[15] S. Basu, A. Cano-Odena, I.F.J. Vankelecom, Asymmetric membrane based on Matrimid® and polysulphone blends for enhanced permeance and stability in binary gas (CO2/CH4) mixture separations, Sep. Purif. Technol. 75 (2010) 15–21. doi:10.1016/j.seppur.2010.07.004.

[16] Y. Zhang, J. Sunarso, S. Liu, R. Wang, Current status and development of membranes for CO2/CH4 separation: A review, Int. J. Greenh. Gas Control. 12 (2013) 84–107. doi:10.1016/j.ijggc.2012.10.009.

[17] A. Bos, I. Pünt, H. Strathmann, M. Wessling, Suppression of gas separation membrane plasticization by homogeneous polymer blending, AIChE J. 47 (2001) 1088–1093. doi:10.1002/aic.690470515.

[18] D.Q. Vu, W.J. Koros, S.J. Miller, Mixed matrix membranes using carbon molecular sieves I . Preparation and experimental results, 211 (2003) 311–334.

[19] T.-S. Chung, L.Y. Jiang, Y. Li, S. Kulprathipanja, Mixed matrix membranes (MMMs) comprising organic polymers with dispersed inorganic fillers for gas separation, Prog. Polym. Sci. 32 (2007) 483–507. doi:10.1016/j.progpolymsci.2007.01.008.

[20] D. Bastani, N. Esmaeili, M. Asadollahi, Polymeric mixed matrix membranes containing zeolites as a filler for gas separation applications: A review, J. Ind. Eng. Chem. 19 (2013) 375–393. doi:10.1016/j.jiec.2012.09.019.

[21] U. Cakal, NATURAL GAS PURIFICATION BY ZEOLITE FILLED POLYETHERSULFONE BASED MIXED MATRIX MEMBRANES, Middle East Technical University, 2009.

[22] B. Zornoza, C. Téllez, J. Coronas, J. Gascon, F. Kapteijn, Metal organic framework based mixed matrix membranes: An increasingly important field of research with a large application potential, Microporous Mesoporous Mater. 166 (2013) 67–78. doi:10.1016/j.micromeso.2012.03.012.

[23] R. Adams, C. Carson, J. Ward, R. Tannenbaum, W. Koros, Metal organic framework mixed matrix membranes for gas separations, Microporous Mesoporous Mater. 131 (2010) 13–20. doi:10.1016/j.micromeso.2009.11.035.

[24] P.S. Goh, A.F. Ismail, S.M. Sanip, B.C. Ng, M. Aziz, Recent advances of inorganic fillers in mixed matrix membrane for gas separation, Sep. Purif. Technol. 81 (2011) 243–264. doi:10.1016/j.seppur.2011.07.042.

[25] N. Keser Demir, B. Topuz, L. Yilmaz, H. Kalipcilar, Synthesis of ZIF-8 from recycled mother liquors, Microporous Mesoporous Mater. 198 (2014) 291–300. doi:10.1016/j.micromeso.2014.07.052.

[26] B. Ghalei, M.-A. Semsarzadeh, A Novel Nano Structured Blend Membrane for Gas Separation, Macromol. Symp. 249-250 (2007) 330–335. doi:10.1002/masy.200750354.

[27] D. Jiang, X.R. Zhang, Y.M. Ma, C.Y. Ma, Compatibility of Polyethersulfone/Polycarbonate Blends, Adv. Mater. Res. 217-218 (2011) 1601–1605. doi:10.4028/www.scientific.net/AMR.217-218.1601.

[28] B. Gholizadeh, A. Arefazar, J. Barzin, Morphology and Gas Permeability of Polymeric Membrane by PC / PA6 / Nanoclay Ternary Nanocomposite, Polym. Polym. Compos. 20 (2012) 271–279.

[29] K. Liang, J. Grebowicz, E. Valles, F.E. Karasz, W.J. MacKnight, Thermal and rheological properties of miscible polyethersulfone/polyimide blends, J. Polym. Sci. Part B Polym. Phys. 30 (1992) 465–476. doi:10.1002/polb.1992.090300506.

[30] G.C. Kapantaidakis, S.P. Kaldis, X.S. Dabou, G.P. Sakellaropoulos, Gas permeation through PSF-PI miscible blend membranes, J. Memb. Sci. 110 (1996) 239–247. doi:10.1016/0376-7388(95)00265-0.

[31] S.S. Hosseini, M.M. Teoh, T.S. Chung, Hydrogen separation and purification in membranes of miscible polymer blends with interpenetration networks, Polymer (Guildf). 49 (2008) 1594–1603. doi:10.1016/j.polymer.2008.01.052.

[32] M. Iqbal, Z. Man, H. Mukhtar, B.K. Dutta, Solvent effect on morphology and CO2/CH4 separation performance of asymmetric polycarbonate membranes, J. Memb. Sci. 318 (2008) 167–175. doi:10.1016/j.memsci.2008.02.040.

[33] J. Han, W. Lee, J.M. Choi, R. Patel, B.R. Min, Characterization of polyethersulfone/polyimide blend membranes prepared by a dry/wet phase inversion: Precipitation kinetics, morphology and gas separation, J. Memb. Sci. 351 (2010) 141–148. doi:10.1016/j.memsci.2010.01.038.

[34] S.S. Hosseini, N. Peng, T.S. Chung, Gas separation membranes developed through integration of polymer blending and dual-layer hollow fiber spinning process for hydrogen and natural gas enrichments, J. Memb. Sci. 349 (2010) 156–166. doi:10.1016/j.memsci.2009.11.043.

[35] G.C. Kapantaidakis, G.H. Koops, High flux polyethersulfone–polyimide blend hollow fiber membranes for gas separation, J. Memb. Sci. 204 (2002) 153–171. doi:10.1016/S0376-7388(02)00030-3.

[36] S. Rafiq, Z. Man, A. Maulud, N. Muhammad, S. Maitra, Effect of varying solvents compositions on morphology and gas permeation properties on membranes blends for CO2 separation from natural gas, J. Memb. Sci. 378 (2011) 444–452. doi:10.1016/j.memsci.2011.05.025.

[37] F. Dorosti, M.R. Omidkhah, M.Z. Pedram, F. Moghadam, Fabrication and characterization of polysulfone/polyimide–zeolite mixed matrix membrane for gas separation, Chem. Eng. J. 171 (2011) 1469–1476. doi:10.1016/j.cej.2011.05.081.

[38] A.F. Ismail, R.A. Rahim, W.A.W.A. Rahman, Characterization of polyethersulfone/Matrimid® 5218 miscible blend mixed matrix membranes for O2/N2 gas separation, Sep. Purif. Technol. 63 (2008) 200–206. doi:10.1016/j.seppur.2008.05.007.

[39] S. Basu, A. Cano-Odena, I.F.J. Vankelecom, Asymmetric Matrimid®/[Cu3(BTC)2] mixed-matrix membranes for gas separations, J. Memb. Sci. 362 (2010) 478–487. doi:10.1016/j.memsci.2010.07.005.

[40] S. Rafiq, Z. Man, A. Maulud, N. Muhammad, S. Maitra, Separation of CO2 from CH4 using polysulfone/polyimide silica nanocomposite membranes, Sep. Purif. Technol. 90 (2012) 162–172. doi:10.1016/j.seppur.2012.02.031.

[41] Ġ Ayas, Effect of the particle size of ZIF-8 on the separation performance of ZIF-8/pNA/PES membranes, Middle East Technical University, 2014.

[42] K.S. Park, Z. Ni, A.P. Côté, J.Y. Choi, R. Huang, F.J. Uribe-Romo, et al., Exceptional chemical and thermal stability of zeolitic imidazolate frameworks., Proc. Natl. Acad. Sci. U. S. A. 103 (2006) 10186–10191. doi:10.1073/pnas.0602439103.

[43] T. Ozawa, A New Method of Analyzing Thermogravimetric Data, Bull. Chem. Soc. Jpn. 38 (1965) 1881–1886. doi:10.1246/bcsj.38.1881.

[44] W.A.W.A. Rahman, FORMATION AND CHARACTERIZATION OF MIXED MATRIX COMPOSITE MATERIALS FOR EFFICIENT ENERGY GAS SEPARATION, 2006.

[45] J. Ahmad, M.-B. Hägg, Development of matrimid/zeolite 4A mixed matrix membranes using low boiling point solvent, Sep. Purif. Technol. 115 (2013) 190–197. doi:10.1016/j.seppur.2013.04.049.

[46] K. Liang, G. Bánhegyi, F.E. Karasz, W.J. MacKnight, Thermal, dielectric, and mechanical relaxation in poly(benzimidazole)/poly(etherimide) blends, J. Polym. Sci. Part B Polym. Phys. 29 (1991) 649–657. doi:10.1002/polb.1991.090290602.

[47] F.W. Billmeyer Jr., Textbook of Polymer Science, 3rd ed., John Wiley & Sons, Ltd, New York, 1984.

[48] E. Karatay, H. Kalıpçılar, L. Yılmaz, Preparation and performance assessment of binary and ternary PES-SAPO 34-HMA based gas separation membranes, J. Memb. Sci. 364 (2010) 75–81. doi:10.1016/j.memsci.2010.08.004.

[49] Y. Zhang, I.H. Musselman, J.P. Ferraris, K.J. Balkus, Gas permeability properties of Matrimid® membranes containing the metal-organic framework Cu–BPY–HFS, J. Memb. Sci. 313 (2008) 170–181. doi:10.1016/j.memsci.2008.01.005.

[50] M. Peydayesh, S. Asarehpour, T. Mohammadi, O. Bakhtiari, Preparation and characterization of SAPO-34 – Matrimid® 5218 mixed matrix membranes for CO2/CH4 separation, Chem. Eng. Res. Des. 91 (2013) 1335–1342. doi:10.1016/j.cherd.2013.01.022.

[51] S. Shahid, K. Nijmeijer, High pressure gas separation performance of mixed-matrix polymer membranes containing mesoporous Fe(BTC), J. Memb. Sci. 459 (2014) 33–44. doi:10.1016/j.memsci.2014.02.009.

[52] E. V. Perez, K.J. Balkus, J.P. Ferraris, I.H. Musselman, Mixed-matrix membranes containing MOF-5 for gas separations, J. Memb. Sci. 328 (2009) 165–173. doi:10.1016/j.memsci.2008.12.006.

[53] M.J.C. Ordoñez, K.J. Balkus, J.P. Ferraris, I.H. Musselman, Molecular sieving realized with ZIF-8/Matrimid® mixed-matrix membranes, J. Memb. Sci. 361 (2010) 28–37. doi:10.1016/j.memsci.2010.06.017.

[54] S. Basu, A. Cano-Odena, I.F.J. Vankelecom, MOF-containing mixed-matrix membranes for CO2/CH4 and CO2/N2 binary gas mixture separations, Sep. Purif. Technol. 81 (2011) 31–40. doi:10.1016/j.seppur.2011.06.037.

[55] K. Díaz, M. López-González, L.F. del Castillo, E. Riande, Effect of zeolitic imidazolate frameworks on the gas transport performance of ZIF8-poly(1,4-phenylene ether-ether-sulfone) hybrid membranes, J. Memb. Sci. 383 (2011) 206–213. doi:10.1016/j.memsci.2011.08.042.

[56] Q. Song, S.K. Nataraj, M. V. Roussenova, J.C. Tan, D.J. Hughes, W. Li, et al., Zeolitic imidazolate framework (ZIF-8) based polymer nanocomposite membranes for gas separation, Energy Environ. Sci. 5 (2012) 8359. doi:10.1039/c2ee21996d.

[57] R.J. Li, W.P. Hsu, T.K. Kwei, A.S. Myerson, Transport of gases in miscible polymer blends above and below the glass transition region, AIChE J. 39 (1993) 1509–1518. doi:10.1002/aic.690390910.

[58] L.M. Robeson, Polymer Blends in Membrane Transport Processes, Ind. Eng. Chem. Res. 49 (2010) 11859–11865. doi:10.1021/ie100153q.

[59] A.L. Khan, X. Li, I.F.J. Vankelecom, SPEEK/Matrimid blend membranes for CO2 separation, J. Memb. Sci. 380 (2011) 55–62. doi:10.1016/j.memsci.2011.06.030.

APPENDIX A

CALCULATION OF SINGLE PERMEABILITIES

Gas permeability results were calculated by depending on the rate of pressure change in permeate with respect to time. Pressure changes were recorded by computer program. A sample rate of change in pressure with respect to time is given in Figure A.1.

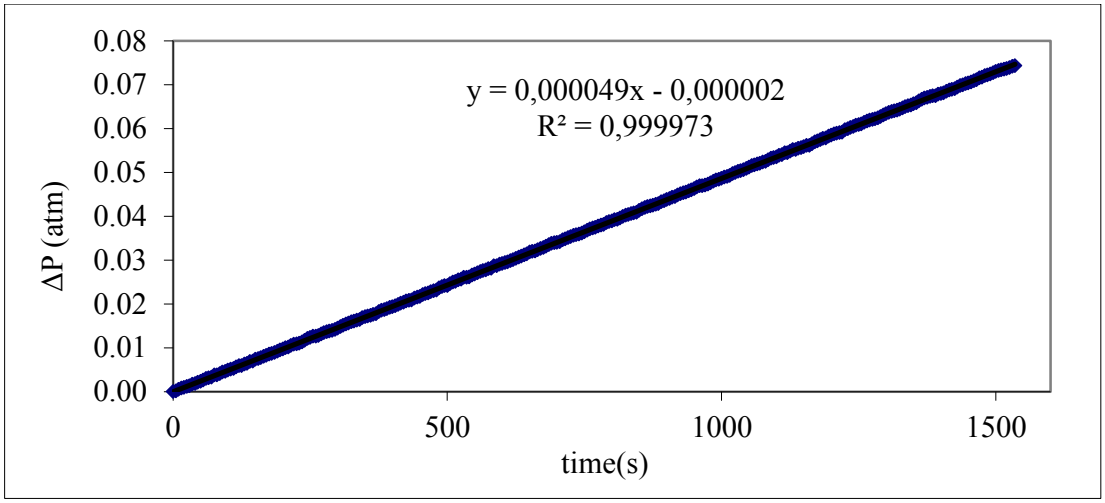

Figure A.1 The time (s) vs. pressure change (atm) graph for H2 permeation test of PES/PI 20/80

The permeability calculation algorithm is started with calculation of ΔP, which is the subtraction of the initial pressure from the n^{th} pressure each time.

$$\Delta P = P_n - P_0 \qquad \text{Equation A. 1}$$

The slope of ΔP vs t graph equals to (ΔP/ Δt). By using this slope the rate of change of moles was calculated.

$$\Delta n/\Delta t\,(\mathrm{mol}/s) = [(\Delta P/\Delta t) * V_d]/RT \qquad \text{Equation A. 2}$$

where V_d is the dead volume of the permeate, T is the test temperature, and R is the gas constant.

The volumetric rate of change is calculated as follows:

$$\Delta V/\Delta t\,(cm^3/s) = [(\Delta n/\Delta t) * M]/\rho \qquad \text{Equation A. 3}$$

where M is the molecular weight of the gas and ρ is the density of the gas.

Flux of the gas through the membrane is the volumetric flow rate per effective membrane area, which is 9.6 cm^2.

$$J(cm^3/cm^2.s) = \Delta V/\Delta t/A \qquad \text{Equation A. 4}$$

The gas permeability of the membrane is calculated as follows:

$$P(Barrer) = J * l/P_f - P_p \qquad \text{Equation A. 5}$$

Where P_f is the feed pressure, P_p is the permeate pressure, which is the average of P_0 and P_n, and l is the membrane thickness.

APPENDIX B

SAMPLE CALCULATION OF ZIF-8 YIELD AND AVERAGE PARTICLE SIZE

ZIF-8 synthesis took place in methanol medium. The yield is calculated from the initial amounts of reactants and final amount of synthesized ZIF-8. The reaction of zinc nitrate hexahydrate and HMIM is given below:

$$6\ Zn(NO_3)_2.6H_2O + 12\ C_4H_6N_2 \xrightarrow{CH_3OH} Zn_6N_{24}C_{48}H_{60}\ \ (ZIF-8)$$

Initial Reaction Mixtures:

- $4.8\ g\ Zn(NO_3)_2.6H_2O\ in\ 180.8\ g\ CH_3OH$
- $10.56\ g\ C_4H_6N_2\ in\ 180.8\ g\ CH_3OH$

where,

- $MW_{Zn(NO_3)_2.6H_2O} = 297.49\ g/mole$
- $MW_{C_4H_6N_2} = 82.11\ g/mole$
- $MW_{CH_3OH} = 32.11\ g/mole$
- $MW_{Zn_6N_{24}C_{48}H_{60}} = 1365.51\ g/mole$

The dried weight of synthesized ZIF-8 was 1.36 g. Consumed and remained amounts of $Zn(NO_3)_2.6H_2O$, HMIM and methanol was calculated as follows:

$$Consumed\ Zn^{2+} = \frac{1.36\ g\ ZIF-8}{1365.51 \frac{g\ ZIF-8}{mole\ ZIF-8}} * \frac{6\ mole\ Zn^{2+}}{1\ mole\ ZIF-8} * \frac{297.49\ g\ Zn^{2+}}{1\ mole\ Zn^{2+}}$$
$$= 1.78\ g\ Zn^{2+}$$

$$Remaining\ Zn^{2+} = Initial\ amount\ of\ Zn^{2+} - Consumed\ amount\ of\ Zn^{2+}$$
$$= 4.8\ g - 1.78\ g = 3.02\ g\ Zn^{2+}$$

$$Consumed\ HMIM = \frac{1.36\ g\ ZIF-8}{1365.51 \frac{g\ ZIF-8}{mole\ ZIF-8}} * \frac{12\ mole\ HMIM}{1\ mole\ ZIF-8} * \frac{82.11\ g\ HMIM}{1\ mole\ HMIM}$$
$$= 0.98\ g\ HMIM$$

$$Remainin\ HMIM = Initial\ amount\ of\ HMIM - Consumed\ amount\ og\ HMIM$$
$$= 9.58\ g\ HMIM$$

$$Remaining\ MeOH$$
$$= 4.8\ g\ Zn^{2+} + 10.56\ g\ HMIM + (180.8 * 2) g\ MeOH$$
$$- 1.78\ g\ ZIF-8 - 3.02\ g\ Zn^{2+} - 9.58\ g\ HMIM$$
$$= 362.58\ g\ MeOH$$

The maximum amount of ZIF-8 that could be synthesized was calculated as follows:

$$Maximum\ amount\ of\ ZIF-8$$
$$= \frac{4.8\ g\ Zn^{2+}}{297.49 \frac{g\ ZIF-8}{mole\ ZIF-8}} * \frac{1\ mole\ ZIF-8}{6\ mole\ Zn^{2+}} * \frac{1365.51 g\ ZIF-8}{1\ mole\ ZIF-8}$$
$$= 3.67\ g\ ZIF-8$$

$$Yield\ \% = \frac{Actual\ amount\ of\ ZIF-8}{Maximum\ amount\ of\ ZIF-8} * 100 = \frac{1.36\ g\ ZIF-8}{3.67\ g\ ZIF-8} = \mathbf{37.06}\ \%$$

Table B.1 Average Particle Size of ZIF-8 Crystals from SEM micrographs

	68.7
	55.6
	81.7
	104.9
	76.6
	65.6
	63.5
	60.4
	93
	99.1
	100.1
	87.2
	83.9
	82.1
	74.7
	113.5
	96.2
Average	82.7
St. Deviation	16.3

APPENDIX C

TGA THERMOGRAMS OF DENSE AND ASYMMETRIC PES/PI 20/80, AND PES/PI/ZIF-8 20/80/10 MEMBRANES

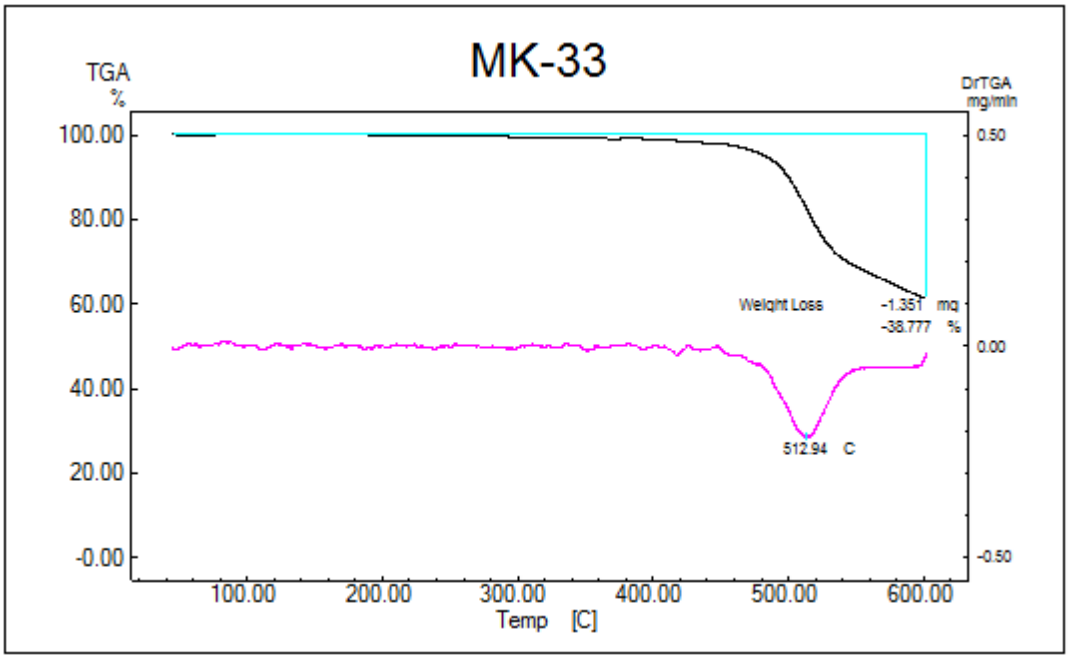

Figure C.1 The TGA thermogram of Dense PES/PI 20/80 Membrane 1

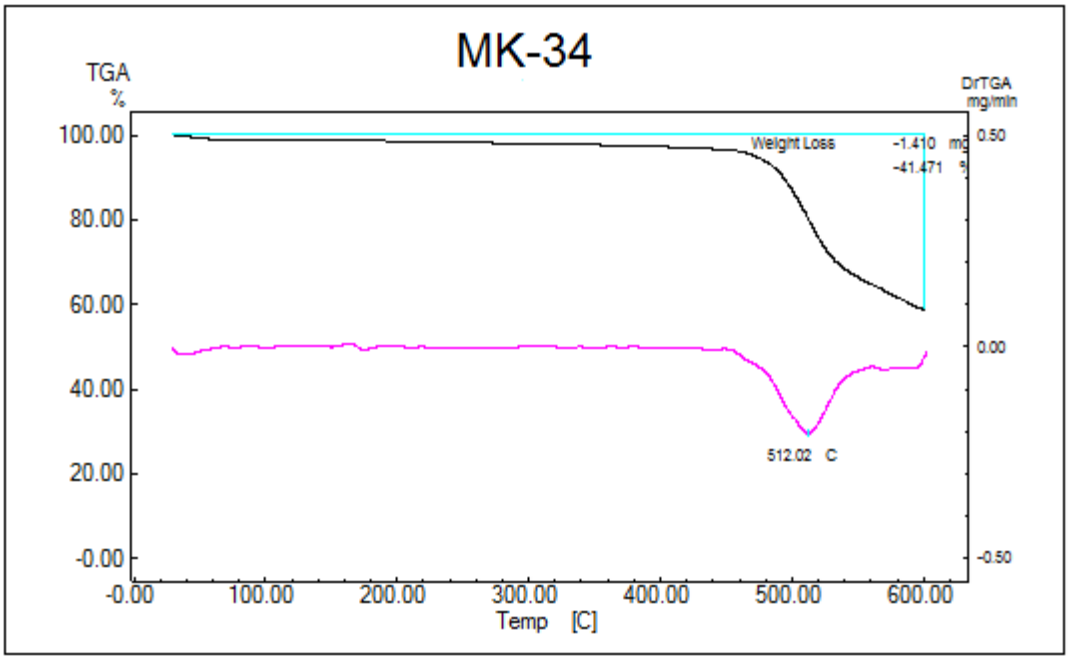

Figure C.2 The TGA thermogram of Dense PES/PI 20/80 Membrane 2

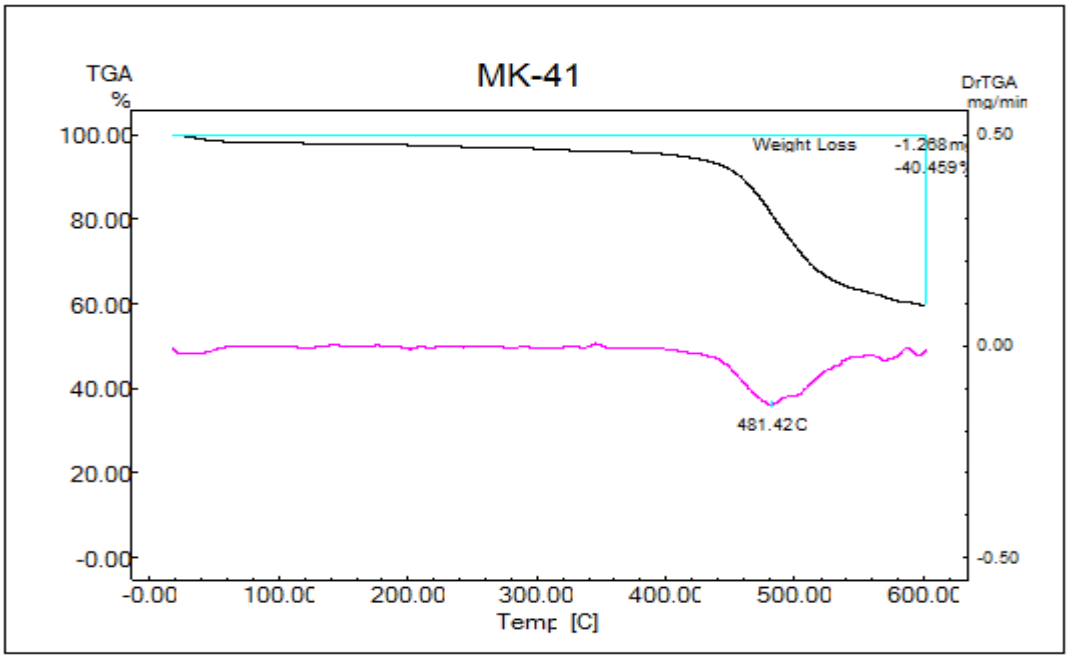

Figure C.3 The TGA thermogram of Dense PES/PI/ZIF-8 20/80/10 Membrane 1

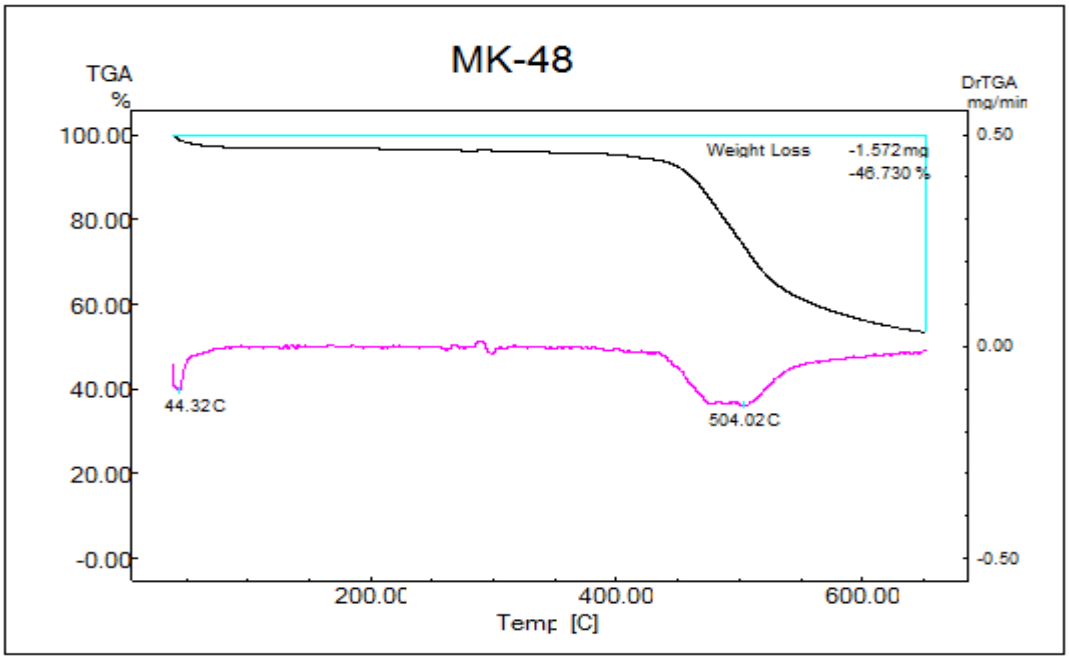

Figure C.4 The TGA thermogram of Dense PES/PI/ZIF-8 20/80/10 Membrane 2

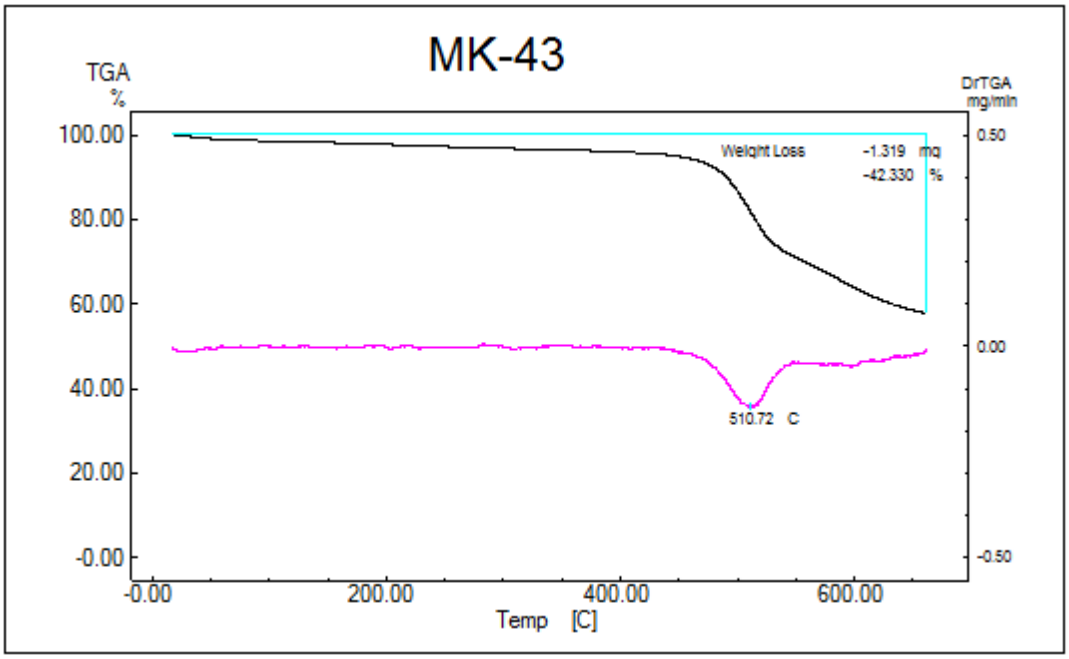

Figure C.5 The TGA thermogram of Asymmetric PES/PI 20/80 Membrane 1

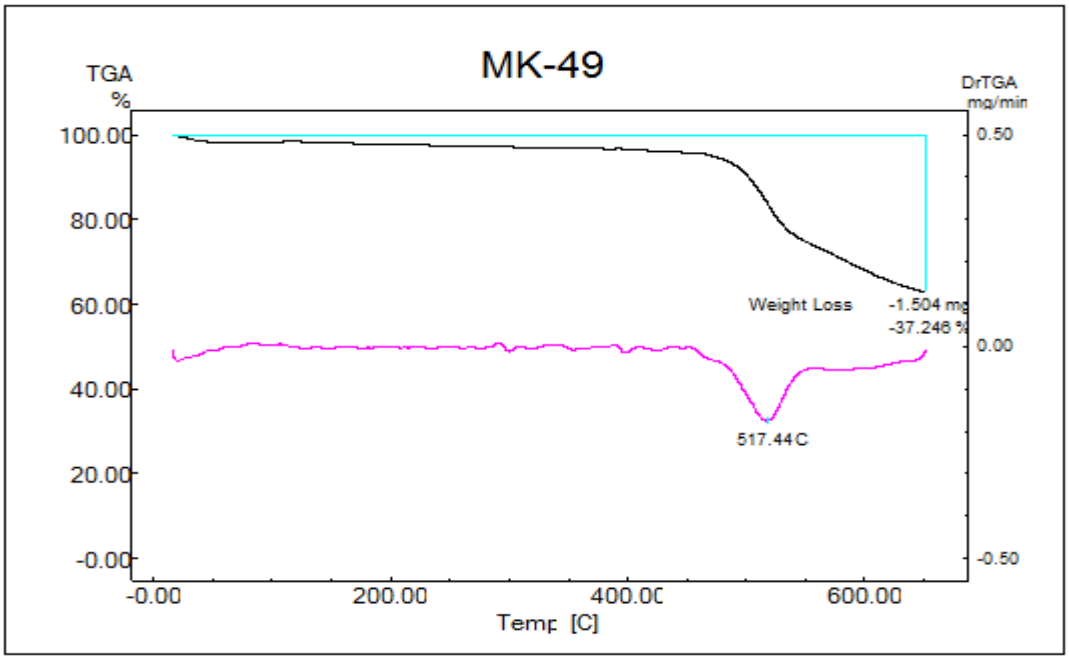

Figure C.6 The TGA thermogram of Asymmetric PES/PI 20/80 Membrane 2

APPENDIX D

DSC SCANS OF PES/PI BLEND MEMBRANES

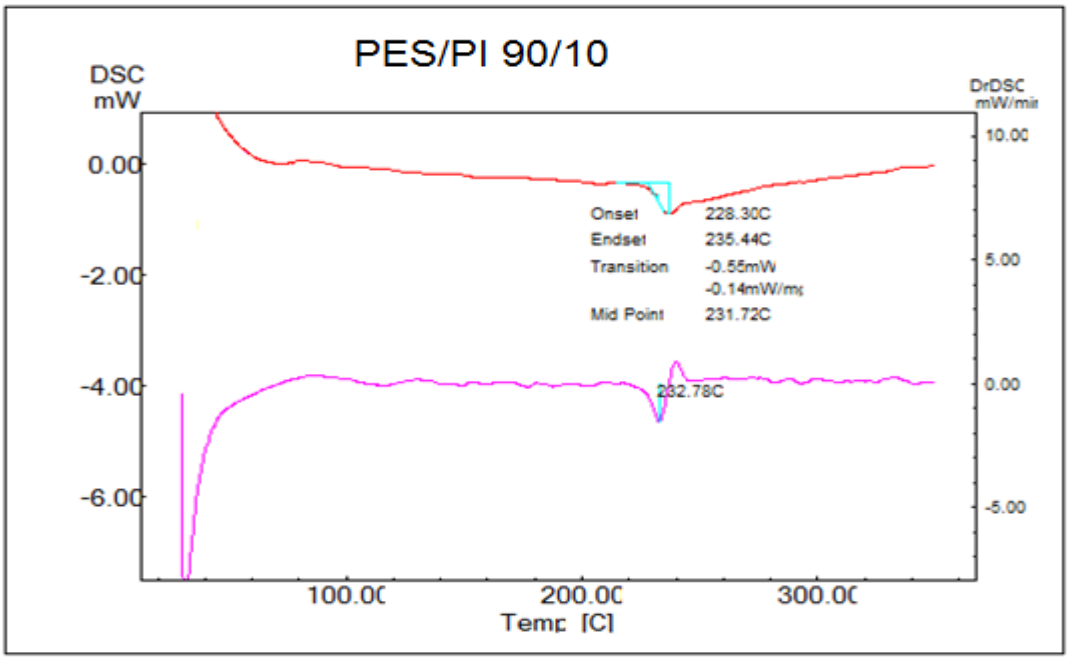

Figure D.1 DSC thermogram of PES/PI 90/10

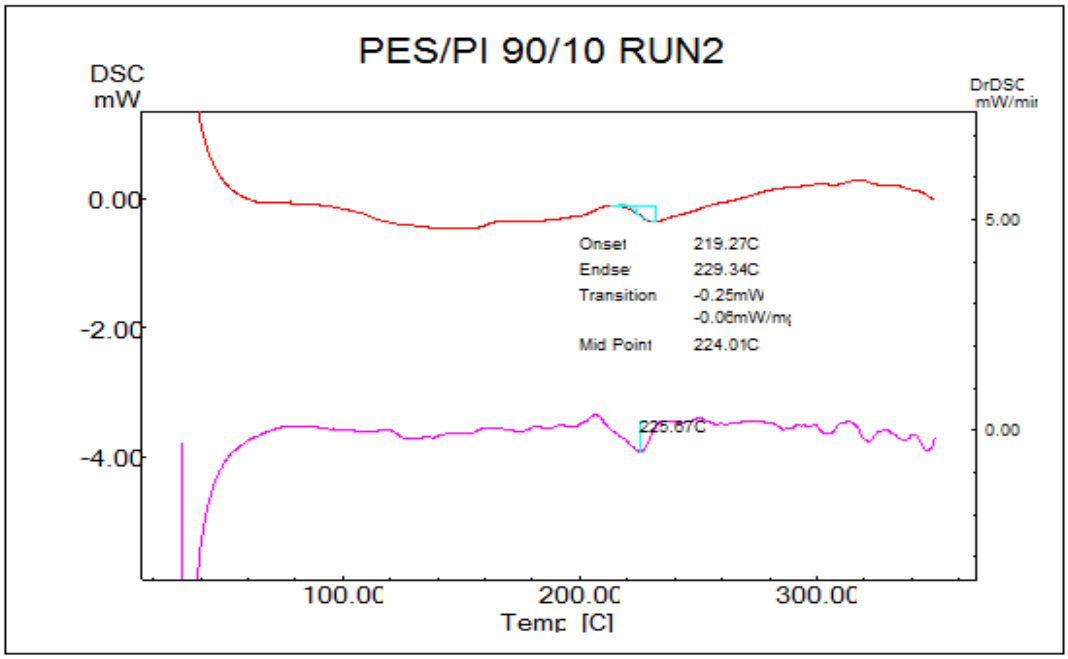

Figure D.2 DSC thermogram of PES/PI 90/10 Run2

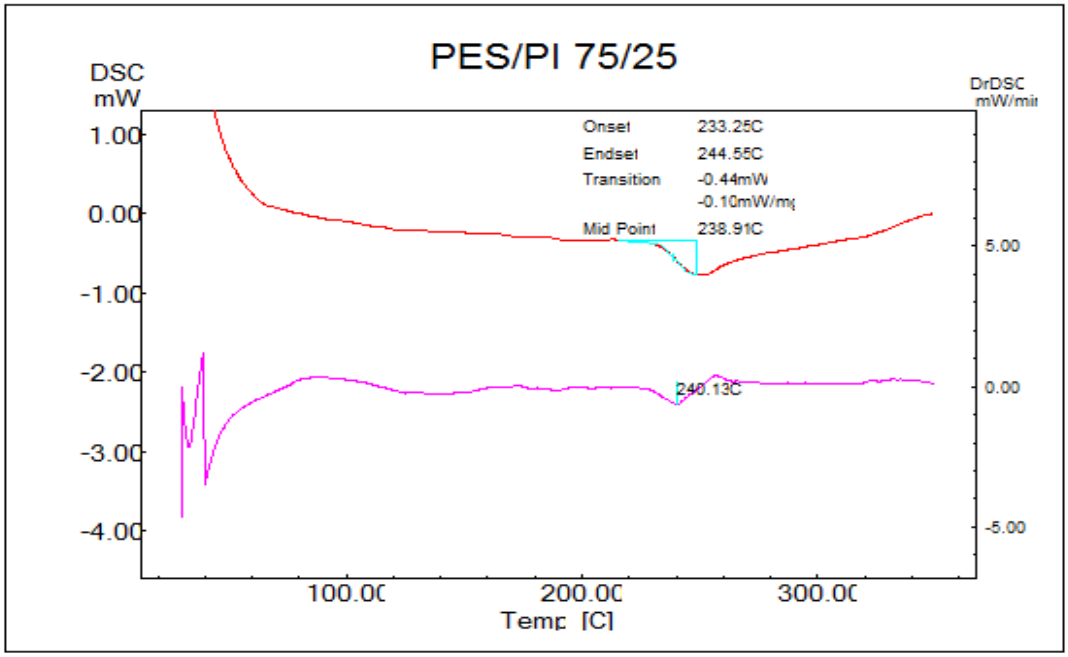

Figure D.3 DSC thermogram of PES/PI 75/25

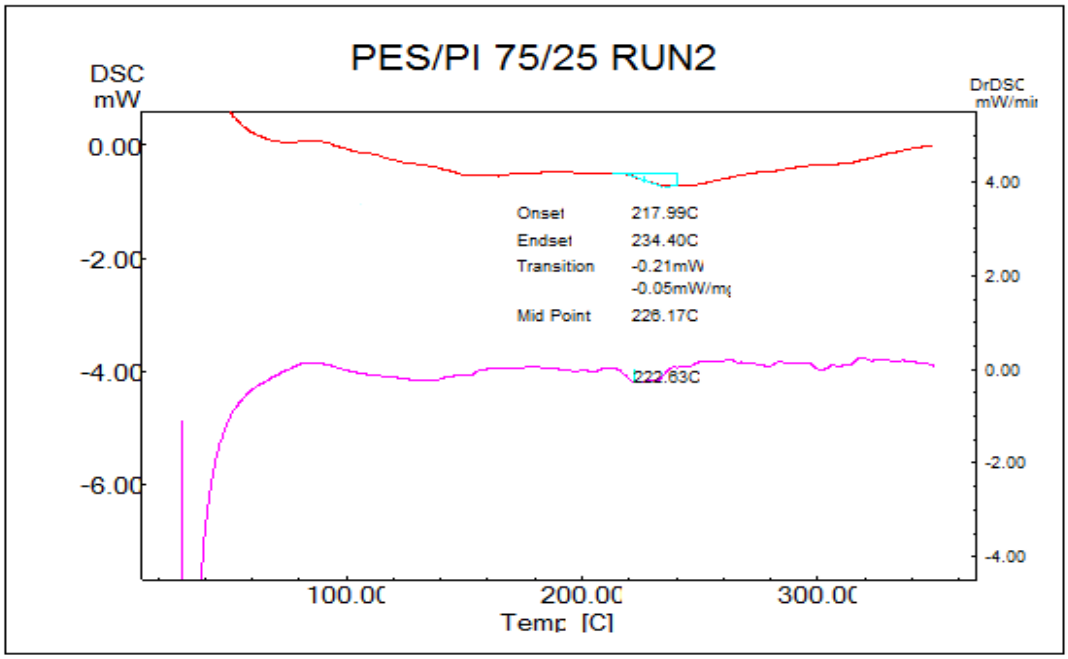

Figure D.4 DSC thermogram of PES/PI 75/25 Run2

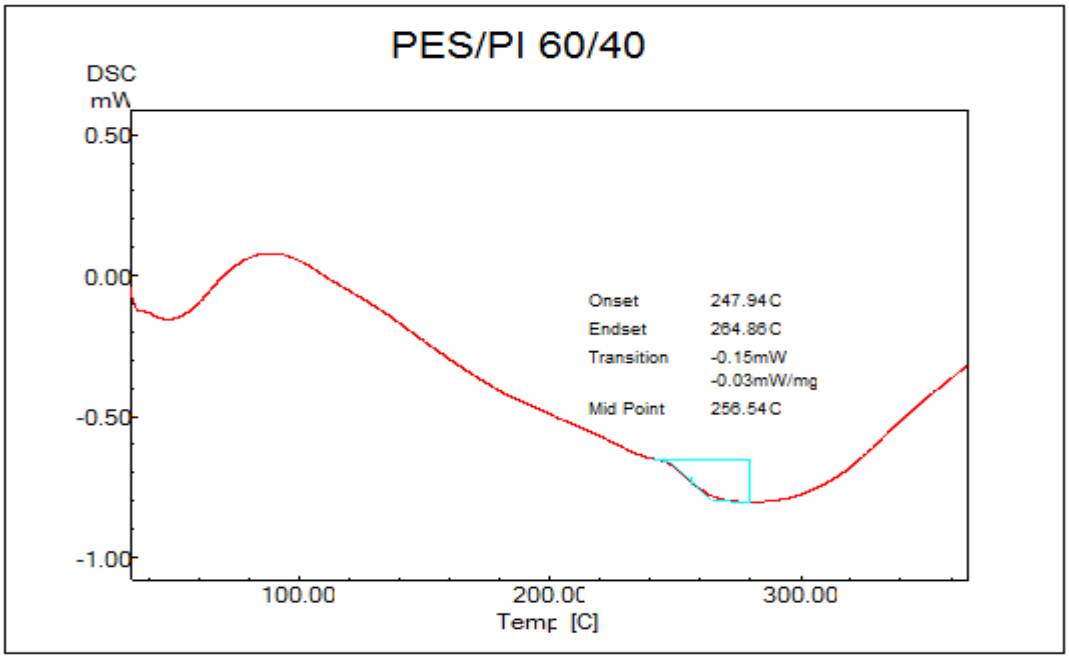

Figure D.5 DSC thermogram of PES/PI 60/40

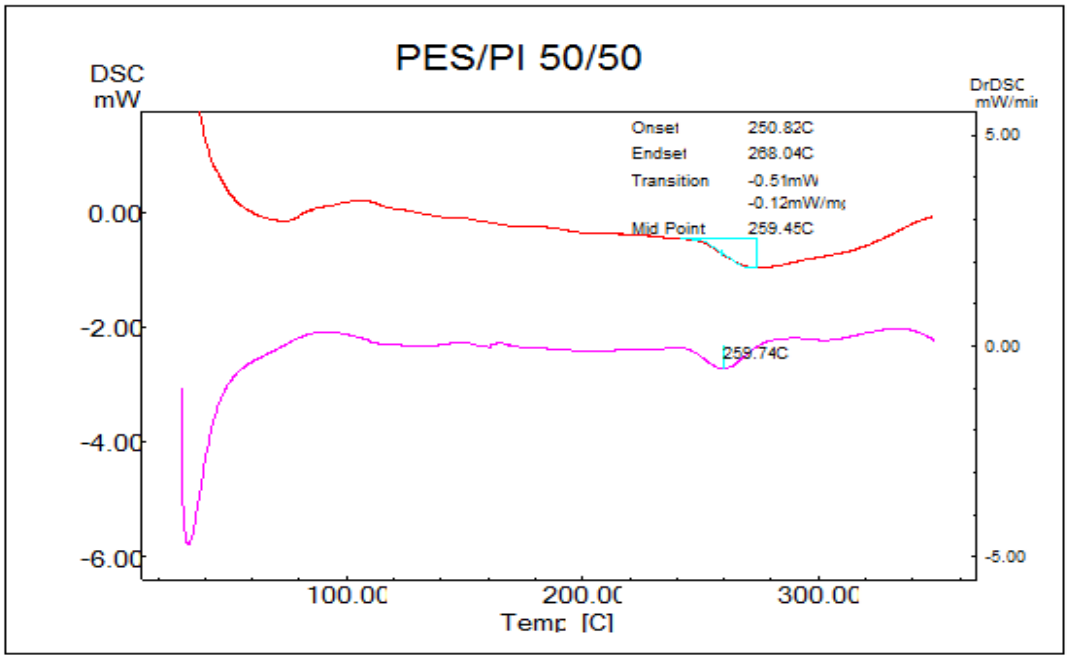

Figure D.6 DSC thermogram of PES/PI 50/50

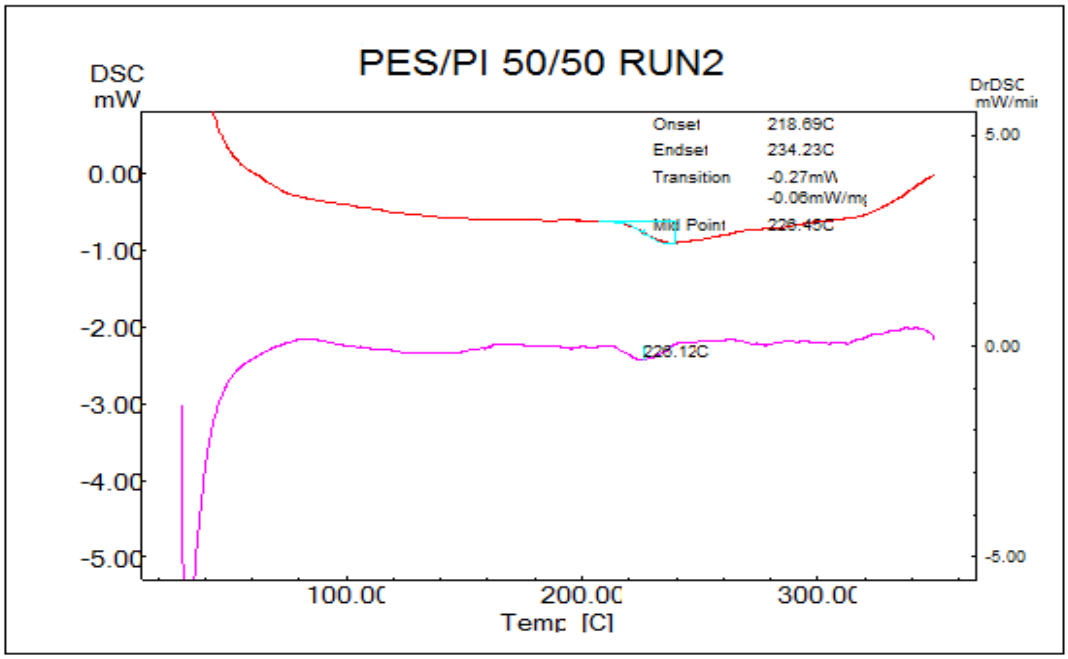

Figure D.7 DSC thermogram of PES/PI 50/50 Run2

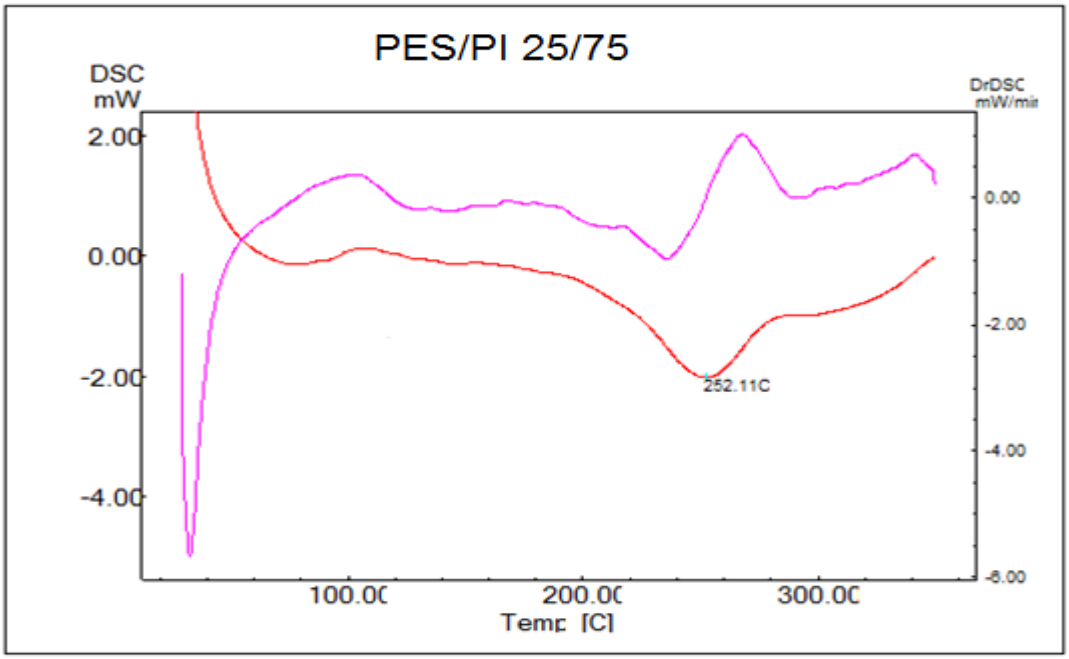

Figure D.8 DSC thermogram of PES/PI 25/75

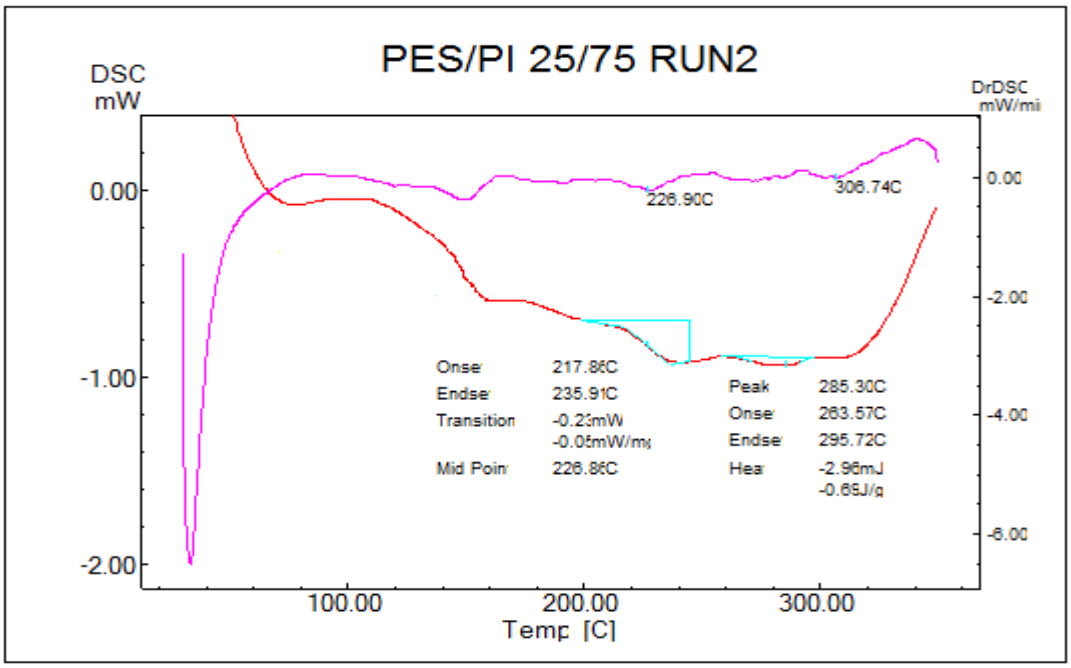

Figure D.9 DSC thermogram of PES/PI 25/75 Run2

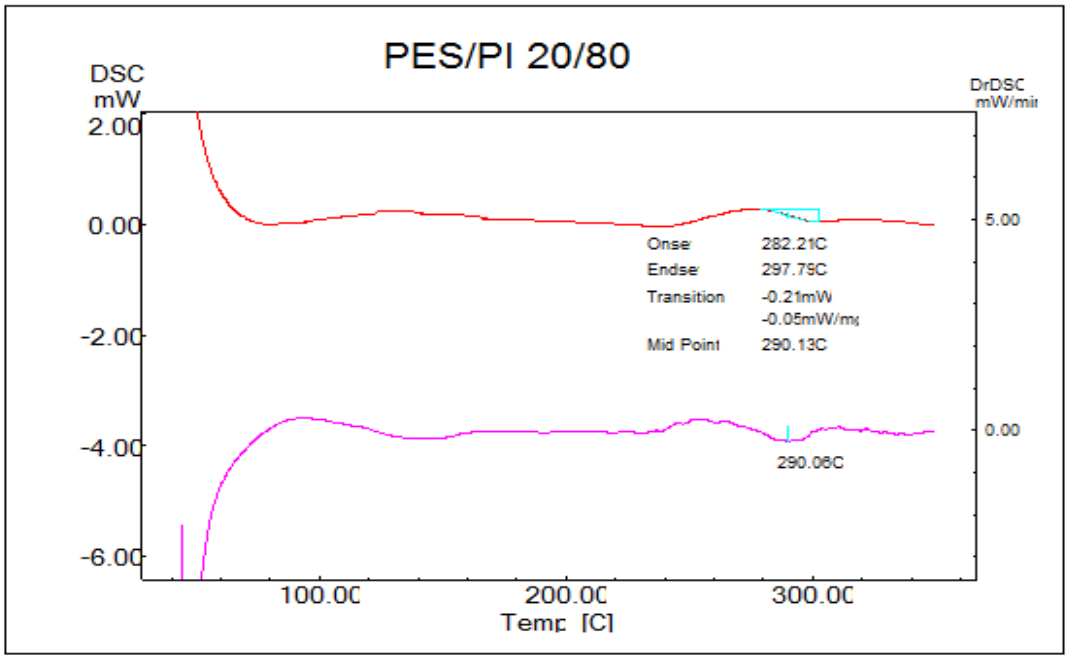

Figure D.10 DSC thermogram of PES/PI 20/80

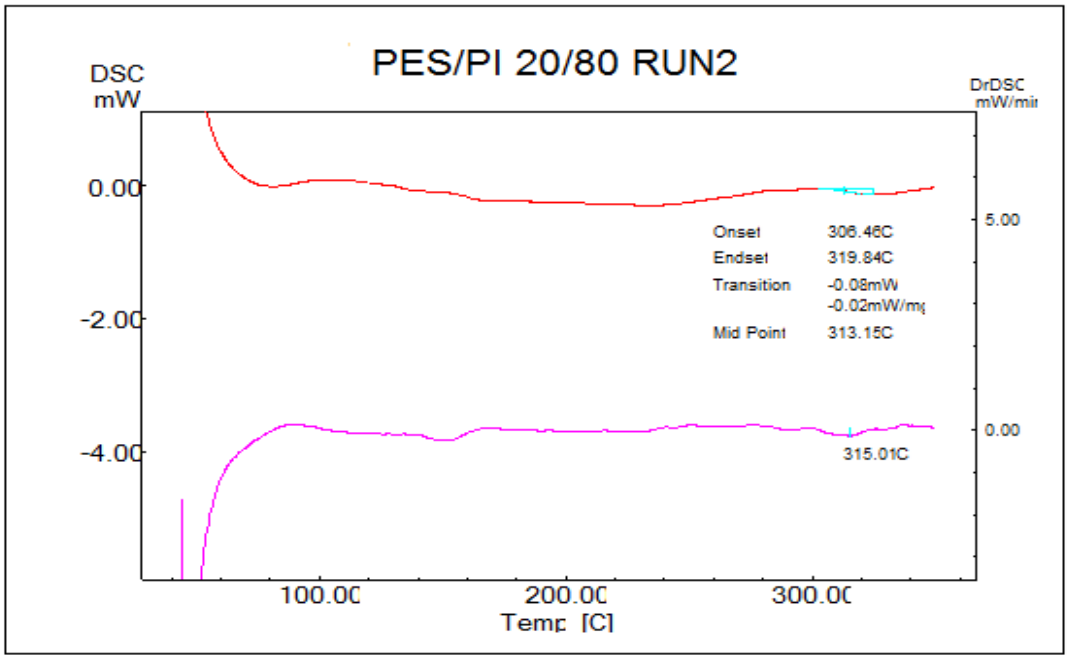

Figure D.11 DSC thermogram of PES/PI 20/80 Run2

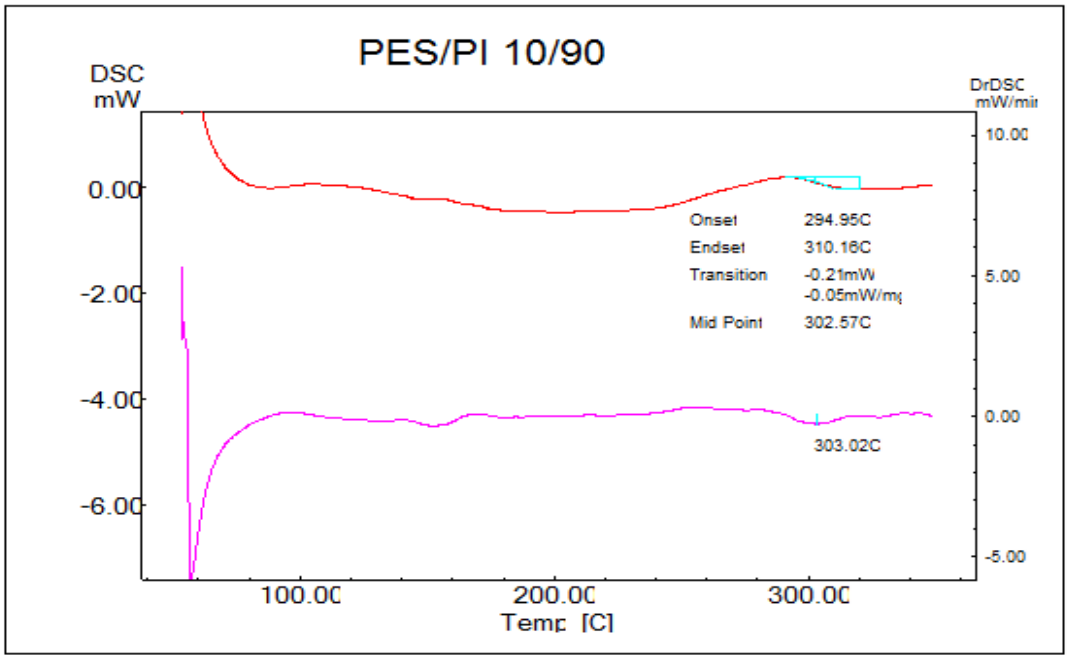

Figure D.12 DSC thermogram of PES/PI 10/90

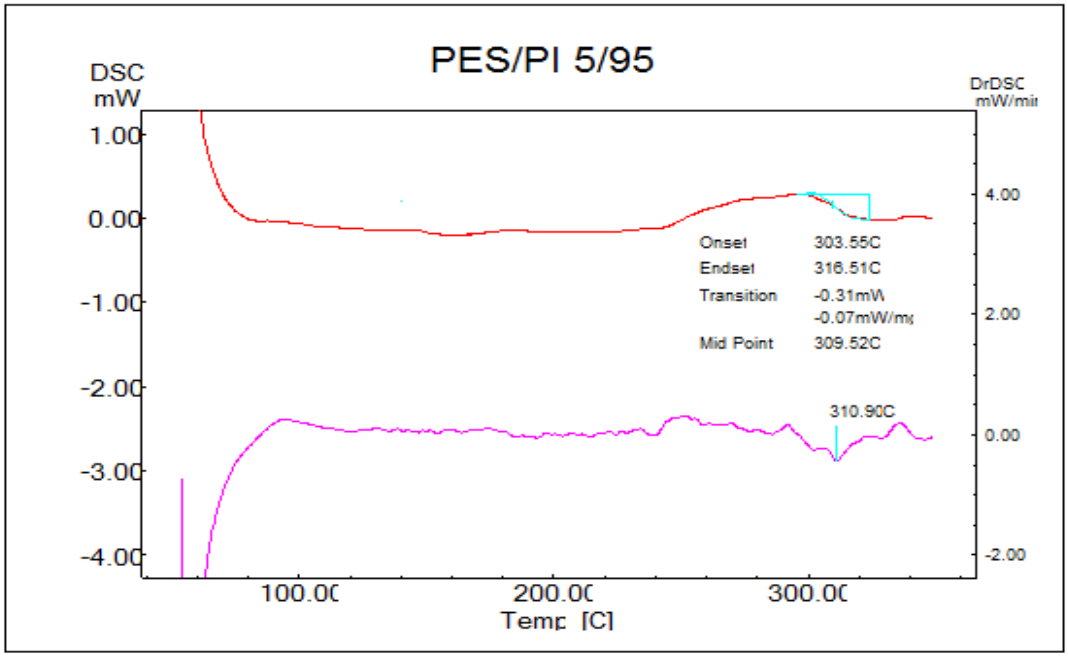

Figure D.13 DSC thermogram of PES/PI 5/95

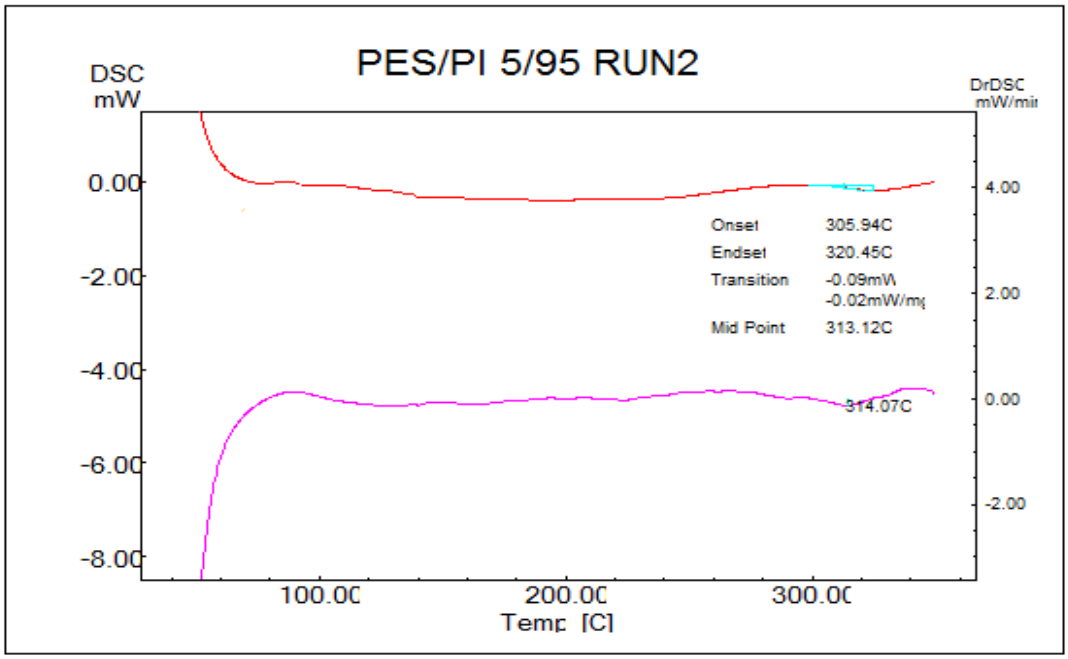

Figure D.14 DSC thermogram of PES/PI 5/95 Run2

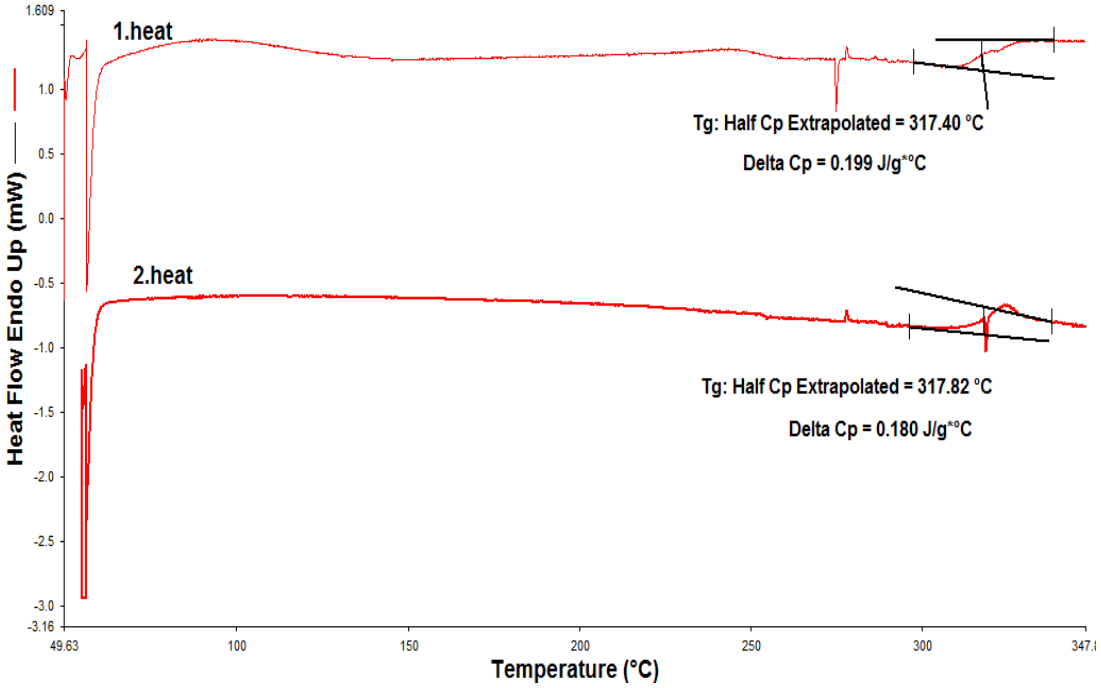

Figure D.15 DSC thermogram of Pure PI

APPENDIX E

REPRODUCIBILITY OF GAS PERMEABILITY EXPERIMENTS

Table E.1 Reproducibility data for PES/PI dense blend membranes

		Permeability (Barrer)			Selectivity		
Experiment Code	%PI	H_2	CO_2	CH_4	H_2/CO_2	CO_2/CH_4	H_2/CH_4
MK8-P2-RUN1	100	31.32	9.52	0.252	3.29	37.81	124.43
MK8-P2-RUN2		31.73	9.61	0.255	3.30	37.70	124.47
MK16-P1-RUN2		32.78	9.25	0.267	3.54	34.68	122.86
MK16-P2-RUN1		34.36	9.83	0.283	3.50	34.70	121.37
MK16-P2-RUN2		32.57	10.01	0.278	3.25	36.00	117.08
Average		32.55	9.64	0.267	3.38	36.18	122.04
Std. Dev.		1.05	0.26	0.012	0.12	1.37	2.73
MK35-P1-RUN1	90	24.26	7.42	0.194	3.27	38.16	124.76
MK35-P1-RUN2		23.98	7.63	0.218	3.15	34.95	109.92
Average		24.12	7.52	0.206	3.21	36.56	117.34
Std. Dev.		0.14	0.10	0.012	0.06	1.61	7.416
MK33-P1-RUN1	80	24.61	7.51	0.216	3.28	34.71	113.75
MK33-P1-RUN2		23.89	7.57	0.221	3.16	34.21	107.94
MK33-P2-RUN1		24.00	7.61	0.212	3.16	35.92	113.33
MK34-P2-RUN1		25.19	8.20	0.213	3.07	38.44	118.06
MK34-P2-RUN2		25.05	8.11	0.233	3.09	34.75	107.28
Average		24.55	7.80	0.219	3.15	35.61	112.07
Std. Dev.		0.53	0.29	0.008	0.07	1.52	4.01

MK13-P1-RUN3	75	23.24	7.35	0.224	3.16	32.82	103.76
MK21-P1-RUN1		20.72	7.11	0.261	2.91	27.29	79.49
MK21-P1-RUN2		21.89	7.27	0.222	3.01	32.74	98.59
MK22-P1-RUN1		20.66	7.17	0.227	2.88	31.64	91.14
MK22-P1-RUN2		20.74	6.76		3.07		
Average		21.45	7.13	0.233	3.01	31.12	93.25
Std. Dev.		1.00	0.20	0.016	0.10	2.26	9.12
MK36-P1-RUN1	70	22.52	8.03	0.198	2.80	40.52	113.60
MK36-P1-RUN2		22.18	8.01	0.201	2.77	39.86	110.29
Average		22.35	8.02	0.200	2.79	40.19	111.95
Std. Dev.		0.17	0.01	0.001	0.02	0.33	1.65
MK31-P2-RUN1	40	16.93	6.43	0.175	2.64	36.78	96.93
MK40-P1-RUN1		17.87	7.21	0.187	2.48	38.55	95.54
MK40-P1-RUN2		17.77	6.83	0.192	2.60	35.56	92.53
Average		17.52	6.82	0.185	2.57	36.96	95.00
Std. Dev.		0.42	0.32	0.007	0.07	1.23	1.84
MK14-P1-RUN1	25	16.17	6.53	0.188	2.48	34.71	85.93
MK14-P1-RUN2		16.18	6.57	0.199	2.46	33.04	81.42
MK14-P2-RUN1		16.03	6.20	0.238	2.58	26.03	67.28
MK14-P2-RUN2		15.89	6.02		2.64		
MK27-P1-RUN1		16.76	6.45	0.362	2.60	17.79	46.26
MK27-P1-RUN2		16.43	6.26	0.320	2.62	19.59	51.39
Average		16.24	6.34	0.261	2.56	31.26	78.21
Std. Dev.		0.284	0.194	0.022	0.069	3.761	7.946
MK5-P1-RUN1	0	10.64	4.92		2.16		
MK5-P1-RUN2		9.76	4.51	0.119	2.16	38.06	82.32
MK5-P2-RUN1		11.06	4.95		2.23		
MK5-P2-RUN2		11.40	4.77	0.160	2.39	29.85	71.35
MK30-P1-RUN1		10.94	4.71	0.139	2.32	33.78	78.54
Average		10.76	4.77	0.139	2.25	33.90	77.40
Std. Dev.		0.56	0.16	0.017	0.09	3.35	4.55

Table E.2 Reproducibility data for PES/PI/ZIF-8 20/80/10

	Permeability (Barrer)			Selectivity		
Experiment Code	H_2	CO_2	CH_4	H_2/CO_2	CO_2/CH_4	H_2/CH_4
MK-41-P1-RUN1	41.13	14.20	0.385	2.90	36.86	106.77
MK-41-P1-RUN2	40.57	14.09	0.389	2.88	36.23	104.30
MK-42-P1-RUN1	38.24	13.09	0.344	2.92	38.06	111.17
MK-44-P1-RUN1	38.34	13.17	0.365	2.91	36.11	105.14
MK-48-P1-RUN1	37.23	13.09	0.356	2.84	36.80	104.65
Average	38.93	13.53	0.368	2.89	36.81	106.41
Std. Dev.	1.42	0.51	0.017	0.03	0.69	2.53